Dipartimento di / Department of

Medicina e chirurgia

Dottorato di Ricerca in / PhD program   Dimet   Ciclo / Cycle XXIX

Curriculum in (se presente / if it is)

TITOLO TESI / THESIS TITLE

AQP8, a redoxtat controlling tyrosine kinase signalling

Cognome / Surname   Bestetti   Nome / Name Stefano

Matricola / Registration number   073108

Tutore / Tutor: Andrea Biondi

Cotutore / Co-tutor: Roberto Sitia
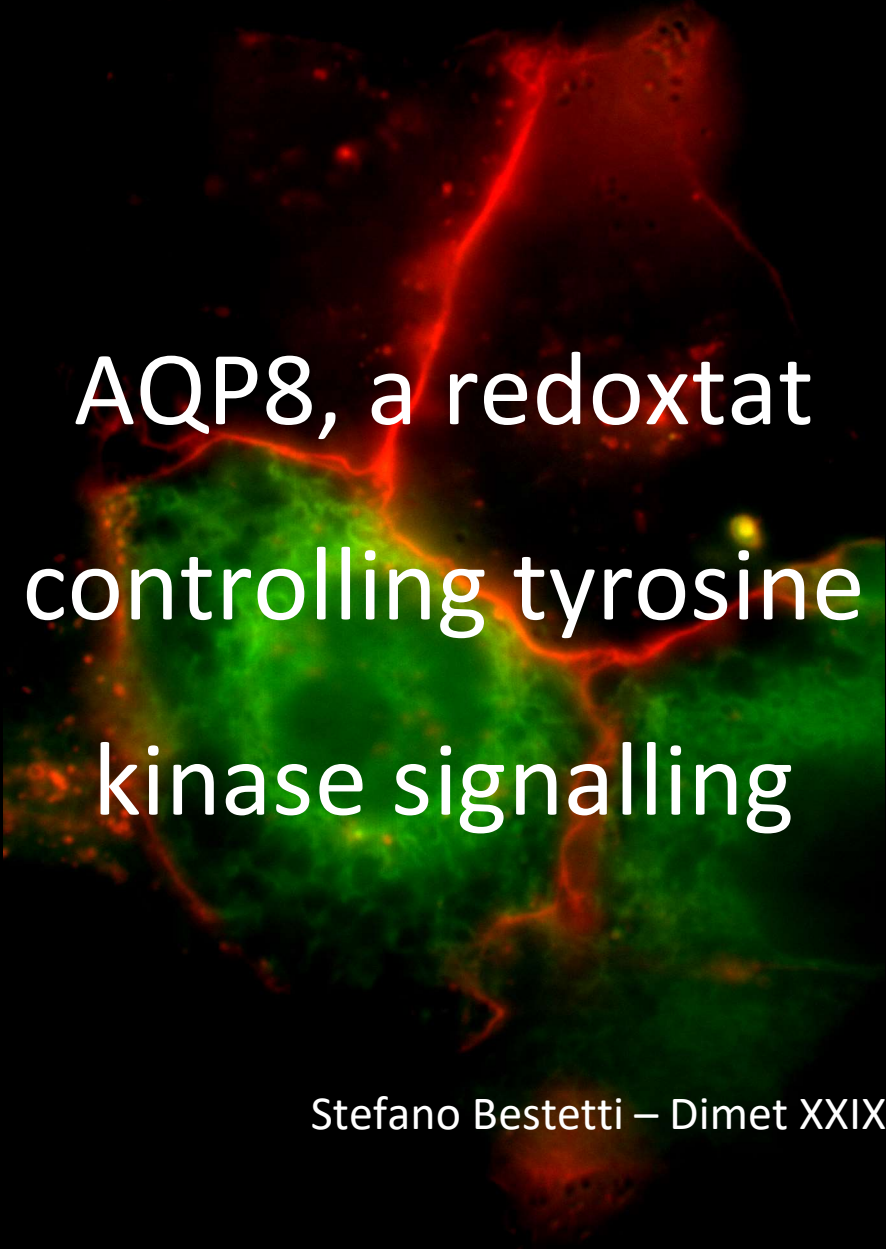(se presente / if there is one)

Supervisor:
(se presente / if there is one)

Coordinatore / Coordinator: Andrea Biondi

ANNO ACCADEMICO / ACADEMIC YEAR   2016/2017

Dimet

AQP8, a redoxtat controlling tyrosine kinase signalling

Stefano Bestetti – Dimet XXIX

"L'essenziale è invisibile agli occhi" .... per questo io uso un microscopio.

[Antoine de Saint-Exupéry]

Table of contents

6

Chapter 1: General Introduction

Life began in an oxygen-free atmosphere (1,2). As a memory of those early days, most biochemical reactions occurring in the cytoplasm require reducing conditions. This is the reason why most cell free transcription and translation protocols require the addition of DTT. The appearance of oxygen on the planet, about 2.5 billion years ago, caused a revolution in most living species.
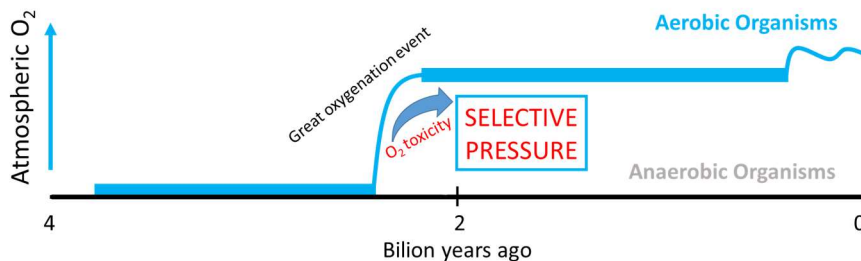
Figure 1. The appearance of oxygen on Earth. The increase of oxygen in the atmosphere 2.4–2.1 billion years ago, commonly known as the Great Oxidation Event (GOE), is believed to lead to the emergence of earliest animals on Earth. On the other hand, oxygen toxicity is thought to exert evolutionary pressure contributing to the diversification of animals. Organisms that could not accommodate to the challenge of oxygen toxicity evolved into anaerobes (adapted from Hong Z. et al., 2016).

On the one hand, oxidants can cause damage to macromolecules. On the other hand, the steep redox gradients across the plasma membrane, and in eukaryotes between organelles, offer unique signalling possibilities. My thesis deals with the mechanisms that link redox and tyrosine kinase signalling pathways.

Redox homeostasis

Owing to the hormetic properties of oxygen, essential yet toxic at high concentrations, cells must reach in order to balance between the need of oxidative species and the potential menace that they can represent. This delicate equilibrium is defined *redox homeostasis (redoxtasis* thereafter) and requires an intricate network of sensors and adaptive pathways. Indeed, *redoxtasis* has a fundamental role in every "breathing" organisms. This need for O_2 obscures the fact that this precious gas is also a toxic mutagen. Organisms (such as obligate anaerobic) that were not able to cope and evolve with the new environment extinguished soon after the "*great oxygenation event*".

ROS

Together with oxygen, its reactive species (ROS) appeared on Earth. These compounds are generated as by-product of the normal oxygen metabolism. In biomedicine, the most relevant species are hydrogen peroxide (H_2O_2), superoxide anion ($O_2^{\cdot -}$), hydroxyl radical ($OH^{\cdot}$) and peroxide ($O_2^{\cdot 2-}$) (Fig. 1).

Reactive Oxygen Species

Oxygen
O_2

Peroxide
$O_2^{.2-}$

Superoxide anion
$O_2^{.-}$

Hydroxyl radical
$OH^{.}$

Hydrogen Peroxide
H_2O_2
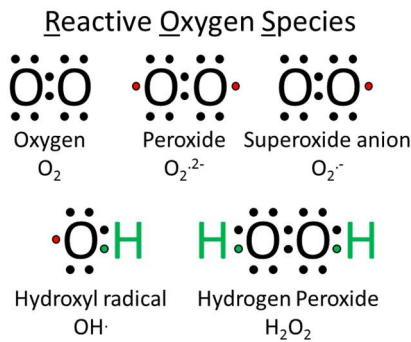
Figure 1. Electron structures of common reactive oxygen species. Each structure is provided with its name and chemical formula. The red dots represent an unpaired electron.

ROS differ for reactivity, stability and specificity of action. The most reactive is peroxide ($O_2^{.2-}$), followed by $OH^{.}$, H_2O_2, $O_2^{.-}$ and finally O_2. Nonetheless, reactivity is not the sole determinant in biological processes. The stability of these compounds is also of paramount relevance.

For example, $OH^{.}$ is the most labile ROS and has a very short diffusion coefficient. These characteristics significantly limit its capability of having selectivity and specificity on biological targets. On the other hand, H_2O_2 has opposite characteristics. As a consequence, H_2O_2 is the most abundant and stable ROS in cells. Moreover, being a weaker oxidant then $OH^{.}$, it has also much higher specificity of action in biological systems. All these features make H_2O_2 an optimal candidate for a role of second messenger. Indeed, it can interact with the active sites of kinases and phosphatases leading, respectively, to an activation or an inhibition of the target protein with huge pathophysiological consequences for cells and organisms (1-4).

ROS production and scavenging

As stated above, redoxtasis is an equilibrium between production and detoxification of ROS. Within cells, there are many enzymes that produce ROS as by-product, differing for localization, type of ROS produced, activity and regulation. These diversities reflect the different oxidative needs of cells in different compartments (Fig. 2).
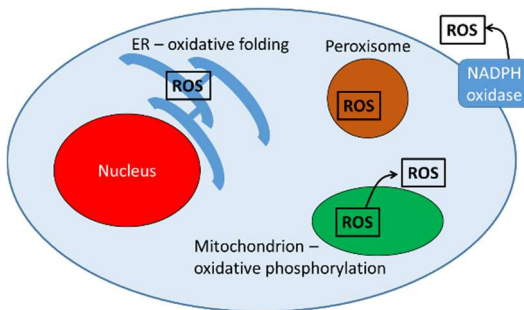
Figure 2. Various organelles within the cell can generate ROS. These include mitochondria, the endoplasmic reticulum and peroxisomes. In addition, various enzymes, including oxidases and oxygenases, generate ROS as part of their enzymatic reaction cycles (adapted from Holmström & Finkel 2014).

Peroxisomes

Peroxisomes are organelles in which several oxidation reactions occur, that lead to the formation of H_2O_2, as the name of the organelle suggest. The levels of H_2O_2 must be kept under strict surveillance because, as pointed out before, H_2O_2 is a dangerous molecule that can seriously damage cells. For this purpose, peroxisomes contain an enzyme called catalase, which decomposes

H_2O_2 generating water and oxygen (Fig. 3), impeding excessive H_2O_2 leakage from this organelle (5).

$$2H_2O_2 \xrightarrow{\text{Catalase}} 2H_2O + O_2$$

Hydrogen peroxide   Water   Oxygen

Figure 3. Typical reaction of a catalase enzyme in which H_2O_2 is detoxified in water and molecular oxygen.

Mitochondria

Another very important site of ROS production are mitochondria. The main function of this organelle is to produce energy for cells, exploiting the conversion of carbohydrates and fatty acids into ATP through the process known as oxidative phosphorylation.

Oxygen is consumed during physiological respiration and is converted into superoxide ($O2^{\cdot-}$), when electrons prematurely leak from the electron transport chain and are abnormally transferred to molecular oxygen (6). Moreover, the mitochondrial functions are very sensitive to oxidative damage and under certain metabolic or stress conditions, mitochondrial superoxide generation is further increased. This increase leads to a decreased ATP production, changes in Ca^{2+} homeostasis and increased mitochondrial membrane permeability. As a consequence, cells undergo apoptosis (7).

Not all the complexes of the mitochondrial respiratory chain produce ROS, the two main site of production of superoxide being

complex I and complex III (8, 9). In these organelles, redox homeostasis is maintained thanks to different enzymes. Superoxide from complex I is released into the matrix, whereas superoxide from complex III can be produced on either side of the inner membrane (10). Superoxide can then cross the outer membrane via a voltage-dependent anion-selective channel (VDAC) or can be dismutated into H_2O_2 in the matrix by superoxide dismutase 2 (SOD2) or in the intermembrane space by SOD1 (11) (Fig. 4). H_2O_2 can then cross mitochondrial membranes (12, 13) (Fig. 4, dashed arrows). Alternatively, it can be detoxified by other mitochondrial enzymes, such as members of the glutathione peroxidase or peroxiredoxin families. In the cytosol, superoxide is converted by SOD1 into H_2O_2, which is further detoxified by the peroxisomal enzyme catalase.
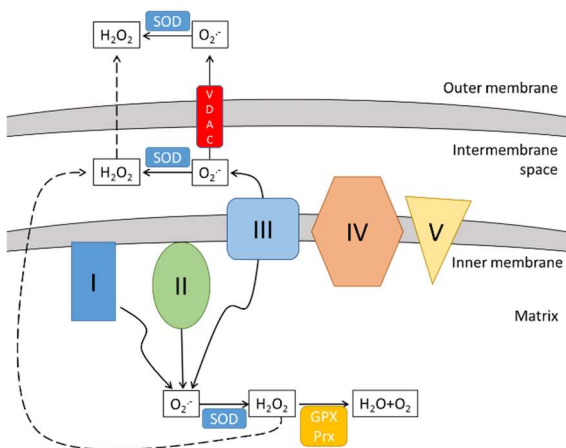
Figure 4. ROS production and detoxification through the process of oxidative phosphorylation by the electron transport chain in mitochondria (adapted from Phillip West A. et al., 2011).

Mitochondrial ROS (mROS) have long been thought just as dangerous by-products of the respiratory chain. However, more and more evidences point out that they are essential for many biological processes. For instance, mROS are fundamental for the mechanisms that regulate insulin secretion (14).

Therefore, we can say that mitochondria are prototype organelles to highlight the double edge effects that ROS can have inside cells, harmful if redox homeostasis is lost, but fundamental when it is strictly maintained.

Endoplasmic reticulum

ROS have a crucial role also in the endoplasmic reticulum (ER), the organelle where oxidative protein folding occurs. In this process, disulphide bonds are formed between cysteine residues in nascent proteins (15). What drives this process is a redox power that allows cysteines, upon their oxidation, to form a disulphide bond. In mammalian cells, a number of different enzymes can provide the oxidative power for this process (Fig. 5). A central role in the process is played by protein disulphide isomerase (PDI). In its oxidised form this multifunctional enzyme can catalyse the formation of a disulphide bond. Once the disulphide is formed PDI must be re-oxidised to begin a new cycle. This process is overseen by ER

oxidoreductase 1 (Ero1), a flavoprotein that is then reduced ($Ero1_{red}$). $Ero1_{red}$ is then oxidised back by molecular oxygen and this reaction produces a molecule of H_2O_2 per disulphide bond formed.

Oxidative folding in the ER
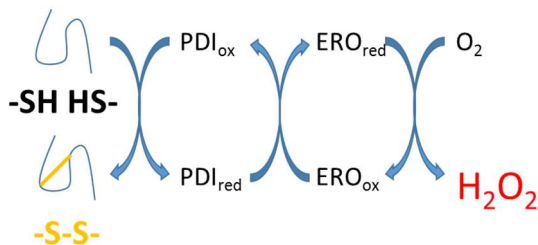
Figure 5. Schematic view of oxidative folding in the ER. Highlighted here the PDI-ERO cycle, fundamental to sustain disulphide bonds formation in the ER off nascent proteins but detrimental because of the formation of hydrogen peroxide as by-product.

This equation has consequences that at first sight could be surprising. Imagine plasma cells, the factories responsible for the production of antibodies in our body. Considering that a single plasma cell produces 10^3 IgM molecules per second, each of which contains 10^2 disulphide bonds, it follows that 10^5 H_2O_2 molecules are generated in the ER each second (16). Similar figures are reached in beta cells of the pancreas during insulin production. Therefore, it is obvious that the ER must be equipped with great anti-oxidant capacity, allowing it to recycle or detoxify the huge amount of H_2O_2 produced during these multiple cycles. Thus ER is able to maintain redox homeostasis and avoid the activation of maladaptive pathways that could lead to cell death (17).

Two types of ER-resident antioxidant enzymes are important in maintaining H_2O_2 levels under control: glutathione peroxidases

(GPX7 and GPX8) (18) and peroxiredoxins (PRX4) (19). They have two major roles: i) reducing H_2O_2 to water, which lead to their oxidation, and ii) transferring their oxidizing power to PDI, hence improving the capacity of the oxidative folding machinery. Therefore, also in the ER H_2O_2 as a Janus-like effect. Generated as a potentially harmful by-product of oxidative folding, it can boost disulphide bond formation increasing the overall folding capacity of the ER.

Prx4, GPx7 and GPx8 reside in the ER, where in addition to PDI over twenty other oxidoreductases reside, to satisfy a diverse secretome in the need of forming the proper array of disulphide bonds. It is of fundamental importance therefore that non-native disulphides are isomerized, or reduced to facilitate the destruction of terminally misfolded proteins. The search for the source of the reducing power that in the ER limits the activity of Ero1 and other oxidases is still open. Recent data (20) suggest a role for thioredoxin reductase (TrxR) though it remains to be explained how this protein - that lacks a leader sequence - negotiates entry into the ER. A plethora of PRX and GPX enzymes reside in the cytosol and other organelles, where disulphide bond formation is rare and often linked to signalling (that needs to be transient) or aggregation (that cells seek to prevent). Prompt reduction of oxidised Prx and GPx is mediated by thioredoxin Trx and TrxR (21). The ultimate reducing power is provided by NADPH.

Plasma membrane

Also on the plasma membrane there are enzymes that produce ROS. These belong to the NADPH oxidases (NOX) family. These enzymes are peculiar, in the sense that they generate superoxide/peroxide as their main products and not as by-product as in many other flavoproteins (22). Their prototype is PhOx, also dubbed NOX2 in the latest nomenclature. This Phagocytic Oxidase is designed to release abundant peroxide in phagosomes so as to kill pathogens. It is hence recruited onto the phagosomes membrane and activated with myeloperoxidase, which uses peroxides to form hypochloric acid. Not surprisingly, NOX2 deficient individuals suffer from a severe immune deficiency, called Chronic granulomatous disease and characterized by recurrent bacterial infections (23, 24). Besides their antibacterial activities, NOXes have been linked with the generation of ROS as important signalling molecules in angiogenesis, inner ear development, and insulin signalling (25). Indeed, NOXes could often be coupled with a tyrosine kinase receptor (TKR) and, after TKR activation, they start producing $O_2^{.-}$ in the extracellular space, which is converted in H_2O_2 by SOD enzymes outside the cells. H_2O_2 can finally enter into cell to exerts its biological role and amplify signalling pathways downstream the

recepto to which NOX is coupled to promote cell growth and/or differentiation (25, 26) (Fig. 6).
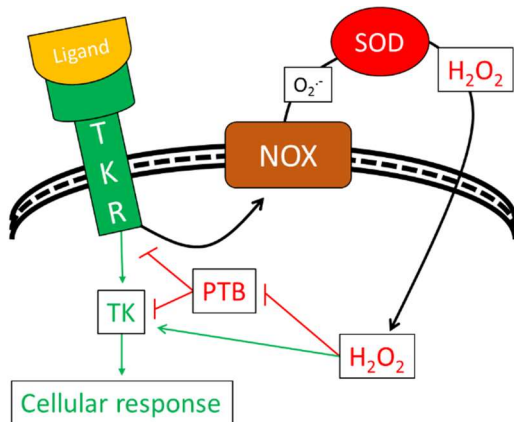
Figure 6. Cartoon representing the pathway that links TKRs and NOXes. Activation of TKR by its ligand, lead to the production of superoxide anion from a NOX that is rapidly converted to H_2O_2 by SOD enzymes in the extracellular space. Finally, NOX-derived H_2O_2 can enter into cells and exerts its physiological functions. In green growth-positive effects and in red growth-negative effects.

Hydrogen peroxide: physiological relevance

ROS, and in particular H_2O_2, are like an atomic reactor, very powerful and useful but only if maintained under tight control. As described above, H_2O_2 can inhibit protein phosphatases and activate protein kinases thus amplifying signalling pathways to stimulate cell proliferation (25, 27), differentiation (28), migration (29), or apoptosis (30, 31). But H_2O_2 must not react randomly with every molecule otherwise all the pathways would be active at the same time causing a sort of cellular atomic fallout. In this view, it is important to notice that most H_2O_2 sensitive proteins must contain

deprotonated cysteine residues (with a low pKa) enabling specific H_2O_2-targeting. H_2O_2 is unable to react with protonated cysteines. Thus, deprotonated thiol groups are utilized as reactive species in the catalytic mechanisms of a multitude of enzymes, rendering many of them susceptible to regulation by oxidation. Indeed, exposure to ROS leads to reversible oxidation of thiol groups of key cysteine residues in many proteins, including transcriptional regulators, kinases, phosphatases, structural proteins and metabolic enzymes.

Many efficient mechanisms evolved to confer specificity to redox signalling pathways precisely channelling H_2O_2 functions to select targets.

First, different H_2O_2 concentrations can activate preferentially one or another pathway: for example, it has been demonstrated that different patterns of p53-regulated gene expression are initiated in response to different levels of H_2O_2. Antioxidants are induced in response to low levels, further decreasing the oxidative burden and hence protecting the cell from DNA damage. In contrast, higher levels of H_2O_2, generated for example in stress conditions, stimulate the expression of pro-oxidants important for apoptosis induction (32). The induction of apoptosis is a defence mechanism which will eliminate cells that have potentially lost their genome stability because of the presence of high ROS levels with the risk of developing malignant mutations.

20

Incidentally, this dual response is one of the main hurdles encountered so far in the educated design of anticancer therapies targeting oxidant/antioxidant pathways.

Second, cells can localize or de-localize H_2O_2 targets and/or scavengers in proximity of the site of production to regulate the initiation, duration and intensity of signalling. A remarkable example of this strategy is the localized inactivation of Prx1 that allows for the transient accumulation of H_2O_2 near the activated tyrosine kinases, where signalling components are concentrated, while preventing the toxic H_2O_2 accumulation elsewhere (33). Similarly, Haj et al. (34) demonstrated that the activated EGFR is internalized and transported by vesicles near the ER, where PTP1B dephosphorylates it. The catalytic activity of PTP is dependent on a reduced cysteine residue in its active site, that is extremely susceptible to oxidation by H_2O_2 (35). Targeting EGFR towards the ER has an explanation in the localization of Nox4 in the ER. Thus, NOX4 produces H_2O_2 that extends the duration of EGFR signalling by PTP1B oxidation, but only when EGFR, NOX4 and PTP1B colocalize in a discrete part of the cell, namely the cytoplasmic face of the ER.

Third, it is now clear, also thank to my work, that H_2O_2 cannot freely diffuse across membranes at physiological concentration (13, 36, 37), but rather requires the presence of specific channels. Indeed, increasing evidences indicate that members of the

aquaporins (AQP) family could have this kind of function. As I will discuss in great detail below, my work contributed to reveal that the regulation of AQP8-dependent H_2O_2 transport across the plasma membrane provides yet another layer of spatial/temporal control of signalling.

AQPs

AQPs family

Peter Agre was awarded the 2003 Nobel prize in Chemistry for the discovery of a protein that increases membrane permeability to water (38). Before this fundamental contribution in 1992, water was thought to freely cross biological membranes. This protein was the first member of the aquaporin family, and was hence named aquaporin 1 (AQP1).

AQPs are membrane channels containing six transmembrane domains connected by 5 loops and two termini protruding into the cytosol. Two loops contain the conserved asparagine-proline-alanine (NPA) signature motif or minor variations thereof (Fig. 7).
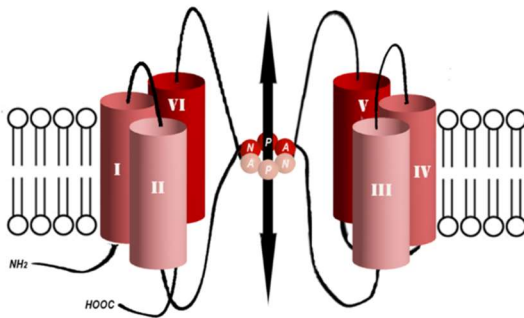
Figure 7. Predicted tertiary structure of an AQP8 monomer. AQP8 monomer is formed by six transmembrane domains that are organised creating a channel that allows the bidirectional flux of solutes.

AQPs have a molecular weight between 20kDa and 40kDa and form tetramers within biological membranes (39). Each monomer in a tetramer is functional (Fig. 8), and contains a narrow hydrophilic channel that selectively exclude charged ions as well as large solutes. In all cases, the gate allows the passage of water.
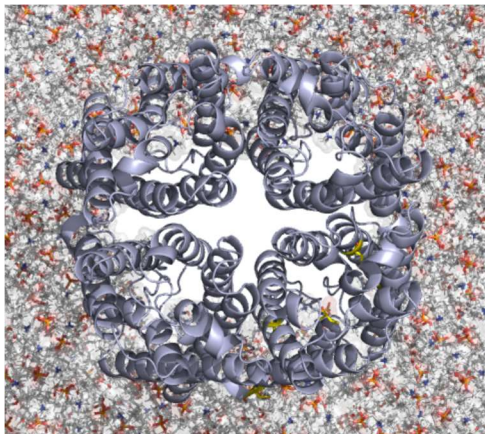
Figure 8. Predicted quarternary structure of AQP8. Each tetramer is formed by 4 functional identical monomers. The function of the putative central pore is still poorly understood.

Other isoforms can transport one or more of the following compounds: glycerol, lactic acid, acetic acid, nitric acid, hydroxylated metalloid acids, CO_2, ammonia, urea and H_2O_2 (39). The human genome encodes 13 AQP genes, with different localization and transport selectivity.

Interestingly, plants have over 70 AQP isoforms, reflecting the need for uptaking and transporting a vast array of substances (Table 1).

Aquaporins	Tissue expression	Other solutes transported
AQP0	Highly expressed in the lens	-
AQP1	Renal tubules, exocrine pancreas, bile ducts, subsets of cells in the intestine, myoepithelial cells of breast and endothelial cells	-
AQP2	Renal tubules	-
AQP3	Epithelial and glandular cells, including renal collecting ducts	Hydrogen peroxide, urea, glycerol
AQP4	CNS, lung, thyroid gland and stomach	-
AQP5	Salivary gland and testis	-
AQP6	Renal tubules	-
AQP7	Adipose and soft tissue	Glycerol, urea
AQP8	Colon, rectum and pancreas	Hydrogen peroxide, ammonia
AQP9	Liver and gallbladder	Hydrogen peroxide, urea, glycerol
AQP10	Small intestine- and duodenum glands	Urea, glycerol
AQP11	Ubiquitous, most abundant in gastrointestinal tract and adrenal gland	-
AQP12	Pancreas and epididymis	-

Table 1. Patterns of expression and solutes transported (different than water) of the 13 mammalian AQPs (*The Human Protein Atlas*).

Over the last two decades, the diversity and phylogeny of AQPs was elucidated (40), crystal structures for some members of the family were revealed (41, 42), and questions such as subcellular localization of AQPs, their spatial and temporal expression patterns and regulation addressed (43). Moreover, it has also been elucidated the role of individual residues for pore selectivity, transport capability, gating and posttranslational modifications (44) and the consequences of post-translational modifications and

heteromerization (in plant AQPs) on the functional- and trafficking-regulation (43, 45, 46).

AQPs-mediated H$_2$O$_2$ transport

The studies of H$_2$O$_2$ transport followed the same steps as it was a decade before for water. Biophysical measurements established that i) H$_2$O$_2$ does not freely diffuse across membranes (though the permeability is quite high), ii) huge differences in H$_2$O$_2$ membrane permeability exist amongst cell types and iii) H$_2$O$_2$ membrane permeability could be inhibited with AQP blockers, first chemical such as mercurial compounds (47, 48) and then genetic, like diseases or experimental silencing assays.

Despite all these experimental evidences and, as described above, the necessity for several metabolic and signalling pathways to tight and fast regulate H$_2$O$_2$ fluxes to gain physiological effectiveness, the dogma long remained that H$_2$O$_2$ crosses membranes via passive diffusion. Moreover, many studies to directly prove the existence of a H$_2$O$_2$ transporter were hampered by the presence of efficient H$_2$O$_2$ decomposing enzymes in living cells and the lack of robust assays to measure H$_2$O$_2$ which become available only recently.

Nonetheless, Henzler and Steudle were the first to hypothesize the existence of channels that can facilitate the

transport of H_2O_2 (49). Comparing the permeability and reflection coefficients of water and H_2O_2 the authors suggested that the two uses partially the same path(s) to cross membranes. Accordingly, mercury chloride, a well-established AQPs inhibitor, reduced the permeability coefficient for H_2O_2 that was then rescued by a treatment with 2-mercaptoethanol (49). This was another evidence pointing to the existence of special aquaporin(s), also called *peroxiporins*, that can facilitate H_2O_2 transport.

The first actual evidence that specific AQPs can transport H_2O_2 came in 2007 when Bienert et al. demonstrated that human AQP8 can facilitate H_2O_2 entry in yeast cells (36). A huge decrease in yeast growth-rates and survival was observed and correlated not only with the amount of H_2O_2 added in the culture medium, but also with the presence or absence of AQP8 (or other plant AQPs that were suspected to transport H_2O_2).

More direct methods were then used to confirm and compare the transport ability of the peroxiporins identified with toxicity assays. Yeast cells were loaded with a H_2O_2 sensitive dye and the kinetics of fluorescence emission changes were monitored and quantified after exposure to H_2O_2. As anticipated, the signal increased significantly only in cells that were transformed with hAQP8 and not with an empty vector confirming the role of specific AQPs in facilitating H_2O_2 uptake. Altogether these experiments

provided convincing evidences demonstrating an AQP-mediated H_2O_2 transport (36).

Thereafter, yeast growth and survival assays in combination with H_2O_2 optical detection assays were used to quantitatively assess whether and which AQPs are permeable to H_2O_2 (39).

Mammalian AQPs in their physiological context

Once it was accepted that AQPs increase membrane permeability to H_2O_2 and the latter is a key signalling molecule, several studies in mammalian cell systems followed promptly to demonstrate that i) AQPs facilitate transmembrane H_2O_2 diffusion in their native expression contexts, ii) AQP-mediated H_2O_2 transport is of physiological relevance and iii) it can be regulated. These were made possible largely thanks to the development of specific H_2O_2 probes of improved specificity, faster kinetics and predetermined subcellular localization, of either chemical nature, as in the case of boronate-based fluorescent dyes (50) or genetically encoded fusion proteins between bacterial OxyR and a permutated fluorescent protein (*HyPer* and variants thereof; (51, 52)). Using these technologies, it was possible to establish that AQP-mediated import of NOX-produced H_2O_2 has an important role amplifying diverse signal transduction cascades (Fig. 6), as detailed below.

AQP3

The first AQP demonstrated to transport H_2O_2 in mammalian cells was AQP3 (37). AQP3-overexpressing human embryonic kidney 293 (HEK293) cells which were loaded with a with chemical or genetically encoded optical sensors, responded with a significant higher fluorescent signal emission upon exposure to H_2O_2 than untrasfected cells (37). Importantly, modifying AQP3 expression altered downstream intracellular H_2O_2 signalling. Thus, knockdown of hAQP3 expression using a specific shRNA decreased the influx of H_2O_2 upon extracellular application or after epidermal growth factor (EGF)-stimulated production. Simultaneously, downstream serine/threonine kinase AKT/protein kinase B phosphorylation circuits were reduced, implying that AQP3-mediated H_2O_2 import is important for intracellular redox signalling (37).

After this first finding, AQP3 it has been demonstrated to be involved also in chemokine-dependent T lymphocyte migration during immune responses in mice (53), in regulation migration of two breast cancer lines (54) and in modulating psoriasis (55) and scleroderma (56) pathogenesis. It has also been reported that AQP3 knockdown reduces spontaneous metastasis in xenografts (54). Importantly de-regulation of intestinal H_2O_2 levels has been clinically connected to early-onset of inflammatory bowel disease and colon

cancer. In this context, it was hypothesized that intestinal H_2O_2 transport across the cell membrane depends on AQP3 (57). These results leave little doubt that AQP3-dependent H_2O_2 transport impacts signalling.

AQP8

As described above, AQP8 facilitates H_2O_2 diffusion across membranes in heterologous expression systems (36). The physiological importance of AQP8 in the transduction of H_2O_2 signals across the plasma membrane was demonstrated in human and murine cells (13, 58). My work contributed to show that AQP8 is an efficient peroxiporin. Accordingly, hAQP8-silencing diminished H_2O_2 entry and dampened EGF signalling. The presence of catalase in the extracellular space phenocopied AQP8 silencing, implying that H_2O_2 generated in response to EGF was produced in the outer leaflet of the plasma membrane, hence accessible to the scavenger and needing to cross a lipid bilayer to promote signalling (13). Other members of the lab then showed that AQP8 is essential to import H_2O_2 generated by NOX2 upon B cell receptor cross-linking, signal amplification being necessary for B cell activation and plasma cell differentiation (58).

The involvement of AQP in signalling cascades was clear also in human acute leukaemia cells (59). When AQP8 expression was positively or negatively modulated, downstream signalling was increased or decreased, respectively. Thus, AQP8-mediated H_2O_2 transport affects signalling and cell proliferation (59). The biochemical consequences of this pathway were investigated also in B1647 cells that constitutively produce vascular endothelial growth factor (VEGF) where AQP8 expression levels were shown to influence the VEGF-induced oxidation of target proteins (60).

Taken together, these examples show that AQP8 can fine-tune cysteine modifications of proteins, modulating intracellular signalling pathways.

Transport across the membranes of organelles

Since AQP8 begins its folding schedule in the ER, it is not surprising that downregulation of the channel also had an impact on H_2O_2 transport across the membrane of this organelle (13). Considering that there are proteins that release H_2O_2 in the ER and, by doing that, they can oxidise and modulate the activity of cytoplasmic enzymes such as PTP1B (61), it is conceivable that peroxiporin-mediated ER H_2O_2 channelling be also used to provide specificity to inter-organelle redox signalling (62).

AQP9

A reverse genetic approach using cell model systems (CHO-K1 and HepG2 cells) and AQP9 knock-out mice have recently implicated AQP9 as an H_2O_2 transporter *in vivo* suggesting that -like AQP3 and AQP8- also this channel might control physiologically important transmembrane H_2O_2 fluxes (63).

All these findings highlighted here are just few pieces of a bigger puzzle underlining the various roles that AQPs play in regulating H_2O_2 and other solutes transport across membranes. The interrelationships between AQPs and ROS action are hence of central biomedical interest and deserve further intensive work.

Cancer and ROS

As described above, H_2O_2 transiently activates certain tyrosine kinases (TK) and inhibits tyrosine phosphatases via reversible cysteine oxidation. In this way, it potentiates signalling circuits that could favour tumour progression. Besides its function as a second messenger, H_2O_2 can also cause oxidative stress that can finally lead to apoptosis if in excess (17). Thus, the relevance of redox circuitry in cancer is of paramount importance. Perhaps only in aging did the interest in redox gain more momentum that in cancer.

Why did many clinical attempts give only marginal, if any definitive result? A key aspect that must be considered is the ability of malignant cells to upregulate antioxidant defences. It is well known that to survive to the stressful microenvironments in which tumour cells live, they must contrive adaptive responses, one of which is the upregulation of antioxidant genes to counteract oxidative stress (64). This defence mechanism has been clearly shown to display pro-tumour effects through mechanisms that are so far only partially understood. All preventive or therapeutic attempts with antioxidants failed or, worse, showed evidence of unexpected harm, as demonstrated by several meta-analyses of randomized clinical trials (65-67).

A meticulous handling of the dangerous ROS-based circuits could hence be a feature that cancer cell exploit during disease progression to improve their tumorigenicity. Increased ROS production is a hallmark of cancer onset since it will increase genomic instability allowing cells to accumulate oncogenic mutations. In a second phase, in order to survive, cancer cells will upregulate also their antioxidant capacity to counteract the increased ROS production that, if prolonged, will have a tumour suppressor activity by inducing apoptosis. Thus, tumour cells will acquire a new redoxtasis which is more prone to be disrupted since

the antioxidant systems are already upregulated, making cancer cells more prone to a second oxidative insult.

Thus, mechanisms that control H_2O_2 production, transport and clearance are of paramount oncological interest: as the reader will find below in chapter 2 section, tilting the redox homeostasis can facilitate radio-chemotherapy, because tumour cells need to optimise growth promoting pathways, usually live on the edge of the delicate redox balance, and hence can be more easily induced to undergo apoptosis (68).

Activation of antioxidant pathways is an intrinsic risk in chemotherapeutic protocols based on generating oxidative stress (69). Indeed, non-lethal oxidative stress induces anti-oxidant responses that increase cell fitness and chemo resistance (69). Accordingly, sulfosalazine, a drug that inhibits xCT-, a protein with antioxidant capacity, impairs antioxidant responses synergising with As_2O_3 and thus increasing the efficacy of cancer treatment (70).

Another example of the strict relationship between ROS and cancer comes from a haematological cancer, multiple myeloma (MM). The genetic and microenvironment differences between normal plasma and MM cells has as a final consequence a different metabolite production. In fact, recent metabolomic studies have unveiled the importance of some pathways potentially involved in redox homeostasis in the neoplastic evolution of MM

cells, especially in the crosstalk with the tumour site (71). On the same line, it is also reported that increasing oxidative stress in MM cells could potentiate bortezomib sensitivity. This concept came thanks to studies focused on redox homeostasis and signalling (72-74). Treatment with buthionine sulfoximine (BSO), a compound that decreases the intracellular pool of glutathione, strongly synergize with bortezomib treatment increasing cell death both in MM cell lines and in MM cells derived from patients, whilst antioxidants protect MM cells from bortezomib-mediated cell death ((72) and Fig. 9).
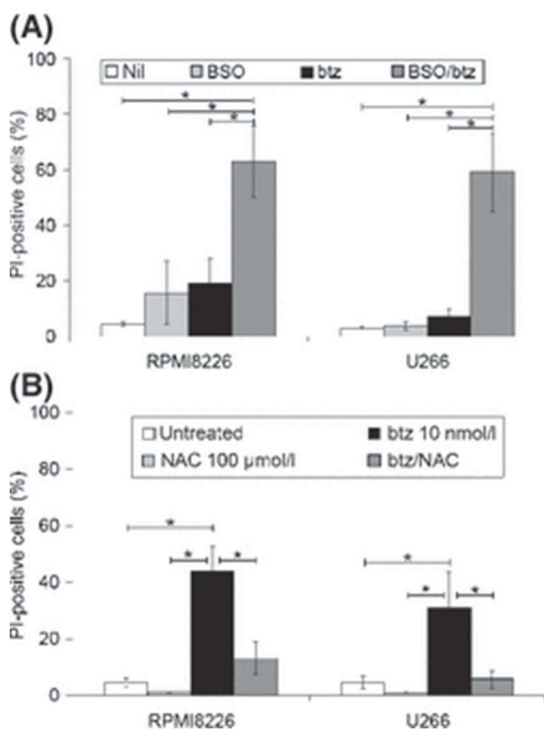
Figure 9. Redox homeostasis modulates the sensitivity of myeloma cells to bortezomib. GSH depletion increases sensitivity to bortezomib (A) whilst antioxidants protect from bortezomib-mediated cell death (B) (British Journal of Haematology Volume 141, Issue 4, pages 494-503, 13 MAR 2008).

Another evidence that perturbing redox home-ostasis in cancer could improve chemo-therapy came from a study where the authors treat either MM cell lines, MM

cells derived from patients or a mouse model with a high dose of iron. It is well known that iron is a very important nutrient and cancer cells could increase their fitness if iron availability is increased. However, excess iron could be toxic since it is a substrate in the Fenton reaction leading to the formation of ROS (75). Thus, co-treatment with iron and bortezomib increases therapy efficacy, showing a strong synergistic effect, as it was for BSO (73, 74).

As early diagnosis and staging are fundamental to improve the patients' response to treatments, the study of these redox-related pathways in a normal plasma cell population compared to MM, could be essential to reveal new strategies to treat this disease.

An independent study showed an additional example of how ROS are interconnected to cancer and how more profound studies could open new opportunity in cancer therapy. NOX1 is highly expressed in colon cancer and its role in cancer development has been recently investigated. The authors demonstrated that NOX1 contributes to decreased growth, blood vessel density, and VEGF and HIF-1 expression in HT-29 xenografts derived from NOX1 knockdown cells (76).

These here reported are just few examples of a promising field rapidly expanding in which ROS are no longer looked as collateral effects of cancer therapy that must be prevented but as important, active player for anticancer treatment.

Cancer and AQPs

Not only ROS but also AQPs were closely associated with tumour functions in more than 20 human cancer cell types ((77, 78) and table 2).

Aquaporins	Tumor type	Correlated function
AQP1	Brain, Breast, Colorectal, Cervical, Laryngeal, Lung, Nasopharyngeal, Ovarian	Tumor grade, prognosis, tumor angiogenesis, tumor necrosis, tumor cell migration, tumor invasion and metastasis
AQP3	Colorectal, Cervical, Liver, Lung, Oesophageal, Renal, Skin, Stomach, Tongue	Tumor grade, prognosis, tumor angiogenesis, tumor invasion, tumor cell migration and tumor energy metabolism
AQP4	Brain, Lung, Thyroid	Tumor grade, migration, tumor-associated edema, adhesion, invasion and tumor apoptosis
AQP5	Breast, Colorectal, Cervical, Leukaemia, Liver, Lung, Oesophageal, Ovarian, Stomach, Tongue	Tumor prognosis, tumor proliferation, tumor invasion, tumor cell migration and drug resistance
AQP7	Thyroid	Unknown
AQP8	Cervical	Tumor cell migration, tumor invasion, tumor metastasis and anti-apoptosis
AQP9	Brain, Ovarian	Tumor grade, drug resistance and energy metabolism

Table 2. AQPs over-expression in different human tumours (from Wang J. et al., 2015).

AQPs have been involved in carcinogenesis, pathogenesis of tumour-associated edema, tumour cell proliferation and migration, or tumour angiogenesis (79-82). For example, AQP1 was up-regulated in lung adenocarcinoma and more importantly inhibiting its expression can inhibit tumour cell invasion (83).

The presence of AQP3 has been demonstrated to be important for cells the proliferation and migration of lung cancer

cells and its downregulation slowed cell cycle progression and promotes apoptosis (84).

Over the last years, many AQP-targeting drugs and monoclonal antibodies have been developed but their clinical application in oncology still limited. The reader is referred to a recent review by Verkman (44) for more details on the pros and cons of this approach. Further studies are required to verify the efficiency and safety of these potential anticancer drugs.

The results from studies in vivo or vitro also show the attractive opportunities for AQP-target therapy. However, there is still a long way to go before we can clearly elucidate the specificity of AQPs in the pathogenesis, metabolisms, and controls of various cancers, or resistance and tolerance to anticancer therapies.

So far AQPs have been linked to cancer mainly for their ability to transport water, as described above for AQP1 and 3. Since specific AQPs can transport also H_2O_2 and given the important role of H_2O_2 in cancer pathology it is of extreme interest to study in deeper details how AQPs-mediated H_2O_2 transport takes place and if it can have an impact on cancer cell fate.

Aim of the thesis

In my undergraduate studies, I have been interested in type-2 diabetes, a condition in which oxidative stress is thought to play an important pathogenetic role. In that period, the possibility of targeting HyPer, a genetically encoded H_2O_2-specific probe, allowed me to investigate the relationship between mitochondria- and ER-produced H_2O_2 generated during a hyperglycaemic stimulus. During this period my interest for the redox field of study blossomed and I had the opportunity to collaborate with the team of Roberto Sitia, which was studying the role of AQP8 in mammalian cells.

A year after I started my PhD project in Roberto's laboratory focused on the investigation of whether and how AQP8-mediated H_2O_2 transport is regulated in physio-pathological contexts. The final objective is to determine if this regulation could be exploited as a new therapeutic approach against cancer. This could be particularly relevant in multiple myeloma, since, as described above, oxidative stress is proved to be a promising treatment in combination with classical chemotherapy to improve prognosis.

References

1.   Reth M. Hydrogen peroxide as second messenger in lymphocyte activation. Nature immunology. 2002;3(12):1129-34.

2.   Bae YS, Kang SW, Seo MS, Baines IC, Tekle E, Chock PB, et al. Epidermal growth factor (EGF)-induced generation of hydrogen peroxide. Role in EGF receptor-mediated tyrosine phosphorylation. The Journal of biological chemistry. 1997;272(1):217-21.

3.   Lee SR, Kwon KS, Kim SR, Rhee SG. Reversible inactivation of protein-tyrosine phosphatase 1B in A431 cells stimulated with epidermal growth factor. The Journal of biological chemistry. 1998;273(25):15366-72.

4.   Sundaresan M, Yu ZX, Ferrans VJ, Irani K, Finkel T. Requirement for generation of H_2O_2 for platelet-derived growth factor signal transduction. Science. 1995;270(5234):296-9.

5.   Wang X, Li S, Liu Y, Ma C. Redox regulated peroxisome homeostasis. Redox biology. 2015;4:104-8.

6.   Orrenius S, Gogvadze V, Zhivotovsky B. Mitochondrial oxidative stress: implications for cell death. Annu Rev Pharmacol Toxicol. 2007;47:143-83.

7.   James AM, Murphy MP. How mitochondrial damage affects cell function. J Biomed Sci. 2002;9(6 Pt 1):475-87.

8.   Koopman WJ, Nijtmans LG, Dieteren CE, Roestenberg P, Valsecchi F, Smeitink JA, et al. Mammalian mitochondrial complex I: biogenesis, regulation, and reactive oxygen species generation. Antioxidants & redox signaling. 2010;12(12):1431-70.

9.   Orrenius S. Reactive oxygen species in mitochondria-mediated cell death. Drug Metab Rev. 2007;39(2-3):443-55.

10.   Murphy MP. How mitochondria produce reactive oxygen species. The Biochemical journal. 2009;417(1):1-13.

11.   Han D, Antunes F, Canali R, Rettori D, Cadenas E. Voltage-dependent anion channels control the release of the superoxide anion from mitochondria to cytosol. The Journal of biological chemistry. 2003;278(8):5557-63.

12.   Yang B, Zhao D, Verkman AS. Evidence against functionally significant aquaporin expression in mitochondria. The Journal of biological chemistry. 2006;281(24):16202-6.

13.   Bertolotti M, Bestetti S, Garcia-Manteiga JM, Medrano-Fernandez I, Dal Mas A, Malosio ML, et al. Tyrosine kinase signal modulation: a matter of H_2O_2 membrane permeability? Antioxidants & redox signaling. 2013;19(13):1447-51.

14.   Leloup C, Tourrel-Cuzin C, Magnan C, Karaca M, Castel J, Carneiro L, et al. Mitochondrial reactive oxygen species are obligatory signals for glucose-induced insulin secretion. Diabetes. 2009;58(3):673-81.

15.   Margittai E, Sitia R. Oxidative protein folding in the secretory pathway and redox signaling across compartments and cells. Traffic. 2011;12(1):1-8.

16.   Tu BP, Weissman JS. The FAD- and O(2)-dependent reaction cycle of Ero1-mediated oxidative protein folding in the endoplasmic reticulum. Molecular cell. 2002;10(5):983-94.

17.   Davies KJ. The broad spectrum of responses to oxidants in proliferating cells: a new paradigm for oxidative stress. IUBMB life. 1999;48(1):41-7.

18.   Nguyen VD, Saaranen MJ, Karala AR, Lappi AK, Wang L, Raykhel IB, et al. Two endoplasmic reticulum PDI peroxidases increase the efficiency of the use of peroxide during disulfide bond formation. Journal of molecular biology. 2011;406(3):503-15.

19.   Zito E, Melo EP, Yang Y, Wahlander A, Neubert TA, Ron D. Oxidative protein folding by an endoplasmic reticulum-localized peroxiredoxin. Molecular cell. 2010;40(5):787-97.

20.   Poet GJ, Oka OB, van Lith M, Cao Z, Robinson PJ, Pringle MA, et al. Cytosolic thioredoxin reductase 1 is required for correct disulfide formation in the ER. The EMBO journal. 2017;36(5):693-702.

21.   Lu J, Holmgren A. The thioredoxin antioxidant system. Free radical biology & medicine. 2014;66:75-87.

22.   Bedard K, Krause KH. The NOX family of ROS-generating NADPH oxidases: physiology and pathophysiology. Physiol Rev. 2007;87(1):245-313.

23.   Rada B, Hably C, Meczner A, Timar C, Lakatos G, Enyedi P, et al. Role of Nox2 in elimination of microorganisms. Semin Immunopathol. 2008;30(3):237-53.

24.   Deffert C, Cachat J, Krause KH. Phagocyte NADPH oxidase, chronic granulomatous disease and mycobacterial infections. Cellular microbiology. 2014;16(8):1168-78.

25.   Geiszt M, Leto TL. The Nox family of NAD(P)H oxidases: host defense and beyond. The Journal of biological chemistry. 2004;279(50):51715-8.

26.   Park L, Anrather J, Zhou P, Frys K, Wang G, Iadecola C. Exogenous NADPH increases cerebral blood flow through NADPH oxidase-dependent and -independent mechanisms. Arterioscler Thromb Vasc Biol. 2004;24(10):1860-5.

27.   Foreman J, Demidchik V, Bothwell JH, Mylona P, Miedema H, Torres MA, et al. Reactive oxygen species produced by NADPH oxidase regulate plant cell growth. Nature. 2003;422(6930):442-6.

28.   Sauer H, Rahimi G, Hescheler J, Wartenberg M. Role of reactive oxygen species and phosphatidylinositol 3-kinase in cardiomyocyte differentiation of embryonic stem cells. FEBS letters. 2000;476(3):218-23.

29.   Ushio-Fukai M. Localizing NADPH oxidase-derived ROS. Sci STKE. 2006;2006(349):re8.

30.   Cai H. Hydrogen peroxide regulation of endothelial function: origins, mechanisms, and consequences. Cardiovascular research. 2005;68(1):26-36.

31.   Gechev TS, Hille J. Hydrogen peroxide as a signal controlling plant programmed cell death. The Journal of cell biology. 2005;168(1):17-20.

32.   Sablina AA, Budanov AV, Ilyinskaya GV, Agapova LS, Kravchenko JE, Chumakov PM. The antioxidant function of the p53 tumor suppressor. Nature medicine. 2005;11(12):1306-13.

33.   Woo HA, Yim SH, Shin DH, Kang D, Yu DY, Rhee SG. Inactivation of peroxiredoxin I by phosphorylation allows localized H(2)O(2) accumulation for cell signaling. Cell. 2010;140(4):517-28.

34.   Haj FG, Markova B, Klaman LD, Bohmer FD, Neel BG. Regulation of receptor tyrosine kinase signaling by protein tyrosine phosphatase-1B. The Journal of biological chemistry. 2003;278(2):739-44.

35.   Meng TC, Fukada T, Tonks NK. Reversible oxidation and inactivation of protein tyrosine phosphatases in vivo. Molecular cell. 2002;9(2):387-99.

36.   Bienert GP, Moller AL, Kristiansen KA, Schulz A, Moller IM, Schjoerring JK, et al. Specific aquaporins facilitate the diffusion of hydrogen

peroxide across membranes. The Journal of biological chemistry. 2007;282(2):1183-92.

37.   Miller EW, Dickinson BC, Chang CJ. Aquaporin-3 mediates hydrogen peroxide uptake to regulate downstream intracellular signaling. Proceedings of the National Academy of Sciences of the United States of America. 2010;107(36):15681-6.

38.   Preston GM, Carroll TP, Guggino WB, Agre P. Appearance of water channels in Xenopus oocytes expressing red cell CHIP28 protein. Science. 1992;256(5055):385-7.

39.   Bienert GP, Chaumont F. Aquaporin-facilitated transmembrane diffusion of hydrogen peroxide. Biochimica et biophysica acta. 2014;1840(5):1596-604.

40.   Abascal F, Irisarri I, Zardoya R. Diversity and evolution of membrane intrinsic proteins. Biochimica et biophysica acta. 2014;1840(5):1468-81.

41.   Tani K, Fujiyoshi Y. Water channel structures analysed by electron crystallography. Biochimica et biophysica acta. 2014;1840(5):1605-13.

42.   Kirscht A, Kaptan SS, Bienert GP, Chaumont F, Nissen P, de Groot BL, et al. Crystal Structure of an Ammonia-Permeable Aquaporin. PLoS Biol. 2016;14(3):e1002411.

43.   Hachez C, Besserer A, Chevalier AS, Chaumont F. Insights into plant plasma membrane aquaporin trafficking. Trends Plant Sci. 2013;18(6):344-52.

44.   Verkman AS, Anderson MO, Papadopoulos MC. Aquaporins: important but elusive drug targets. Nature reviews Drug discovery. 2014;13(4):259-77.

45.   Maurel C, Verdoucq L, Rodrigues O. Aquaporins and plant transpiration. Plant, cell & environment. 2016;39(11):2580-7.

46.   Verdoucq L, Rodrigues O, Martiniere A, Luu DT, Maurel C. Plant aquaporins on the move: reversible phosphorylation, lateral motion and cycling. Curr Opin Plant Biol. 2014;22:101-7.

47.   Bienert GP, Schjoerring JK, Jahn TP. Membrane transport of hydrogen peroxide. Biochimica et biophysica acta. 2006;1758(8):994-1003.

48.   Bienert GP, Heinen RB, Berny MC, Chaumont F. Maize plasma membrane aquaporin ZmPIP2;5, but not ZmPIP1;2, facilitates transmembrane diffusion of hydrogen peroxide. Biochimica et biophysica acta. 2014;1838(1 Pt B):216-22.

49.   Henzler T, Steudle E. Transport and metabolic degradation of hydrogen peroxide in Chara corallina: model calculations and measurements with the pressure probe suggest transport of H(2)O(2) across water channels. Journal of experimental botany. 2000;51(353):2053-66.

50.   Lin W, Chen T. A vinblastine fluorescent probe for pregnane X receptor in a time-resolved fluorescence resonance energy transfer assay. Analytical biochemistry. 2013;443(2):252-60.

51.   Belousov VV, Fradkov AF, Lukyanov KA, Staroverov DB, Shakhbazov KS, Terskikh AV, et al. Genetically encoded fluorescent indicator for intracellular hydrogen peroxide. Nat Methods. 2006;3(4):281-6.

52.   Bilan DS, Belousov VV. HyPer Family Probes: State of the Art. Antioxidants & redox signaling. 2016;24(13):731-51.

53.   Hara-Chikuma M, Chikuma S, Sugiyama Y, Kabashima K, Verkman AS, Inoue S, et al. Chemokine-dependent T cell migration requires aquaporin-3-mediated hydrogen peroxide uptake. J Exp Med. 2012;209(10):1743-52.

54.   Satooka H, Hara-Chikuma M. Aquaporin-3 Controls Breast Cancer Cell Migration by Regulating Hydrogen Peroxide Transport and Its Downstream Cell Signaling. Molecular and cellular biology. 2016;36(7):1206-18.

55.   Hara-Chikuma M, Satooka H, Watanabe S, Honda T, Miyachi Y, Watanabe T, et al. Aquaporin-3-mediated hydrogen peroxide transport is required for NF-kappaB signalling in keratinocytes and development of psoriasis. Nature communications. 2015;6:7454.

56.   Luo J, Liu X, Liu J, Jiang M, Luo M, Zhao J. Activation of TGF-beta1 by AQP3-Mediated H_2O_2 Transport into Fibroblasts of a Bleomycin-Induced Mouse Model of Scleroderma. The Journal of investigative dermatology. 2016;136(12):2372-9.

57.   Thiagarajah JR, Chang J, Goettel JA, Verkman AS, Lencer WI. Aquaporin-3 mediates hydrogen peroxide-dependent responses to environmental stress in colonic epithelia. Proceedings of the National Academy of Sciences of the United States of America. 2017;114(3):568-73.

58.   Bertolotti M, Farinelli G, Galli M, Aiuti A, Sitia R. AQP8 transports NOX2-generated H_2O_2 across the plasma membrane to promote signaling in B cells. Journal of leukocyte biology. 2016;100(5):1071-9.

59.   Vieceli Dalla Sega F, Prata C, Zambonin L, Angeloni C, Rizzo B, Hrelia S, et al. Intracellular cysteine oxidation is modulated by aquaporin-8-mediated hydrogen peroxide channeling in leukaemia cells. BioFactors. 2016.

60.   Vieceli Dalla Sega F, Zambonin L, Fiorentini D, Rizzo B, Caliceti C, Landi L, et al. Specific aquaporins facilitate Nox-produced hydrogen peroxide transport through plasma membrane in leukaemia cells. Biochimica et biophysica acta. 2014;1843(4):806-14.

61.   Chen K, Kirber MT, Xiao H, Yang Y, Keaney JF, Jr. Regulation of ROS signal transduction by NADPH oxidase 4 localization. The Journal of cell biology. 2008;181(7):1129-39.

62.   Appenzeller-Herzog C, Banhegyi G, Bogeski I, Davies KJ, Delaunay-Moisan A, Forman HJ, et al. Transit of H_2O_2 across the endoplasmic reticulum membrane is not sluggish. Free radical biology & medicine. 2016;94:157-60.

63.   Watanabe S, Moniaga CS, Nielsen S, Hara-Chikuma M. Aquaporin-9 facilitates membrane transport of hydrogen peroxide in mammalian cells. Biochem Biophys Res Commun. 2016;471(1):191-7.

64.   Castellani P, Balza E, Rubartelli A. Inflammation, DAMPs, tumor development, and progression: a vicious circle orchestrated by redox signaling. Antioxidants & redox signaling. 2014;20(7):1086-97.

65.   Wang Z, Joshi AM, Ohnaka K, Morita M, Toyomura K, Kono S, et al. Dietary intakes of retinol, carotenes, vitamin C, and vitamin E and colorectal cancer risk: the Fukuoka colorectal cancer study. Nutr Cancer. 2012;64(6):798-805.

66.   Fritz H, Kennedy D, Fergusson D, Fernandes R, Cooley K, Seely A, et al. Selenium and lung cancer: a systematic review and meta analysis. PloS one. 2011;6(11):e26259.

67.   Cortes-Jofre M, Rueda JR, Corsini-Munoz G, Fonseca-Cortes C, Caraballoso M, Bonfill Cosp X. Drugs for preventing lung cancer in healthy people. Cochrane Database Syst Rev. 2012;10:CD002141.

68.   Cenci S, Sitia R. Managing and exploiting stress in the antibody factory. FEBS letters. 2007;581(19):3652-7.

69.   Landriscina M, Maddalena F, Laudiero G, Esposito F. Adaptation to oxidative stress, chemoresistance, and cell survival. Antioxidants & redox signaling. 2009;11(11):2701-16.

70.   Balza E, Castellani P, Delfino L, Truini M, Rubartelli A. The pharmacologic inhibition of the xc- antioxidant system improves the antitumor efficacy of COX inhibitors in the in vivo model of 3-MCA tumorigenesis. Carcinogenesis. 2013;34(3):620-6.

71.   Tavel L, Fontana F, Garcia Manteiga JM, Mari S, Mariani E, Caneva E, et al. Assessing Heterogeneity of Osteolytic Lesions in Multiple Myeloma by (1)H HR-MAS NMR Metabolomics. International journal of molecular sciences. 2016;17(11).

72.   Nerini-Molteni S, Ferrarini M, Cozza S, Caligaris-Cappio F, Sitia R. Redox homeostasis modulates the sensitivity of myeloma cells to bortezomib. British journal of haematology. 2008;141(4):494-503.

73.   Campanella A, Santambrogio P, Fontana F, Frenquelli M, Cenci S, Marcatti M, et al. Iron increases the susceptibility of multiple myeloma cells to bortezomib. Haematologica. 2013;98(6):971-9.

74.   Bordini J, Galvan S, Ponzoni M, Bertilaccio MT, Chesi M, Bergsagel PL, et al. Induction of iron excess restricts malignant plasma cells expansion and potentiates bortezomib effect in models of multiple myeloma. Leukemia. 2016.

75.   Gozzelino R. The Pathophysiology of Heme in the Brain. Curr Alzheimer Res. 2016;13(2):174-84.

76.   Juhasz A, Markel S, Gaur S, Liu H, Lu J, Jiang G, et al. NADPH Oxidase 1 Supports Proliferation of Colon Cancer Cells by Modulating Reactive Oxygen Species-Dependent Signal Transduction. The Journal of biological chemistry. 2017.

77.   Papadopoulos MC, Saadoun S. Key roles of aquaporins in tumor biology. Biochimica et biophysica acta. 2015;1848(10 Pt B):2576-83.

78.   Wang J, Feng L, Zhu Z, Zheng M, Wang D, Chen Z, et al. Aquaporins as diagnostic and therapeutic targets in cancer: how far we are? J Transl Med. 2015;13:96.

79.   Wang J, Li X, Zhang DQ, Yang CS, Qi Y, Li MS, et al. Quantitative analysis of aquaporin-4 antibody in longitudinally extensive transverse myelitis. J Neuroimmunol. 2015;278:26-9.

80.   Nico B, Annese T, Tamma R, Longo V, Ruggieri S, Senetta R, et al. Aquaporin-4 expression in primary human central nervous system lymphomas correlates with tumour cell proliferation and phenotypic heterogeneity of the vessel wall. Eur J Cancer. 2012;48(5):772-81.

81. Guan G, Dong Z, Sun K. [Correlation between the expression of aquaporin 1 and the micro-angiogenesis in laryngeal carcinoma]. Lin Chung Er Bi Yan Hou Tou Jing Wai Ke Za Zhi. 2009;23(5):219-21.

82. Saadoun S, Papadopoulos MC, Davies DC, Krishna S, Bell BA. Aquaporin-4 expression is increased in oedematous human brain tumours. J Neurol Neurosurg Psychiatry. 2002;72(2):262-5.

83. Hoque MO, Soria JC, Woo J, Lee T, Lee J, Jang SJ, et al. Aquaporin 1 is overexpressed in lung cancer and stimulates NIH-3T3 cell proliferation and anchorage-independent growth. The American journal of pathology. 2006;168(4):1345-53.

84. Xiong G, Chen X, Zhang Q, Fang Y, Chen W, Li C, et al. RNA interference influenced the proliferation and invasion of XWLC-05 lung cancer cells through inhibiting aquaporin 3. Biochem Biophys Res Commun. 2017;485(3):627-34.

Chapter 2: Stress Regulates Aquaporin-8 Permeability to Impact Cell Growth and Survival.

Medraño-Fernandez I*, Bestetti S*, Bertolotti M, Bienert GP, Bottino C, Laforenza U, Rubartelli A, Sitia R.

* These authors contributed equally to this work.

Abstract

Aquaporin-8 (AQP8) allows the bidirectional transport of water and hydrogen peroxide across biological membranes. Depending on its concentration, H_2O_2 exerts opposite roles, amplifying growth factor signalling in physiological conditions but causing severe cell damage when in excess. Thus, H_2O_2 permeability is likely to be tightly controlled in living cells.

Aims: In this study, we investigated whether and how the transport of H_2O_2 through plasma membrane AQP8 is regulated, particularly during cell stress.

Results: We show that diverse cellular stress conditions, including heat, hypoxia and ER stress, reversibly inhibit the permeability of AQP8 to H_2O_2 and water. Preventing the accumulation of intracellular reactive oxygen species (ROS) during stress counteracts AQP8 blockade. Once inhibition is established, AQP8-dependent transport can be rescued by reducing agents. Neither H_2O_2 and water transport are impaired in stressed cells expressing a mutant AQP8 in which cysteine 53 had been replaced by serine. Cells expressing this mutant are more resistant to stress-, drug- and radiation-induced growth arrest and death.

Innovation and conclusion: The control of AQP8-mediated H_2O_2 transport provides a novel mechanism to regulate cell signalling and survival during stress.

Introduction

The pathophysiology of H_2O_2 exemplifies how reactive oxygen species (ROS) are double-edged swords in the cell signalling armamentarium: H_2O_2 is toxic at high concentrations, but at the same time it is an essential second messenger in charge of modulating diverse signalling pathways (12,15,17,36). Among these, H_2O_2 inactivates tyrosine phosphatases by oxidising essential cysteines in their active sites and activates certain kinases, including members of mitogen-activated kinase family (MAPKs). The sum of these activities results in the amplification of tyrosine phosphorylation cascades (35,38). Therefore, the mechanisms that control H_2O_2 production, transport, diffusion and clearance in human cells are of paramount biomedical interest (21).

Owing to their membrane topology, NADPH-oxidases (NOXes) generate superoxide in the external leaflet of the plasma membrane or in the lumen of endocytic and exocytic organelles (4). Dismutases rapidly convert superoxide into H_2O_2 that must then

cross a lipid bilayer to reach its cytosolic targets. Recently, members of the aquaporin protein family (AQP), initially described as bidirectional water transporters (1), have been found to channel also H_2O_2 (7). We have recently shown that aquaporin-8 (AQP8) is essential to allow effective transport of H_2O_2 across the plasma membrane, thus potentiating tyrosine phosphorylation induced by growth factors (6), a notion later corroborated by others (57). These data confirmed that H_2O_2 acts as a rheostat of tyrosine kinase signalling and demonstrated that AQP8 guarantees efficient cytosolic import of H_2O_2 likely produced by NOXes. AQP8 silencing inhibited in part the transport of H_2O_2 through the ER membrane, but had little if any effect on mitochondria (6), where a fraction of AQP8 has been reported to localize (9). In other cell types, AQP3 (18,39) and possibly also different channels can allow efficient H_2O_2 transport.

Considering its importance in modulating growth factor downstream pathways, we surmised that AQP8-dependent H_2O_2 transport could be finely tuned during stress conditions, known to entail the production of ROS (51,52). Accordingly, we found that diverse cellular stresses reversibly inhibit AQP8-dependent transport impacting cell growth and survival. The expression of an AQP8 mutant that does not undergo this inhibition increases the resistance of cells to heat-, arsenic trioxide- and radiation-induced stress.

Results

Membrane permeability to H_2O_2 is impaired during cell stress

The hormetic properties of H_2O_2 -essential for cell survival, but toxic at high concentrations- imply tight regulation of its intracellular levels. We reasoned that, being more sensitive to oxidant toxicity (11,42), cells undergoing stress might deploy mechanisms that limit H_2O_2 import. To test this possibility, we exposed human HeLa cells expressing an H_2O_2-specific ratiometric sensor in their cytosol (HyPerCyto (5)) to diverse chemical or physical stresses and followed the entry of exogenous H_2O_2 by live imaging. As shown in Fig. 1A, non-stressed cells (red line) display a characteristic shift in the ratio of HyPerCyto fluorescence emission (488/405nm) as exogenously added H_2O_2 enters the cytosol. The addition of extracellular catalase after H_2O_2 during our time-course analyses rapidly eliminated this shift (Fig. S1A). Thus, in control conditions, intracellular ROS produced in response to exposure to H_2O_2 plays a minor if any role in the activation of HyPerCyto, which detects mostly H_2O_2 imported through the plasma membrane. Having validated a system that allows us to register primarily the entry of exogenous molecules, we measured H_2O_2 permeability in

stressed cells. Clearly, the activation of HyperCyto was inhibited in cells exposed to different stressors, i.e. the Hsp90 inhibitor geldanamycin, the glycolytic inhibitor 2-deoxyglucose, the ER stressor tunicamycin, heat-shock and hypoxia (Fig. 1A). Similar results were obtained on different cells types, such as the murine B-lymphoma I.29μ+ or the human myeloma OPM2 (data not shown). In view of its efficacy and ease of control, we used heat-shock for most experiments of stress induction.

H_2O_2 transport inhibition is redox-dependent

The observation that different stressors inhibit H_2O_2 transport suggests the existence of mechanisms that reversibly gate its channel under stress conditions. As diverse stresses share the property of triggering ROS production by activating oxidases in target cells (23,27,50), we hypothesised that the increase in the levels of ROS generated during stress was involved in the inhibition of exogenous H_2O_2 influx observed (13,24,32,53). To verify this prediction, HeLa cells were exposed to heat stress in the presence of either diphenyleneiodonium (DPI), a compound that limits ROS production by inhibiting membrane-bound NOXes and other flavoproteins (31), or N-acetyl-cysteine (NAC), a widely used ROS scavenger. As shown in Fig. 1B, addition of DPI or NAC during the

exposure to high temperature (grey bars) prevented the stress-induced inhibition of H_2O_2 uptake.

Fig. 1A. Kinetics of *HyPerCyto* activation in stressed HeLa cells upon addition of exogenous H_2O_2 (50µM) reveals an impairment of its transport though the plasma membrane. Data are shown as mean fold changes of the 488/405nm ratio measured by confocal laser scanning, plotted against time ± standard error of the mean (SEM). Ctrl, control conditions; 2-DG, 2-Deoxyglucose; Geld, Geldanamycin; Tun, Tunicamycin; Heat, Heat stress; Hyp, Hypoxia.

Similar results were obtained on different cells types, such as the murine B-lymphoma I.29µ[+] or the human myeloma OPM2 (data not shown). In view of its efficacy and ease of control, we used heat-shock for most experiments of stress induction.

H_2O_2 transport inhibition is redox-dependent

The observation that different stressors inhibit H_2O_2 transport suggests the existence of mechanisms that reversibly gate its channel under stress conditions. As diverse stresses share the property of triggering ROS production by activating oxidases in target cells (23,27,50), we hypothesised that the increase in the levels of

ROS generated during stress was involved in the inhibition of exogenous H_2O_2 influx observed (13,24,32,53). To verify this prediction, HeLa cells were exposed to heat stress in the presence of either diphenyleneiodonium (DPI), a compound that limits ROS production by inhibiting membrane-bound NOXes and other flavoproteins (31), or N-acetyl-cysteine (NAC), a widely used ROS scavenger. As shown in Fig. 1B, addition of DPI or NAC during the exposure to high temperature (grey bars) prevented the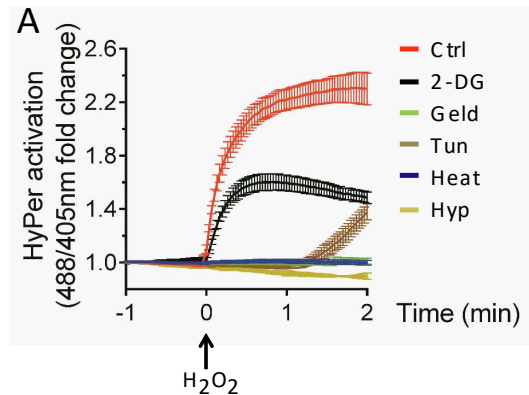 stress-induced inhibition of H_2O_2 uptake. Similar results were obtained when cells were treated with tunicamycin or cultured in hypoxic conditions in the presence of DPI (Fig. S2). These observations suggested that elements of the transport mechanism are controlled by redox-mediated modification(s).
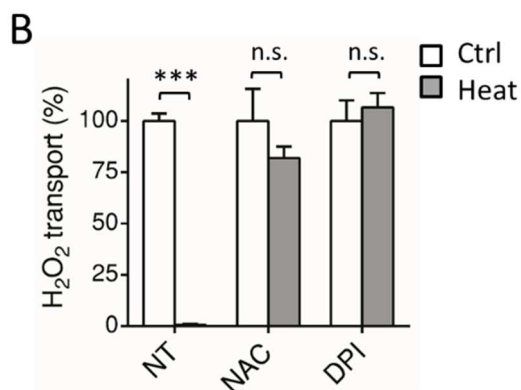

Fig. 1B. Quantification of H_2O_2-uptake performed 90 seconds after addition of exogenous H_2O_2 to HyPerCyto-HeLa cells before or after heat stress with or without either 10μM DPI or 2mM NAC. The data were normalized to the uptake of DPI- or NAC-treated unstressed cells. Average of ≥3 experiments ±SEM. NT, non-treated cells.

AQP8 is the target of the stress-dependent redox regulation

Having shown before that human AQP8 is essential for efficient entry of H_2O_2 into living HeLa cells (6), we investigated whether this channel is the target of the regulatory modification(s) that hamper H_2O_2 uptake by stressed cells. To this end, cells silenced for AQP8 expression, and thus unable to import exogenous H_2O_2, were reconstituted with a vector driving the expression of a silencing-resistant Halo-tagged AQP8 (HaloAQP8), and stained using the Halo technology (40). Confirming our previous results (6), H_2O_2 transport was restored upon expression of the chimeric transgene (decorated in white in the pseudocolor scale used in Fig. 2A and supplemental Movie SM1). Moreover, heat stress prevented H_2O_2 entry also in reconstituted cells (Fig. 2B, upper panels, and Fig. 2C, blue trace). Thus, HaloAQP8 transgene maintains the properties of the endogenous channel proteins. Following our hypothesis, if the channel were controlled by redox-mediated modification(s), incubating heat-stressed cells with the reducing agent dithiothreitol (DTT) immediately before exposure to exogenous H_2O_2 should recover transport only in cells expressing HaloAQP8. In fact, 5-minute exposure to DTT partially rescued H_2O_2 entry only in the positive transfected cells (Fig. 2B, lower panels, Fig. 2C orange trace

and see supplemental Movie SM2). The reducing agent caused an apparent small delay in H_2O_2 uptake when given to unstressed cells (Fig. 2B, black trace), which presumably reflects a potentiation of intracellular antioxidant systems and the consequent rapid detoxification of the first internalized H_2O_2 molecules.

Altogether, these observations further support the notion that AQP8 is a key target of the stress-induced redox regulatory modification(s).
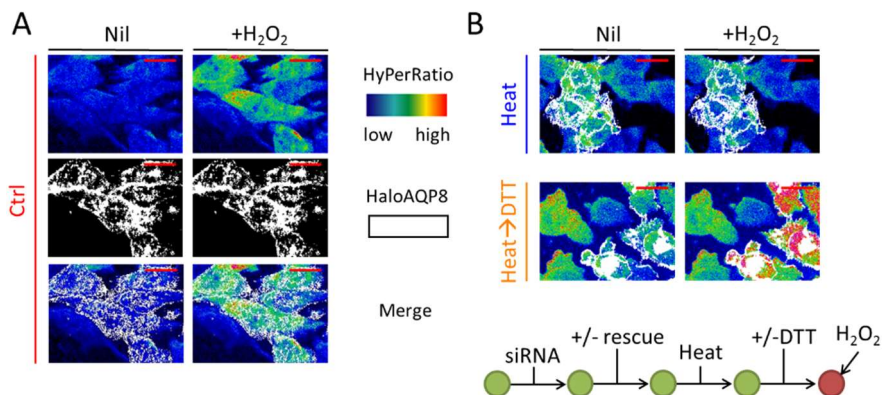
Fig. 2. AQP8 is the target of the redox-dependent regulation of H_2O_2 permeability. A. Frames extracted from a representative video out of ≥3 experiments, highlighting the kinetics of H_2O_2 import into silenced HeLa cells reconstituted with HaloAQP8 before (left panel) and after (right panel) addition of 50µM exogenous H_2O_2. The 488/405nm ratio is shown in pseudo-colour (upper panel, the scale used is indicated in the insert). Cells positively transfected with HaloAQP8 wt are coloured in white (middle panel). HyPer fluorescence ratio at baseline is variable from cell to cell, but the mean within a cell population is nearly the same in all experiments. The variability at the single cell level explains why the basal colours presented in panels or figures sometimes differ. The scale bars correspond to 50µm. Nil, non-treated cells.

B. The upper panels correspond to frames extracted from a video as in panel A, showing no changes in the HyPerCyto-ratios in HeLa cells reconstituted with HaloAQP8 under stress. The frames in lower panels show that recovery of H_2O_2 transport occurs only in cells expressing the transgene (coloured in white) after a 5-minute treatment with 5mM DTT and two washes before the analysis. The experimental flow is depicted on the lower scheme for clarity.
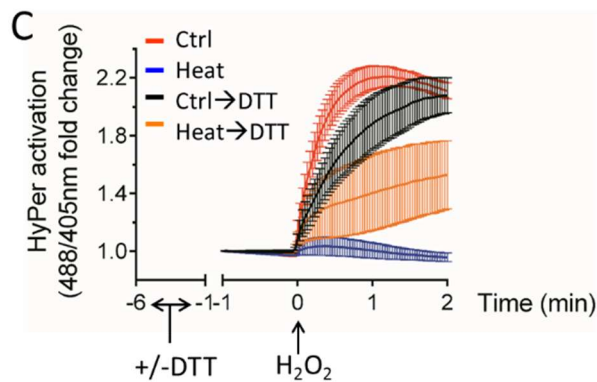
C. Kinetics of H_2O_2 import into HeLa cells in which AQP8 was silenced and then reconstituted with a silencing-resistant vector driving the expression of HaloAQP8. Cells were heat-shocked and then incubated with (orange trace) or without (blue trace) 5mM DTT for 5min. Results represent the mean fold changes of the 488/405nm ratio measured by confocal laser scanning, plotted against time. Average of ≥3 experiments ±SEM.

AQP8 cysteine mutants display different sensitivities to stress-induced transport inhibition

The sensitivity to DTT and the rapidity by which the reducing agent rescued transport suggested that, upon stress, ROS-induced modification(s) of one or more of the six cysteine residues present in human AQP8 lead to the closure of the channels. If this were the case, mutating them could generate AQP8 variants that become insensitive to the stress-dependent blockade. Therefore, we individually replaced the six cysteines in AQP8 for serine. Serine

residues should retain the approximate size and geometry of cysteines residues but be unable to form disulphide bonds or undergo other redox modifications affecting channel structure and conductivity. Accordingly, all single cysteine-to-serine replacements assayed were able to promote efficient water and H_2O_2 transport when expressed in yeast (Fig. S3A and B), showing that mutating those residues did not hamper AQP8 activity in control conditions. HeLa cells were then transfected with wild type (wt) HaloAQP8 or, separately, with the six mutants, and the uptake of exogenous H_2O_2 evaluated before or after heat stress. Like in yeast, none of the cysteine mutants displayed significant impairment in H_2O_2 transport in control conditions in HeLa cells (data not shown). However, clear differences were evident when H_2O_2 import was analysed after heat stress (Fig. 3A). In each sample, care was taken to average only cells expressing the transgenes, as detected by staining with fluorescent Halo ligands (Fig. 3B). In this experiments, negative cells served as powerful internal controls. Neither untransfected cells nor transfectants expressing wt, C8S, C38S, C208S or C247S HaloAQP8 displayed HyPer oxidation upon exposure to H_2O_2. In contrast, C53S transfectants were resistant to the stress-induced inhibition (Fig. 3B, lower right two panels). A HyPer-fluorescence shift was also patent in cells expressing C173S HaloAQP8 after H_2O_2 addition (Fig. 3B, upper right two panels), albeit this mutant was not as efficient as

58

AQP8 C53S in rescuing the entry of H_2O_2 into heat-stressed HeLa cells (about 90% and 30% of the H_2O_2 transported by unstressed cells, respectively).
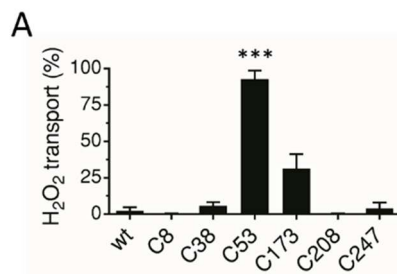
Fig. 3. The expression of AQP8 mutants impacts H_2O_2 and water transport. A. Quantification of H_2O_2 transport after heat stress in HeLa cells expressing diverse AQP8 mutants at 90 seconds of addition of 50µM of H_2O_2. The data are normalized to the cells expressing wt recombinant protein in control conditions ±SEM.
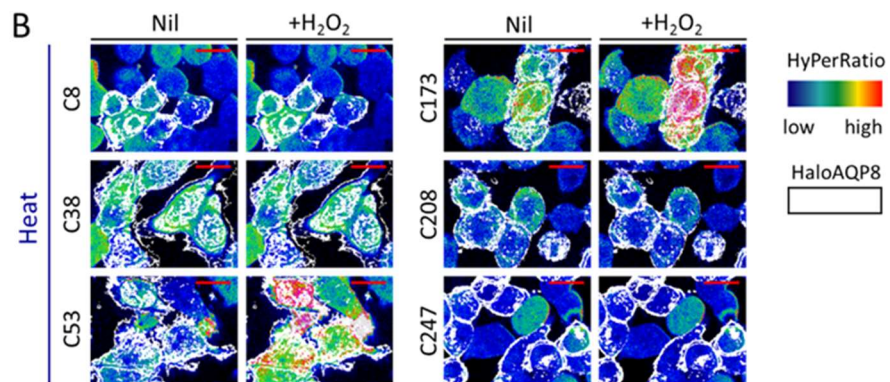
B. Frames extracted from a representative video out of ≥3 similar experiments, showing the kinetics of H_2O_2 import into HeLa cells stably expressing HyPerCyto (ratio in pseudo-colour) and transfected with each of the six single cysteine AQP8 mutants. See legend to Fig. 2A for more details.

Stress inhibits also the AQP8-dependent transport of water

Like other aquaporins, AQP8 can transport water (22). Their expression allows fast changes in the cell volume upon exposure to osmotic gradients, which correspond to the kinetics of water transport across the plasma membrane (48). We therefore measured water fluxes in HeLa cells stably expressing HaloAQP8 wt or the C53S mutant by stopped-flow experiments (Fig. 3C). Staining with Halo ligands confirmed that ≥60% of the cells analysed expressed the transgenes (data not shown). In agreement with our results on H_2O_2 import (Fig. 3A), water fluxes were similar in the two transfectants under control conditions (Fig. 3C, white bars). Remarkably, heat stress had a strong inhibitory effect on cells expressing HaloAQP8 wt, but not in C53S transfectants (Fig. 3C, black bars). Indeed, the latter were able to import water after stress as efficiently as in control conditions, suggesting that in HeLa cells, AQP8 is the main, if not the sole, target of the stress-mediated water transport inhibition. This observation is further supported by the fact that, in contrast with what observed before for H_2O_2 transport, water transport was only partially inhibited in AQP8 wt-expressing HeLa cells, which express other water-transporting members of the AQP family not bearing the regulatory C53 residue, i.e. AQP1 and

AQP4 (data not shown). Noteworthy, a short pre-treatment with DTT was sufficient to restore permeability to water in cells expressing the stress-sensitive HaloAQP8 wt (Fig. 3C, grey bars) as observed when analysing H_2O_2 transport.
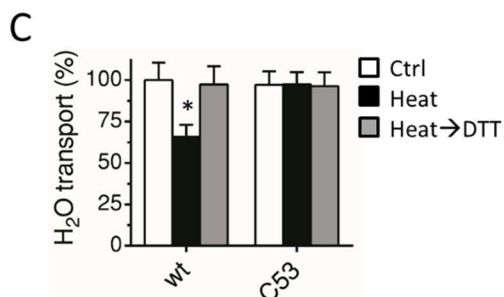
Fig. 3C. Quantification of osmotic water permeability measured in stable wt- or C53S-expressing HeLa cells in control conditions (white bars) or after heat stress either with (grey bars) or without (black bars) a short treatment of DTT performed immediately before of the analysis. Values are means of the initial rate constant (K) of cell volume changes, expressed as percentage of control cells ±SEM of 10-15 single shots for each of ≥3 different experiments.

Thus, stress-induced, redox-based mechanism(s) involving AQP8 inhibit the transport not only of H_2O_2, but also of water.

Mechanisms of AQP8 inhibition

Several mechanisms have been proposed to modulate transport through aquaporins, including oxidative gating and phosphorylation-dependent internalisation from the plasma membrane (25,43,47,59). We first considered the possible role of the latter in preventing AQP8-dependent transport. Unfortunately, our efforts to obtain trustworthy AQP8-specific antibodies were unsuccessful. As a consequence, we followed the movements of

61

HaloAQP8 by total internal reflection microscopy (TIRF) assays (3). By restricting the excitation to 90nm below the plasma membrane, this technology allows visualising only the basal region of cells adhered to glass slides. Intense fluorescence was detected in control cells, implying the presence of abundant HaloAQP8 molecules in the basal membrane. However, no significant differences could be recorded between control and heat-stressed cells (Fig. S4A). As the resolution of TIRF cannot formally exclude AQP8 internalisation, we generated a recombinant AQP8 protein in which a myc tag was inserted in the first extracellular loop (HaloAQP8 myc-out). The capability of this protein to transport water or H_2O_2 was verified in yeast (Fig. S3A and B). As revealed by quantitative cytofluorimetric analyses, the binding of myc-specific antibodies was not significantly perturbed upon exposure of HeLa transfectants to heat-shock (Fig. S4B). Taken together, these data indicated that the stress-induced inhibition of H_2O_2 and water transport is not due to internalisation of AQP8.

In view of the critical role of cysteines 53 and, to a lesser extent 173, we then sought evidence for redox modifications of the channel proteins. Non-reducing gels did not show proof of inter- or intra-chain disulphide bonds (Fig. S5A). Dimedone-based chemical probes (41,46) were used then to verify whether C53 was a target of sulphenylation. Although the amount of sulphenylated proteins

increased in cells treated with increasing concentrations of H_2O_2 (Fig. S5B), we could not obtain compelling evidence for oxidative modifications directly or indirectly impacting AQP8 (Fig. S5B and C). Noteworthy, a clear increase in the amount of intracellular sulphenylated proteins was evident in cells exposed to elevated temperature (Fig. S5C). This increase was less pronounced in cells expressing C53S.

Inhibition of AQP8-mediated transport determines cell fate after stress

Whether stress culminates in survival or death is determined by different factors, such as its intensity and duration, the cell type and other environmental cues (16). To ascertain whether AQP8-mediated transport can impact the cellular responses to stress, we compared several key physiological parameters in HeLa cells stably expressing HaloAQP8 wt or the C53S mutant (Fig. 4). Crystal violet-based clonogenic assays were used to measure proliferation and/or cell survival as counting the number and size of colonies obtained after plating cells before or after exposure to stress provides an estimate of stress resistance. Consistent with the previous results, no significant differences were observed when HaloAQP8 wt or C53S transfectants were cultured in control conditions.

However, the expression of the non-inhibitable AQP8 variant (C53S) rendered cells more able to survive to a severe heat stress than did wt channels (Fig. 4A).

Fig. 4A. Clonogenic assays comparing the ability of stable HaloAQP8 wt- or C53S-expressing HeLa cells to form clonal colonies before and after heat stress. Wells are the result of 2-fold serial dilutions to allow visualization of single-cell derived colonies. Results are represented as percentage of surviving colonies. Average of 3 experiments ±SEM.
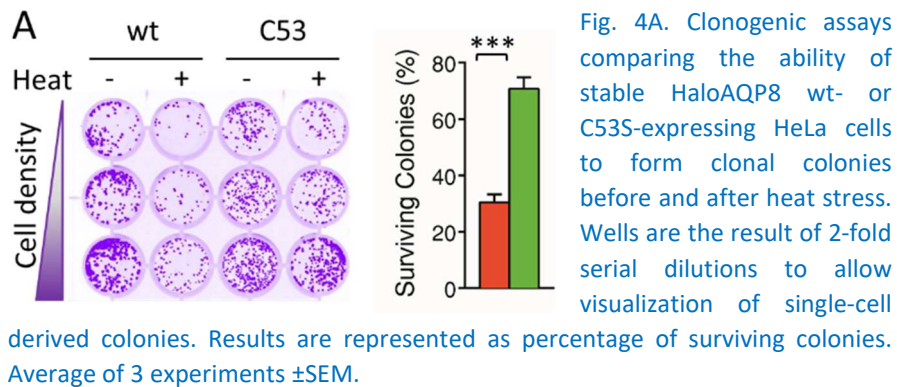
The C53S transfectants yielded about 70% of the colonies obtained by plating unstressed cells, whilst only 30% were recovered in cells expressing HaloAQP8 wt. Noteworthy, similar percentages of colonies were obtained at the three different cell concentrations, arguing against cell cooperativity in the resistance to stress. The size of colonies roughly depends on the number of divisions that a cell undergoes after having successfully attached to the plate. C53S-expressing cells formed slightly but significantly larger colonies than cells expressing the wt protein (Fig. 4B).
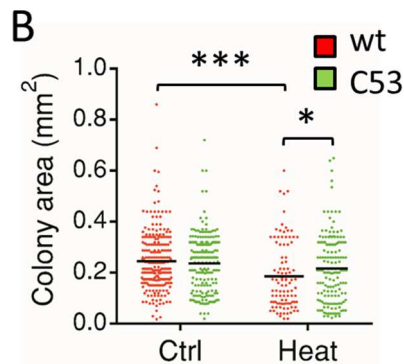
Fig. 4B. Measurement of colony area distribution in both AQP8 wt and C53S-expressing HeLa cells before and after the stress. Each dot is single colony and their area is displayed in mm^2.

Thus, maintaining open AQP8 channels confers adaptive advantages, allowing cells to grow also when they are subjected to harsh conditions.

It is generally accepted that radiotherapy, as well as most chemotherapeutic drugs, kill neoplastic cells by inducing a lethal oxidative stress (54,60). To investigate whether C53S-expression confers a surviving advantage to cells exposed to established anti-tumour therapies, we performed clonogenic assays after either X-irradiation or treatment with arsenic trioxide (As2O3). As shown in Figs. 4C and D, cells expressing AQP8 C53S are more resistant to either treatment than the wt-expressing ones.
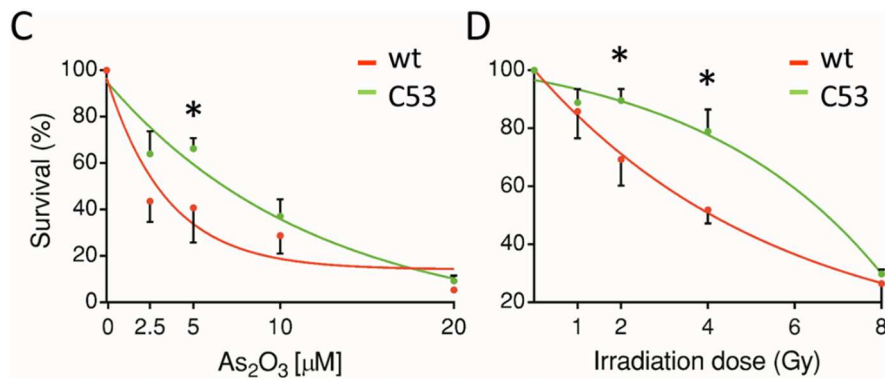
Fig. 4. Expression of C53S AQP8 confers stress-resistance to HeLa cells
C. Quantification of the clonogenic capacity of stable HaloAQP8 wt and C53S-expressing HeLa cells after 7 days from irradiation with different doses. Data are represented as percentage of surviving colonies with respect to the number of colonies grown in control conditions ±SEM. D. Quantification of the clonogenic capacity of stable HaloAQP8 wt and C53S-expressing HeLa cells after 7 days from a 24h-treatment with the indicated doses of arsenic trioxide. Data are represented as in C.

Therefore, dysregulation of AQP8 permeability may represent a protective mechanism activated by cells against endogenous or exogenous stressful stimuli.

Expression of C53S counteracts stress-induced growth arrest

The smaller size of the colonies recovered after heat-shock (see Fig. 4B) is in line with the notion that severe stresses cause transient growth arrest (10). To further investigate the role of AQP8,

we compared cells expressing wt or C53S variants for their efficiency in replenishing an empty territory (Fig. 5A and supplementary movies SM3-6). In principle, these 'gap filling' assays measure the combined rates of cell division and motility, but owing to the proliferative capabilities of HeLa cells, the former prevail in our experimental setting, despite the use of low serum concentrations. Also in these experiments, no significant differences were observed between untreated wt- and C53S-expressing cells (see quantifications in Fig. 5A). Instead, after heat stress, gap closure started sooner and was significantly more efficient in cells expressing C53S, strongly suggesting that these cells were less sensitive to growth arrest in response to stress.
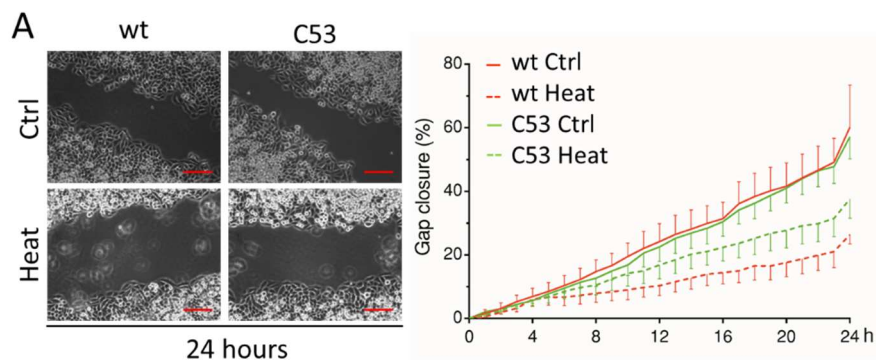
Fig. 5. AQP8 inhibition by stress causes reversible growth arrest
A. The images show frames of a representative video taken at time 0 or after 24h of culture at 37°C in which HaloAQP8 wt- or AQP8 C53S-expressing cells fill a 500µm gap, before or after a 3-hour heat stress. Scale bars correspond to 200µm. The results of ≥3 independent experiments are averaged on the right panel and represented as percentage of gap closure against time ±SEM.

Cell cycle analyses confirmed that AQP8 wt expressing cells were arrested in S phase (Fig. 5B, left panel). In contrast, the consequent increase in the S/G2 ratio was not observed in cells expressing the non-inhibitable AQP8 C53S mutant (Fig. 5B, right panel). Stable transfectants producing AQP8 wt recombinant proteins were able to resume growth after incubation at 37°C, indicating that the stress-derived proliferative block is reversible and can be overcome if the duration and/or strength of the stress is limited (Fig. 5B, left panel).
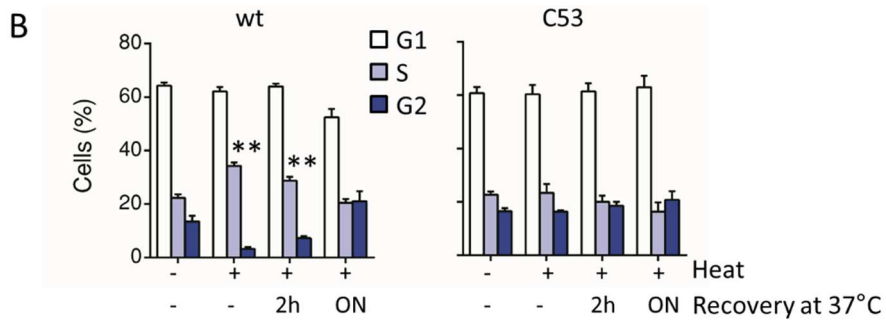
Fig. 5. AQP8 inhibition by stress causes reversible growth arrest B. Cell cycle phase distribution of AQP8 wt- or AQP8 C53S-expressing cells was compared before, immediately after heat stress or after further 2-hour or overnight incubation at 37°C, as indicated. Data are represented as the percentage of cells in each phase relative to the total cell number (average of 3 experiments ±SEM). ON, overnight.

Expression of AQP8 C53S limits stress-induced signalling and apoptosis.

Next, we investigated whether the expression of a non-inhibitable AQP8 protects cells from damage-induced cell death. Staining with Annexin-V (56) confirmed that expression of HaloAQP8 C53S conferred resistance to stress-induced apoptosis. The percentage of Annexin-V positive cells was lower in AQP8 C53S than in wt transfectants either immediately upon stress or after 24h of recovery at 37°C (Fig. 6A). These results mirror the lower efficiency of cells expressing AQP8 wt in gap filling assays (see quantification in Fig. 5A).
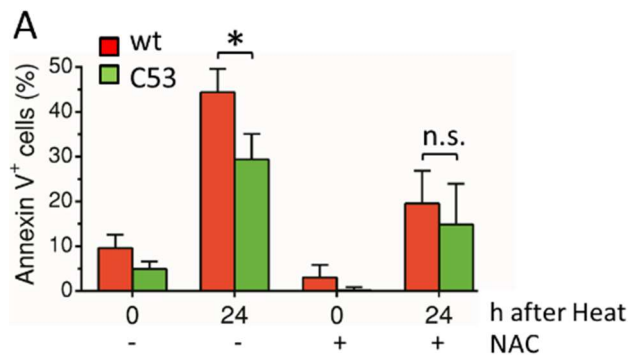
Fig. 6. AQP8 mutation in C53S influences stress-induced p38 phosphorylation A. Apoptosis in stable HaloAQP8 wt and C53S-expressing HeLa cells was monitored by Annexin-V staining, both immediately after inducing stress with or without 2mM NAC or after 24 hours of culture at 37°C. Data are expressed in percentage of Annexin-V positive cells ±SEM.

It is well established that different stress conditions cause phosphorylation of p38 via circuits involving ROS production (55). Accordingly, phosphorylation of p38 was increased over 4-fold upon heat stress in HeLa transfectants expressing wt AQP8 (Fig. 6B), but to a lesser extent in cells expressing C53S (compare lanes 1-4 and the quantification of 8 independent experiments on the right). As expected, addition of NAC during temperature stress prevented p38 phosphorylation (lanes 5-6). p38 phosphorylation was partially inhibited by NAC also in C53S mutants, possibly because only 60% of cells express the mutant protein. NAC was also able to reduce the differences in stress-induced apoptosis between AQP8 wt- and C53S-expressing cells (Fig. 6A). The higher activation of p38 in AQP8 wt cells correlate with the higher levels of apoptotic cells in stressed AQP8 wt-expressing cells, which is consistent with the known role of activated p38 as inducer of apoptosis (55). Along this line, the lower phosphorylation of p38 in AQP8 C53S-expressing cells is in accordance with their increased viability, in part providing a plausible explanation of the stress-resistant phenotype.
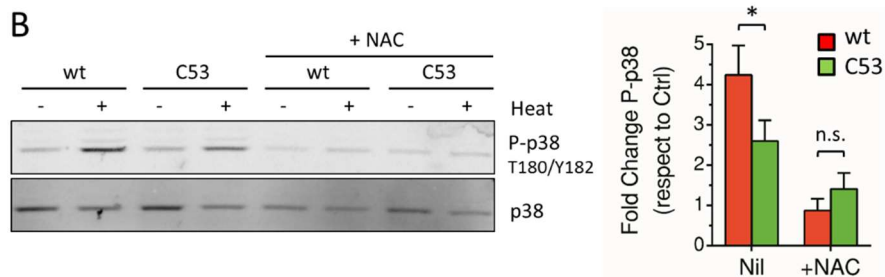
Fig. 6. AQP8 mutation in C53S influences stress-induced p38 phosphorylation B. The image shows a representative western blot analysis, showing changes in phosphorylation of p38 on whole HeLa cell extracts. Cells stably expressing HaloAQP8 wt or C53S mutant were cultured for 3h at 37 or 42°C with or without 2mM NAC. The right panel shows the quantification of phospho-p38 signal normalized against its total levels. Data are represented as fold change of p38 phosphorylation under stress conditions respect to the signal obtained with unstressed controls. Average of 8 experiments ±SEM.

Finally, we investigated whether AQP8 wt- and C53S-expressing cells differed in their sensitivity to hypoxia, a condition known to generate intracellular ROS (20). Cells expressing the non-inhibitable C53S mutant accumulated less HIF1α after 24h of culture at 1% oxygen (supplementary Fig. S6A), in consonance with the possibility that permeant AQP8 channels allow extrusion of excess ROS, limiting their accumulation (Figs. S4C and 7) and consequently HIF1α-stabilization. Expression of AQP8 C53S allowed cells to form bigger colonies when cultured after hypoxic stress (supplementary Fig. S6B), in line with our finding (Fig. 4B) that non-restrained H_2O_2 transport across the plasma membrane confers growth advantages.

71

Discussion

In this study, we show that the transport of both H_2O_2 and water through AQP8 is inhibited following diverse cellular stresses. Mutation of conserved cysteine residues in AQP8 confers resistance to stress. These observations, together with the finding that stress-mediated inhibition of AQP8 wt is prevented by reducing agents, sustain the redox-dependency of the regulatory mechanisms and provide key information on its target. Importantly, substitution of AQP8 cysteine residues does not impact protein activity in basal conditions. In contrast, the role of cysteines 53 and to a lesser extent 173 in modulating channel function under stress is compelling, albeit the underlying molecular mechanism(s) are only partially clarified. In fact, we demonstrated that different stresses converge in gating AQP8-mediated H_2O_2 transport via reversible modifications that preferentially target C53, directly or indirectly, and that DTT recovers the activity of stressed AQP8.

Because of their reactivity, only functional cysteines tend to be conserved during evolution (37,49). Thus, the presence of C53-like residues in AQP8 and AQP3, both known to transport H_2O_2 (6,39), points to relevant role(s) of these cysteines as redox regulatory switches. Computational predictions of the AQP8 structure

(obtained by homology modelling on the web server SWISS-MODEL (2) using the Uniprot entry for human AQP8 O94778) argue against the formation of disulphide bridges between C53 and C173. Accordingly, we did not detect intra- or inter-molecular disulphides linkages in AQP8 upon stress. However, the vicinity of R213 could favour C53 deprotonation rendering it a target of oxidative posttranslational modifications, such as sulphenylation, persulphidation or nitrosation. It is also possible that other molecules are modified so as to inhibit AQP8 in a C53-dependent fashion. Care was taken to exclude the internalization of AQP8, a mechanism utilized to remove other aquaporins from the plasma membrane and often induced by phosphorylation (43,47). Interestingly, also water transport through AQP8 wt, but not the C53S mutant, is inhibited by stress, and is recovered by exposure to reducing agents. The finding that also water fluxes are blocked by stress further confirms that redox-dependent circuits targeting C53 modulate AQP8 activity and excludes artifactual modifications of the redox-sensitive HyPerCyto probe due to H_2O_2 transport.

Our results also show that the stress-dependent gating of AQP8 has important consequences on the outcome of stress. Severe stress is followed by growth arrest and cell death, which limits proliferation of damaged or transformed cells. Stresses most often induce intracellular production of ROS. In this scenario, blocking

AQP8-dependent transport can provide a dual defence against oxidative damage: if the stress is mild, cells resume growth once the problem is solved; if it is harsh, cells undergo apoptosis, limiting the deleterious effects of ROS at the organism level. Cells expressing the non-inhibitable AQP8 C53S variant are more resistant to stress-induced growth arrest and ROS-triggered apoptosis, thus increasing survival. Stress-induced inhibition of water transport may also contribute to the cell responses to stresses: in this regard, a recent report shows that knocking-down AQP2 or AQP4 impacts water transport, resulting in an increase of survival in nematodes during hypotonic-anoxic stress (30).

Figure 7 summarizes a plausible scenario emerging from our results. In normal conditions (panel A), growth factor stimulation activates NOXes to produce H_2O_2 that reaches its cytosolic targets via AQP8 or other channels (6,39). The downstream protein kinase (PKs) circuits promote proliferation. In contrast, severe stress can induce apoptosis via the Ask1-p38 phosphorylation pathway (panel B). This is a ROS-dependent event (55), which can be prevented by the addition of NAC during stress. Gating of AQP8 impedes the bidirectional transport of H_2O_2 (1), yielding two important consequences. On the one hand, NOX-derived H_2O_2 cannot exert its growth-promoting effects. On the other, the excess of H_2O_2 produced intracellularly upon stress cannot be extruded through

AQP8, facilitating growth arrest and apoptosis. The expression of AQP8 C53S (panel C) allows cells to proliferate sooner after stress, because they can eliminate the excess of H_2O_2 and/or still uptake the molecule to promote growth.
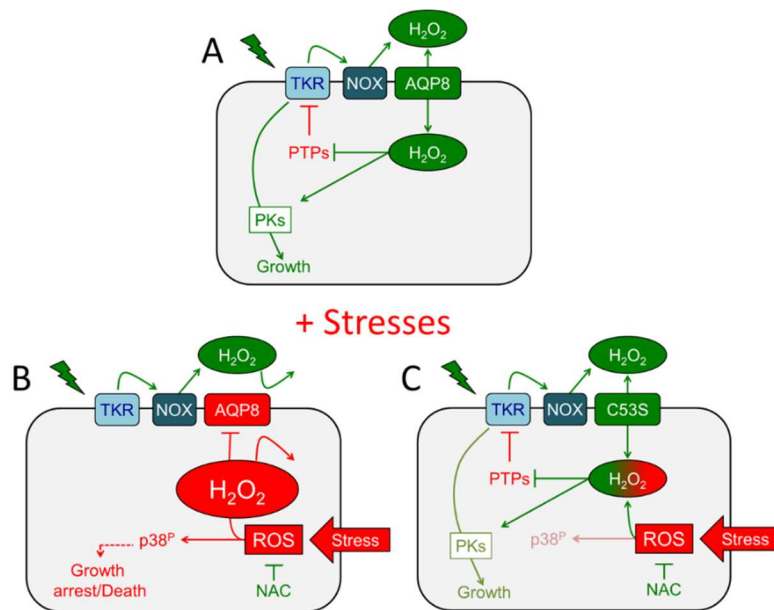
Fig. 7. Schematic model of H_2O_2 generation and transport during signalling. Membrane NOXes are activated upon tyrosine kinase receptor (TKR) engagement to produce H_2O_2, which enters the cells via AQP8 and amplifies downstream signalling (panel A). Under stress conditions, redox-dependent modifications inhibit H_2O_2 transport. Consequently, TKR-dependent phosphorylation cascades are down-regulated and apoptosis is promoted through ROS-dependent p38 activation (panel B). In contrast, the presence of non-inhibitable AQP8 (C53S) restores transport and leads to a stress-resistant phenotype (panel C). The stress-induced pro-apoptotic and H_2O_2 grow-promoting events are depicted in red and green, respectively, highlighting the dichotomous H_2O_2 effects.

To explain the coexistence of opposite redox pathways, the model implies that signalling outcome is controlled either by the dose or the duration of H_2O_2 production, and that topological and/or biochemical restraints limit its diffusion in the cytoplasm. Accordingly, it has been shown that receptor stimulation locally inactivates peroxiredoxin-1 (Prx1), spatially allowing H_2O_2-driven signal amplification (58). Although a fraction of AQP8 has been reported to localize to mitochondria (9), in our hands AQP8 silencing had little if any effect on H_2O_2 transport across the membrane of these organelles (6), suggesting that, in this context, stress does not target mitochondrial AQP8. Probes capable of dissecting H_2O_2 diffusion within the cytosol with improved resolution are needed to pursue this exciting line of investigation.

Cancer cells often experience stressful conditions, like hypoxia, low pH or starvation, that increase ROS production (33). In conflict with the traditional view, a number of recent studies have shown that while the increase of ROS often causes severe damage and cell death, overexpression of antioxidant defences is itself a direct promoter of cancer development and progression, and is responsible for drug resistance (14,19). Our clonogenic assays indicates that the inability of gating AQP8 upon stress, due to mutation in the C53 residue, not only causes increased survival, but also results in resistance to pro-oxidant anti-cancer treatments (45).

Also, the reduced sensitivity to hypoxia might be due to the capacity of stressed cells expressing a non-inhibitable AQP8 to get rid of excess ROS. In this way, ROS intracellular accumulation and the consequent cell damage and apoptosis are prevented. This is particularly important in cancer cells, where the ability to cope with elevated ROS levels limits many therapeutic approaches. Thus, characterising the mechanisms that inhibit the activity of AQP8 and identifying protocols to modulate them may open the way to unforeseen therapeutic opportunities.

Innovation

Our study reveals a novel layer of control in the redox signalling circuitry that impacts cell resistance to stress and survival. The key finding is that living cells can regulate the permeability of AQP8 to H_2O_2 and H2O, particularly during stress. The mechanism we disclose influences cell life-death decisions and can lead to the identification of drug targets with wide implications in tumour biology and other stress-related pathological conditions.

Material and Methods

Cell culture

HeLa cells were cultured in DMEM+Glutamax™-I medium (Life Technologies, Carlsbad, CA, U.S.A.) supplemented with 10% fetal bovine serum (FBS, EuroClone, Pero, Italy) and 5mg/ml penicillin-streptomycin (Lonza, Basel, Switzerland).

Plasmids, siRNAs and transfection procedures

The plasmid for expression of the HyPer probe targeted to the cytosol (HyPerCyto) was a generous gift of Dr. V. Belousov (IBCh, Moscow, Russian Federation), while silencing‑resistant Halo‑AQP8 (HaloAQP8) plasmid was generated as previously described (6), and used as template to create the single cysteine mutants by site-directed mutagenesis using the following primers: HaloAQP8 C8S: Fw - 5' GATAGCCATGTCTGAGCCTGAATTTGGC 3'; Rv - 5' GCCAAATTCAG-GCTCAGACATGGCTATC 3'; HaloAQP8 C38S: Fw 5' – GTGCAGCCATCT-CTGGTCGAAC 3'; Rv - 5' GTTCGACCAGAGATGGCTGCAC 3'; HaloAQP8 C53S: Fw 5' – CTTCATCGGGTCCCTGTCGGTC 3'; Rv - 5' GACCGACAGG-GACCCGATGAAG 3'; HaloAQP8 C173S: Fw 5' – CCTGGCTGTATCCATG-GGTGCC 3'; Rv - 5' GGCACCCATGGATACAGCCAGG 3'; HaloAQP8

C208S: Fw 5' – GTCTGGAGGCTCCATGAATCCC 3'; Rv - 5'
GGGATTCATGGAGCCTCCAGAC 3'; HaloAQP8 C247S: Fw 5' – GCTCAT-
TAGGTCCTTCATTGGAGATGGG 3'; Rv - 5' CCCATCTCCAATGAAGGAC-
CTAATGAGC 3'. All constructs were validated by sequencing.

The AQP8 insert including a myc tag in the first extracellular loop
(loop A) and flanked by two glycines to confer flexibility, was
synthetized by Eurofins Genomics (Ebersberg, Germany). HaloAQP8
myc-out-expressing plasmid was constructed by cloning the
synthetic insert into the pHTN-HaloTag® vector (Promega, Fitchburg,
WI, U.S.A.).

The AQP8-specific siRNA oligonucleotide (5' UUUGGCAAUGACAAG-

GCCA 3') and an unrelated control (Block‐it™) were purchased

from Ambion (Life Technologies, Carlsbad, CA, U.S.A.) and their
efficiency monitored by real-time RT-PCR as reported before (6).

For silencing experiments, 8x104 HyperCyto-expressing HeLa stable
transfectants (see below) were grown overnight in 6-well plates and
transfected with 90pmol of siRNA, using RNAiMAX lipofectamin
(Invitrogen, Carlsbad, CA, U.S.A.), according to the manufacturer
instructions. Cells were analysed for efficient silencing and used after
72h of transfection.

For experiments in which AQP8 expression was reconstituted
transiently using HaloAQP8-wt or the mutant recombinant proteins,

cells were first silenced for 24h and then transfected by Polyethylenimine (PEI) (8) and cultured for further 48h before imaging or biochemical analyses.

Generation of stable HeLa cell lines

HeLa transfectants stably expressing either HyPerCyto, HaloAQP8 wt or HaloAQP8 C53S, were generated by PEI transfection.

After 4 days in selection with 0.5 mg/ml of G418 (Sigma, Saint Louis, MO, U.S.A.), HeLa-HyPerCyto cells were directly sorted at 488 and 405nm using a MoFlo XDP cell sorter (Beckman Coulter, Pasadena, CA, U.S.A.). To obtain HeLa transfectants stably expressing HaloAQP8 wt- and HaloAQP8 C53S, cells were stained overnight with 2nM of HaloTag® TMR Direct Ligand (Promega), and sorted at 534nm.

Reagents and stress treatments

Tunicamycin, 2-deoxyglucose, and geldanamycin, were purchased from Sigma and used at the final concentrations of 10μg/ml for 4h, 6mM overnight, and 1μM overnight, respectively. Arsenic trioxide (As2O3) was a generous gift of Dr. Rosa Bernardi (IRCSS San Raffaele, Milan, Italy) and was incubated overnight at 37°C at the indicated concentrations.

Heat-shock treatment was performed by putting the plates, each containing 1.8x106 cells in 2% FBS medium, in a water bath set at 42°C with or without 10µM diphenyleneiodonium (DPI, Sigma) or with 2mM of N-Acetyl-cysteine (NAC, Sigma). After 3h at 42°C, cells were either lysed for biochemical assays or utilised for live imaging or FACS analyses.

Cell irradiation was performed in a Biobeam gamma-irradiator device (Gamma-service Medical Gmbh, Leipzig, Germany) using the pre-programmed manufacturer setups for the indicated gray (Gy).

Hypoxic conditions were induced either by culturing the cells for 3h or 24h at 1% oxygen in a hypoxia workstation (Invivo2 400, Ruskinn Technology, Ltd., Bridgend, South Wales, UK).

Imaging HyPer oxidation

To perform confocal live imaging experiments, 8x104 HyperCyto‑expressing HeLa cells were silenced and/or transfected on glass‑coverslips as described above. To identify HaloAQP8‑expressing cells, 2nM HaloTag® TMR Direct Ligand was added 24h after transfection. After 24h of culture with the fluorescent ligand, cells on coverslips were equilibrated in Ringer Buffer (RB: 140mM NaCl, 2mM CaCl2, 1mM MgSO4, 1.5mM K2HPO4, 10mM Glucose, pH 7.3) for

10min at room temperature (RT) prior to addition of 50µM of H_2O_2 or 5000U/ml extracellular catalase (both from Sigma), all freshly prepared in RB. When indicated, cells were equilibrated for 5min in RB and then treated 5min with 5mM DTT (Sigma) diluted in RB, washed and analysed.

Confocal images were collected every 2sec for 3min or more by dual excitation with a 488nm argon and a 405nm violet diode lasers. We used an Ultraview confocal laser-scanning microscope equipped with a 40X oil‑immersion lens (Perkin Elmer, Waltham, MA). The 488/405nm ratios were calculated by ImageJ software for ≥25 cells, averaged, and showed as mean fold change ratio plotted against time ±SEM. Alternatively, we averaged the data obtained after 90 seconds from H_2O_2 addition in the time-course experiments performed, and represented them as the percentage of H_2O_2 transport in stressed cells relative to the corresponding non-stressed cells to facilitate quantification and statistical analyses. At least three independent experiments were performed for each condition and/or mutant, except for non-stressed cells treated with NAC and mutant AQP8 C8S stressed cells, in which two different experiments gave almost identical results.

Stopped-flow experiments

Osmotic water permeability was measured by stopped-flow light scattering method as described before (28). Briefly, HeLa-HaloAQP8 wt and -HaloAQP8 C53S were seeded in culture flasks and grown until they reached approximately 90% of confluence. Cells were scraped off from the flasks and incubated at 37°C or 42°C for 3h and then treated with or without DTT. Then, cells were centrifuged, resuspended in Hank's solution and used for the osmotic permeability measurements. The analysis of cell swelling caused by exposure to a hypotonic gradient (150mosm/L) was performed on a stopped-flow apparatus (RX2000, Applied Photophysics, Leatherhead, UK) with a pneumatic drive accessory (DA.1, Applied Photophysics) coupled with a Varian Cary 50 spectrometer (Varian Australia Pty Ltd, Australia). Scattered light intensity at RT with a dead time of 6ms was recorded at a wavelength of 450nm. The time course of swelling was measured for 60s at the acquisition rate of one reading/0.0125s. The gradient caused osmotic water influx, cell swelling, and decreased light scattering. The initial rate constant of cells volume changes (k) was obtained by fitting the time course of light scattering with a one phase exponential decay up to 12s (GraphPad Prism 4.00, 2003). Results were represented as percentage of water transport under stressed conditions relative to

the transcript in control conditions ±SEM. All experiments were performed at least three times.

Clonogenic assay

The colony-forming ability of HeLa cells stably expressing HaloAQP8 wt or mutant C53S was assessed before or after stress. Briefly, cells were incubated in p35 plates at 37°C or 42°C, treated with arsenic trioxide, irradiated or cultured in 1% oxygen as described above, carefully counted and subsequently re-seeded in a 24-well plate at serial 2-fold dilutions starting from 5000 cells/well. Once plated, cells were placed at 37°C and incubated there for 7 days, a time corresponding to six potential cell divisions. After that period, cells were stained with crystal violet (44). Briefly, wells were washed once with PBS and cells were fixed with 2% Formaldehyde for 10min before permeabilisation with 2% methanol for 10min at RT. Then, the colonies were stained with 0.2% crystal violet for 5min at RT with gentle shaking. All of these reagents were from Sigma. Wells were washed with distilled water until a clear background was visible and left to dry at RT for 24h. Resulting colonies were scanned, counted, and their individual areas measured using the Colony counter ImageJ plug-in. The percentages of colonies formed by stressed cells were calculated relative to unstressed cells and the resulting averages are

shown ±SEM. When indicated, averaged data were interpolated with a non-linear regression (curve fit) analysis using Prism software. The area of individual colonies was represented using a distribution graph and expressed in mm2. For heat-shock and As2O3 treatment clonogenic assays, three independent experiments were performed, and n≥2 wells counted. For X-irradiation treatment, two different experiments gave consistent results, and n≥2 wells were counted. For the hypoxic treatment 1 experiment was performed and n≥3 wells were counted.

Apoptosis and cell cycle analyses

Subconfluent HeLa cultures (60-90%) were synchronized by culturing them in DMEM medium at low (2%) FBS concentrations for 3h at 42°C or 37°C with or without 2mM of NAC, and stained with Annexin-V following the protocol provided by the manufacturer (eBioscence, San Diego, CA, U.S.A.), soon after stress or 24h after recovery at 37°C. Data were acquired in a FACSCanto cytometer (BD Biosciences, San Jose, CA, U.S.A.), analyzed with FCS Express 4 Flow software (De Novo Software, Los Angeles, CA, U.S.A.) and represented as percentage of Annexin-V positive cells ±SEM. Experiments were performed at least three independent times. For cell cycle analyses, HaloAQP8 wt or HaloAQP8 C53S stable transfectants were stained

with propidium iodide (PI) immediately after stress or after either a 2h- or overnight-recovery at 37°C. Briefly, cells were washed twice with PBS without Ca++/Mg++ (EuroClone), fixed in 70% cold ethanol, incubated in 0.5ml of PBS without Ca++/Mg++ supplemented with 50μg/ml PI, 0.1% Sodium citrate, 50μg/ml ribonuclease A (all from Sigma) for 30min at RT and acquired in a FACSCanto cytometer (BD Biosciences). Data were analysed with the FCS Express 4 Flow software adjusting cell cycle profiles with the predefined autofit +S order=1 model, and represented as the percentage of cells in each phase relative to the total cell number ±SEM (mean of three experiments).

Gap filling assays

To perform this assay 6.5 x104 cells were seeded in each well of a μ-dish, 35mm, low, culture-insert plate (Ibidi, Martinsried, Germany). In these plates, a silicone dam of 500μm separates the plating space in two identical wells in which cells expressing the same or different AQP8 variants were cultured until confluence was reached. Cells were then incubated at either 37°C or 42°C in 2% FBS for 3h as described. After that period, dams were removed leaving a defined cell-free gap and the medium was increased to 5% FBS to stimulate gap filling. In some experiments 2nM TMR ligand was added to

identify transfectants expressing the protein of interest. Time-lapse 10X photographs of gap closure were taken each 5min for up to 24h using a Zeiss Axiovert S100 TV2 microscope (Zeiss, Oberkochen, Germany) equipped with a Hamamatsu OrcaII-ER camera (Hamamatsu City, Japan) and analysed using ImageJ or Oko-vision (Okolab, Ottaviano, NA, Italy) software. Five independent experiments were performed. Data are represented as the average percentage of gap closure plotted against time ±SEM.

Analysis of p38 activation and oxidative modifications of HaloAQP8

To follow p38 phosphorylation, subconfluent HeLa cultures (80-90%) stably expressing AQP8 wt or AQP8 C53S recombinant proteins were cultured in 2% FBS for 3h at 37°C or 42°C with or without 2mM NAC. Cells were then washed once with ice-cold PBS and scraped in a buffer containing 62.5mM Tris, 1% sodium dodecyl sulfate (SDS), 10% glycerol and 5mM DTT supplemented with freshly added protease inhibitors (Roche, Basel, Switzerland), 10mM N-Ethylmaleimide (NEM), 0.4mM Na_3VO_4 and 10mM NaF (all from Sigma). Cell lysates were sonicated twice at maximum intensity for 10min and aliquots resolved by standard SDS–PAGE electrophoresis followed by western blotting. The experiments were performed

eight times (p38 phosphorylation) or at least twice (NAC inhibition of p38 phosphorylation), giving similar results.

To analyse the changes in mobility of the HaloAQP8 recombinant protein, subconfluent HeLa cultures (80-90%) stably expressing AQP8 wt were washed once with ice-cold PBS and scraped in RIPA buffer (0.1% SDS, 1% NP40, 150mM NaCl, 50mM Tris, pH 7.4) supplemented with freshly added protease inhibitors, 10mM N-Ethylmaleimide (NEM), 0.4mM Na_3VO_4 and 10mM NaF. Whole HeLa cell lysates were centrifuged at 15000rpm 15min 4°C and used in standard reducing and non-reducing electrophoresis followed by western blotting. The experiments were repeated at least three times and gave similar results.

To investigate the sulphenylation of HaloAQP8 recombinant protein, subconfluent HeLa cultures (80-90%) transiently expressing myc-tagged AQP8 wt or C53S cells were either treated with the indicated concentrations of H_2O_2 or subjected to heat stress, washed with ice-cold PBS and scraped in RIPA buffer supplemented with freshly added protease inhibitors, 0.4mM Na_3VO_4, 10mM NaF and 250mM of the sulphenylation-detecting probe DCP-Bio1 (EMD Millipore, Billerica, MA, U.S.A.). Whole HeLa cell lysates were centrifuged at 15000rpm 15min 4°C and post-nuclear surnatant was quantified. 1mg of total protein was then used for immunoprecipitation with

homemade crosslinked anti-myc sepharose beads and eluted by boiling in SDS-containing sample buffer.

Antibodies and western blotting

Primary antibodies rabbit α-p38 and rabbit α-Phospho-p38 (Thr180/Tyr181) were purchased from Cell Signaling Technology (Danvers, Massachusetts, U.S.A.). Anti-Halo antibody was purchased from Promega. Rabbit α-HIF1a was from Cayman Chemical (Ann Harbor, MI, U.S.A.), while mouse anti-tubulin was from Sigma. Secondary antibodies α-rabbit AlexaFluor-488 or -AlexaFluor-647, were purchased from Invitrogen.

Images were acquired using a Typhoon FLA-9000 (GE HealthCare, Little Chalfont, U.K.), processed with ImageJ and densitometrically quantified when indicated by ImageQuant TL software (GE HealthCare, Little Chalfont, UK) ±SEM.

Water transport in yeast

S. cerevisiae wild type strain BY4741 was transformed with pYeDP60u mock vector or pYeDP60u containing indicated AQP8 variant encoding genes. Transformants were selected on synthetic medium (2% agar, 2% glucose, 50mM succinic acid/Tris base, pH 5.5, and 0.7% YNB (yeast nitrogen base) without amino acids (Difco,

Franklin Lakes, NJ, U.S.A.)) supplemented according to the auxotrophic requirements with histidine, methionine and leucine. Transformants were grown in 4ml of above described synthetic medium for 12h at 30°C and then transferred to 25ml of synthetic medium (2% glucose replaced by 2% galactose) for 36h at 30°C. After centrifugation, cells were resuspended in 3ml of 50mM KH_2PO_4 (pH 7.2) plus 6µl of 2-mercaptoethanol, and incubated for 15min at 30°C. 6ml of spheroplasting buffer (2.4M sorbitol, 50mM KH2PO4 (pH 7.2), 200mg bovine serum albumin, and 10mg of Zymolase 20T (Amsbio, Abingdon, UK)) was added to the cell suspension. The cells were incubated for 60min at 30°C. Following centrifugation, spheroplasts were washed once and finally resuspended in 10mM Tris/MES, pH 8.0, 5mM CaCl2, 50mM NaCl, and 1.8M sorbitol, at an A600 of 1.5. Kinetics of spheroplasts swelling was measured essentially as described previously (29). Cell osmotic water permeability was measured after exposing spheroplasts to hypoosmotic conditions (transfer from 1.8mM to 1.2mM sorbitol buffer). Volume changes were recorded via light scattering at an angle of 90° and 450nm using a fast kinetics instrument (SFM-3000, BioLogic, Claix, France) at 25°C with a dead time of 1.5ms. The time course of swelling was measured for 3s to 8s at the acquisition rate of one measurement/0.0005s. All data presented are averages of 15 to 30 trace recordings. The rate constant of the decrease of scattered light intensity is proportional

to the water permeability coefficient (9,26). Rate constants were calculated by fitting the curves using non-linear regression as described by Liu et al. (34). One-exponential functions were used for control spheroplasts and two-exponential functions were used for AQP8 and its variants expressing spheroplasts. At least two independent experiments were performed and gave consistent results.

Growth assay with hydrogen peroxide

For H_2O_2 growth toxicity assays, S. cerevisiae wild type strain BY4741 was transformed with pYeDP60u mock vector or pYeDP60u carrying indicated AQP8 variant encoding genes. Transformants were selected on synthetic medium as described above. The toxicity growth assay was performed as described by Bienert et al. (7). Transformants were spotted on synthetic medium supplemented with different concentrations of H_2O_2 and galactose instead of glucose as a carbon source necessary for the induction of the galactose inducible promoter. After 5-9 days of incubation at 30°C, differences in growth and survival in the different assays were recorded. All yeast growth assays were performed in three independent experiments with consistent results.

Total Internal Reflection Microscopy (TIRF)

In TIRF microscopy a thin layer close to the coverslip/sample interface is illuminated via a collimated beam impinging on the coverslip at an angle of incidence larger than the critical angle. The beam is totally reflected and only the evanescent field with a penetration depth of approximately 90nm excites the sample in the case of a glass-oil interface and an excitation wavelength of 534nm. This method is ideal for imaging thin layers, such as the plasma membrane of a cell, with minimum background fluorescence, and hence allow us to study AQP8 movements from the plasma membrane. Briefly, 3x105 HeLa cells stably expressing HaloAQP8 wt, were seeded 48h before the experiment and labelled with 2nM HaloTag® TMR Direct Ligand for 24h. TIRF images were collected every minute for 2h by excitation with a 530nm laser on a Widefield Leica SR GSD 3D TIRF (Leica, Wetzlar, Germany) equipped with an incubator set at 42°C with controlled CO_2 pressure, using a 63X oil ‑immersion lens. Two independent experiments were performed leading to identical results.

FACS analyses

To quantify AQP8 membrane expression by FACS, HeLa cells were transiently transfected with a plasmid driving the expression of

HaloAQP8 myc-out. 48h later, cells were incubated for 3h at 37°C or 42°C, detached from plates on ice and counted. 4x105 cells were stained with standard 9E10 anti-myc antibodies followed by detection with α-mouse AlexaFluor-488. Non-trasfected cells were used as negative control while binding of the TMR Halo ligand was used as transfection control. FACS analyses (≥3 experiments) were performed in a FACSCanto cytometer and surface expression represented using the FCS Express 4 Flow software.

Statistical analyses

Statistics were calculated either by using the two-sample t-Test for independent samples or the one-way ANOVA method for multiple samples. When using the latter, the Tukey HSD post-hoc test was also applied to find out which groups were significantly different from which others.In all cases statistical significance was defined as $P<0.05$ (*), $P<0.01$ (**) or $P<0.001$(***).

Acknowledgements

Author disclosure statement

The authors declare that they have no conflict of interest.

Author Contributions

IMF and SB performed and analysed the experiments. UL and CB performed and analysed the water transport experiments. GPB measured and analysed water permeability and H_2O_2 sensitivity in yeast. AR suggested the DPI experiments and helped in interpreting

the results. MB performed part of the experiment in figure 1A. RS conceived and supervised the study. IMF, SB, AR and RS wrote the manuscript.

References

1.   Agre P. The aquaporin water channels. Proc Am Thorac Soc 3: 5-13, 2006.
2.   Arnold K, Bordoli L, Kopp J, Schwede T. The SWISS-MODEL workspace: a web-based environment for protein structure homology modelling. Bioinformatics 22: 195-201, 2006.
3.   Axelrod D, Thompson NL, Burghardt TP. Total internal inflection fluorescent microscopy. J Microsc 129: 19-28, 1983.
4.   Bedard K, Krause KH. The NOX family of ROS-generating NADPH oxidases: physiology and pathophysiology. Physiol Rev 87: 245-313, 2007.
5.   Belousov VV, Fradkov AF, Lukyanov KA, Staroverov DB, Shakhbazov KS, Terskikh AV, Lukyanov S. Genetically encoded fluorescent indicator for intracellular hydrogen peroxide. Nat Methods 3: 281-6, 2006.
6.   Bertolotti M, Bestetti S, Garcia-Manteiga JM, Medrano-Fernandez I, Dal Mas A, Malosio ML, Sitia R. Tyrosine kinase signal modulation: a matter of H_2O_2 membrane permeability? Antioxid Redox Signal 19: 1447-51, 2013.
7.   Bienert GP, Moller AL, Kristiansen KA, Schulz A, Moller IM, Schjoerring JK, Jahn TP. Specific aquaporins facilitate the diffusion of hydrogen peroxide across membranes. J Biol Chem 282: 1183-92, 2007.
8.   Boussif O, Lezoualc'h F, Zanta MA, Mergny MD, Scherman D, Demeneix B, Behr JP. A versatile vector for gene and oligonucleotide transfer into cells in culture and in vivo: polyethylenimine. Proc Natl Acad Sci U S A 92: 7297-301, 1995.
9.   Calamita G, Ferri D, Gena P, Liquori GE, Cavalier A, Thomas D, Svelto M. The inner mitochondrial membrane has aquaporin-8 water

95

channels and is highly permeable to water. J Biol Chem 280: 17149-53, 2005.

10.   Campisi J, d'Adda di Fagagna F. Cellular senescence: when bad things happen to good cells. Nat Rev Mol Cell Biol 8: 729-40, 2007.

11.   Cenci S, Mezghrani A, Cascio P, Bianchi G, Cerruti F, Fra A, Lelouard H, Masciarelli S, Mattioli L, Oliva L, Orsi A, Pasqualetto E, Pierre P, Ruffato E, Tagliavacca L, Sitia R. Progressively impaired proteasomal capacity during terminal plasma cell differentiation. EMBO J 25: 1104-13, 2006.

12.   Chiarugi P, Pani G, Giannoni E, Taddei L, Colavitti R, Raugei G, Symons M, Borrello S, Galeotti T, Ramponi G. Reactive oxygen species as essential mediators of cell adhesion: the oxidative inhibition of a FAK tyrosine phosphatase is required for cell adhesion. J Cell Biol 161: 933-44, 2003.

13.   Clark CB, Rane MJ, El Mehdi D, Miller CJ, Sachleben LR, Jr., Gozal E. Role of oxidative stress in geldanamycin-induced cytotoxicity and disruption of Hsp90 signaling complex. Free Radic Biol Med 47: 1440-9, 2009.

14.   DeNicola GM, Karreth FA, Humpton TJ, Gopinathan A, Wei C, Frese K, Mangal D, Yu KH, Yeo CJ, Calhoun ES, Scrimieri F, Winter JM, Hruban RH, Iacobuzio-Donahue C, Kern SE, Blair IA, Tuveson DA. Oncogene-induced Nrf2 transcription promotes ROS detoxification and tumorigenesis. Nature 475: 106-9, 2011.

15.   DeYulia GJ, Jr., Carcamo JM, Borquez-Ojeda O, Shelton CC, Golde DW. Hydrogen peroxide generated extracellularly by receptor-ligand interaction facilitates cell signaling. Proc Natl Acad Sci U S A 102: 5044-9, 2005.

16.   Fulda S, Gorman AM, Hori O, Samali A. Cellular stress responses: cell survival and cell death. Int J Cell Biol 2010: 214074, 2010.

17.   Geiszt M, Leto TL. The Nox family of NAD(P)H oxidases: host defense and beyond. J Biol Chem 279: 51715-8, 2004.

18.   Hara-Chikuma M, Satooka H, Watanabe S, Honda T, Miyachi Y, Watanabe T, Verkman AS. Aquaporin-3-mediated hydrogen peroxide transport is required for NF-kappaB signalling in keratinocytes and development of psoriasis. Nat Commun 6: 7454, 2015.

19.   Harris IS, Treloar AE, Inoue S, Sasaki M, Gorrini C, Lee KC, Yung KY, Brenner D, Knobbe-Thomsen CB, Cox MA, Elia A, Berger T, Cescon DW, Adeoye A, Brustle A, Molyneux SD, Mason JM, Li WY, Yamamoto K,

Wakeham A, Berman HK, Khokha R, Done SJ, Kavanagh TJ, Lam CW, Mak TW. Glutathione and thioredoxin antioxidant pathways synergize to drive cancer initiation and progression. Cancer Cell 27: 211-22, 2015.

20.   Hielscher A, Gerecht S. Hypoxia and free radicals: role in tumor progression and the use of engineering-based platforms to address these relationships. Free Radic Biol Med 79: 281-91, 2015.

21.   Holmstrom KM, Finkel T. Cellular mechanisms and physiological consequences of redox-dependent signalling. Nat Rev Mol Cell Biol 15: 411-21, 2014.

22.   Ishibashi K, Kuwahara M, Kageyama Y, Tohsaka A, Marumo F, Sasaki S. Cloning and functional expression of a second new aquaporin abundantly expressed in testis. Biochem Biophys Res Commun 237: 714-8, 1997.

23.   Jiang F, Zhang Y, Dusting GJ. NADPH oxidase-mediated redox signaling: roles in cellular stress response, stress tolerance, and tissue repair. Pharmacol Rev 63: 218-42, 2011.

24.   Kasanuma Y, Watanabe C, Kim CY, Yin K, Satoh H. Effects of mild chronic heat exposure on the concentrations of thiobarbituric acid reactive substances, glutathione, and selenium, and glutathione peroxidase activity in the mouse liver. Tohoku J Exp Med 185: 79-87, 1998.

25.   Kim YX, Steudle E. Gating of aquaporins by light and reactive oxygen species in leaf parenchyma cells of the midrib of Zea mays. J Exp Bot 60: 547-56, 2009.

26.   Kozono D, Ding X, Iwasaki I, Meng X, Kamagata Y, Agre P, Kitagawa Y. Functional expression and characterization of an archaeal aquaporin. AqpM from methanothermobacter marburgensis. J Biol Chem 278: 10649-56, 2003.

27.   Kultz D. Molecular and evolutionary basis of the cellular stress response. Annu Rev Physiol 67: 225-57, 2005.

28.   Laforenza U, Cova E, Gastaldi G, Tritto S, Grazioli M, LaRusso NF, Splinter PL, D'Adamo P, Tosco M, Ventura U. Aquaporin-8 is involved in water transport in isolated superficial colonocytes from rat proximal colon. J Nutr 135: 2329-36, 2005.

29.   Laize V, Gobin R, Rousselet G, Badier C, Hohmann S, Ripoche P, Tacnet F. Molecular and functional study of AQY1 from Saccharomyces cerevisiae: role of the C-terminal domain. Biochem Biophys Res Commun 257: 139-44, 1999.

30.   LaMacchia JC, Roth MB. Aquaporins-2 and -4 regulate glycogen metabolism and survival during hyposmotic-anoxic stress in Caenorhabditis elegans. Am J Physiol Cell Physiol 309: C92-6, 2015.

31.   Li Y, Trush MA. Diphenyleneiodonium, an NAD(P)H oxidase inhibitor, also potently inhibits mitochondrial reactive oxygen species production. Biochem Biophys Res Commun 253: 295-9, 1998.

32.   Lim EJ, Heo J, Kim YH. Tunicamycin promotes apoptosis in leukemia cells through ROS generation and downregulation of survivin expression. Apoptosis 20: 1087-98, 2015.

33.   Liou GY, Storz P. Reactive oxygen species in cancer. Free Radic Res 44: 479-96, 2010.

34.   Liu K, Nagase H, Huang CG, Calamita G, Agre P. Purification and functional characterization of aquaporin-8. Biol Cell 98: 153-61, 2006.

35.   Lo Conte M, Carroll KS. The redox biochemistry of protein sulfenylation and sulfinylation. J Biol Chem 288: 26480-8, 2013.

36.   Marinho HS, Real C, Cyrne L, Soares H, Antunes F. Hydrogen peroxide sensing, signaling and regulation of transcription factors. Redox Biol 2: 535-62, 2014.

37.   Marino SM, Gladyshev VN. Proteomics: mapping reactive cysteines. Nat Chem Biol 7: 72-3, 2011.

38.   Meng TC, Fukada T, Tonks NK. Reversible oxidation and inactivation of protein tyrosine phosphatases in vivo. Mol Cell 9: 387-99, 2002.

39.   Miller EW, Dickinson BC, Chang CJ. Aquaporin-3 mediates hydrogen peroxide uptake to regulate downstream intracellular signaling. Proc Natl Acad Sci U S A 107: 15681-6, 2010.

40.   Mossuto MF, Sannino S, Mazza D, Fagioli C, Vitale M, Yoboue ED, Sitia R, Anelli T. A dynamic study of protein secretion and aggregation in the secretory pathway. PLoS One 9: e108496, 2014.

41.   Nelson KJ, Klomsiri C, Codreanu SG, Soito L, Liebler DC, Rogers LC, Daniel LW, Poole LB. Use of dimedone-based chemical probes for sulfenic acid detection methods to visualize and identify labeled proteins. Methods Enzymol 473: 95-115, 2010.

42.   Nerini-Molteni S, Ferrarini M, Cozza S, Caligaris-Cappio F, Sitia R. Redox homeostasis modulates the sensitivity of myeloma cells to bortezomib. Br J Haematol 141: 494-503, 2008.

43.   Nielsen S, Chou CL, Marples D, Christensen EI, Kishore BK, Knepper MA. Vasopressin increases water permeability of kidney collecting duct by inducing translocation of aquaporin-CD water channels to plasma membrane. Proc Natl Acad Sci U S A 92: 1013-7, 1995.

44.   Ovalle S, Gutierrez-Lopez MD, Olmo N, Turnay J, Lizarbe MA, Majano P, Molina-Jimenez F, Lopez-Cabrera M, Yanez-Mo M, Sanchez-Madrid F, Cabanas C. The tetraspanin CD9 inhibits the proliferation and tumorigenicity of human colon carcinoma cells. Int J Cancer 121: 2140-52, 2007.

45.   Pani G, Galeotti T, Chiarugi P. Metastasis: cancer cell's escape from oxidative stress. Cancer Metastasis Rev 29: 351-78, 2010.

46.   Paulsen CE, Truong TH, Garcia FJ, Homann A, Gupta V, Leonard SE, Carroll KS. Peroxide-dependent sulfenylation of the EGFR catalytic site enhances kinase activity. Nat Chem Biol 8: 57-64, 2012.

47.   Potokar M, Stenovec M, Jorgacevski J, Holen T, Kreft M, Ottersen OP, Zorec R. Regulation of AQP4 surface expression via vesicle mobility in astrocytes. Glia 61: 917-28, 2013.

48.   Preston GM, Carroll TP, Guggino WB, Agre P. Appearance of water channels in Xenopus oocytes expressing red cell CHIP28 protein. Science 256: 385-7, 1992.

49.   Putker M, Vos HR, van Dorenmalen K, de Ruiter H, Duran AG, Snel B, Burgering BM, Vermeulen M, Dansen TB. Evolutionary acquisition of cysteines determines FOXO paralog-specific redox signaling. Antioxid Redox Signal 22: 15-28, 2015.

50.   Reth M. Hydrogen peroxide as second messenger in lymphocyte activation. Nat Immunol 3: 1129-34, 2002.

51.   Santos CX, Tanaka LY, Wosniak J, Laurindo FR. Mechanisms and implications of reactive oxygen species generation during the unfolded protein response: roles of endoplasmic reticulum oxidoreductases, mitochondrial electron transport, and NADPH oxidase. Antioxid Redox Signal 11: 2409-27, 2009.

52.   Shaughnessy DT, McAllister K, Worth L, Haugen AC, Meyer JN, Domann FE, Van Houten B, Mostoslavsky R, Bultman SJ, Baccarelli AA, Begley TJ, Sobol RW, Hirschey MD, Ideker T, Santos JH, Copeland WC, Tice RR, Balshaw DM, Tyson FL. Mitochondria, energetics, epigenetics, and cellular responses to stress. Environ Health Perspect 122: 1271-8, 2014.

53.   Shutt DC, O'Dorisio MS, Aykin-Burns N, Spitz DR. 2-deoxy-D-glucose induces oxidative stress and cell killing in human neuroblastoma cells. Cancer Biol Ther 9: 853-61, 2010.

54.   Tiligada E. Chemotherapy: induction of stress responses. Endocr Relat Cancer 13 Suppl 1: S115-24, 2006.

55.   Tobiume K, Matsuzawa A, Takahashi T, Nishitoh H, Morita K, Takeda K, Minowa O, Miyazono K, Noda T, Ichijo H. ASK1 is required for sustained activations of JNK/p38 MAP kinases and apoptosis. EMBO Rep 2: 222-8, 2001.

56.   Vermes I, Haanen C, Steffens-Nakken H, Reutelingsperger C. A novel assay for apoptosis. Flow cytometric detection of phosphatidylserine expression on early apoptotic cells using fluorescein labelled Annexin V. J Immunol Methods 184: 39-51, 1995.

57.   Vieceli Dalla Sega F, Zambonin L, Fiorentini D, Rizzo B, Caliceti C, Landi L, Hrelia S, Prata C. Specific aquaporins facilitate Nox-produced hydrogen peroxide transport through plasma membrane in leukaemia cells. Biochim Biophys Acta 1843: 806-14, 2014.

58.   Woo HA, Yim SH, Shin DH, Kang D, Yu DY, Rhee SG. Inactivation of peroxiredoxin I by phosphorylation allows localized H_2O_2 accumulation for cell signaling. Cell 140: 517-28, 2010.

59.   Ye Q, Steudle E. Oxidative gating of water channels (aquaporins) in corn roots. Plant Cell Environ 29: 459-70, 2006.

60.   Zhou S, Ye W, Shao Q, Zhang M, Liang J. Nrf2 is a potential therapeutic target in radioresistance in human cancer. Crit Rev Oncol Hematol 88: 706-15, 2013.

Supplementary data
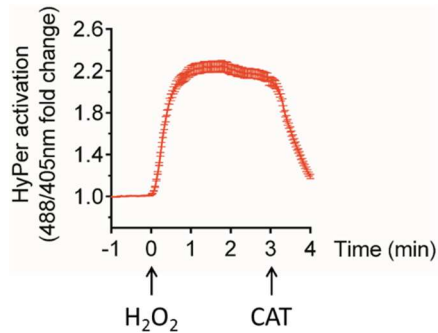
Fig. S1. *HyPerCyto* **detects mainly H$_2$O$_2$ imported through the plasma membrane**

Addition of extracellular catalase (CAT, 5000U/ml) after H$_2$O$_2$ exposure causes the rapid reduction of *HyPerCyto* by cytosolic antioxidant systems, indicating that continuous entry of exogenous H$_2$O$_2$ is needed to sustain re-oxidation of the sensor. These data also indicate that most if not all *HyPer* oxidation depends on exogenously added H$_2$O$_2$. The data represent the mean fold changes of the 488/405nm ratio measured by confocal laser scanning, plotted against time ± SEM.
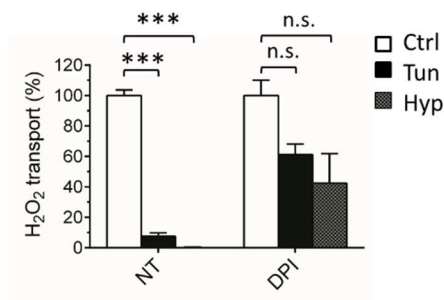
Fig. S2. DPI treatment partially prevents tunicamycin- and hypoxia-induced AQP8 blockade

Cells were subjected to tunicamycin or hypoxic treatment with or without 10μM DPI. The data were normalized to the uptake of DPI-treated unstressed cells. Average of 2 experiments ± SEM. NT, non-treated cells; Ctrl, control; Tun, Tunicamycin; Hyp, Hypoxia.
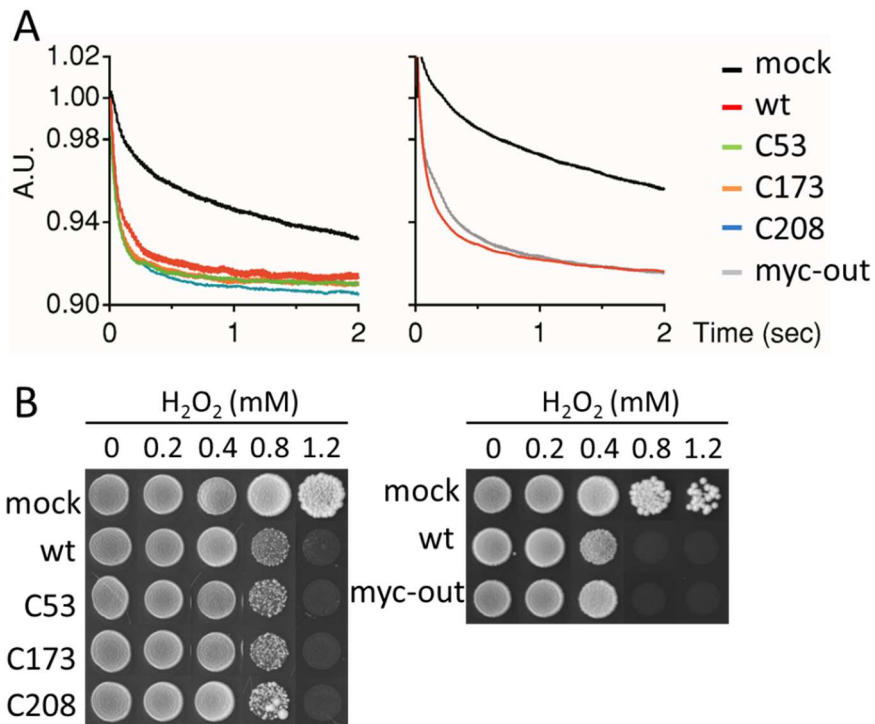
Fig. S3. Transport and survival of yeast expressing different human AQP8 mutants A. Water transport assays in yeasts by stopped-flow spectroscopy after a hypotonic shock. Spheroplasts from BY4741wt yeast cells, transformed with the mock vector pYeDP60u or pYeDP60u containing the indicated hAQP8 versions, were suspended in a 1.8M sorbitol buffer at an A600 of 1.5 and mixed in a fast kinetics instrument (SFM3000, Bio-Logic) with a hypotonic 1.2M sorbitol buffer of equal volume. Scattered 450nm light intensity was measured at 90° and with a photomultiplier connected to the PMS 250 control unit. Each line represents the average of 8-19 (left panel) or 42 (right panel) sample recordings, respectively. The averaging was automatically calculated by the Stopped-Flow Bio-Logic Software Bio-

Kine32. Data points are shown each 500μsec for 2sec. A representative experiment of three (left panel) or two (right panel) independent biological replications is displayed.

B. Yeast growth and survival assay on synthetic medium supplied with different concentrations of H_2O_2. BY4741wt yeast cells, transformed with the mock vector pYeDP60u or pYeDP60u containing the indicated hAQP8 versions, were spotted at an A600 of 2 on medium containing indicated concentrations of H_2O_2. Growth was recorded after 5-8 days at 30°C. All growth assays were replicated with consistent results in three independent experiments.
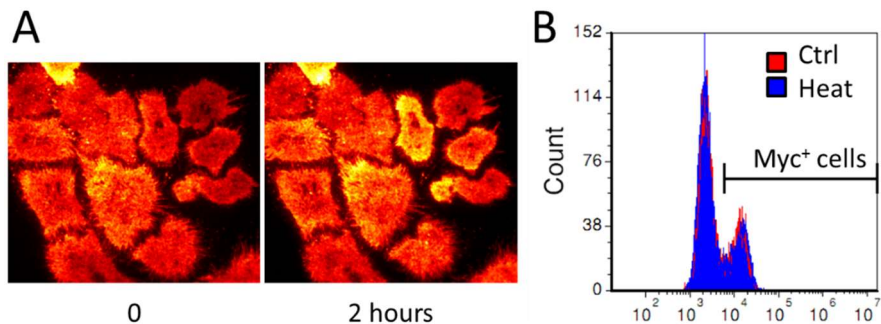
Fig. S4. Inhibition of H_2O_2 transport is not **due to internalization of HaloAQP8.** A. HeLa cells expressing HaloAQP8 wt were decorated with HaloTag® TMR Direct Ligand (in red), cultured at 42°C and 0.5% CO_2 and recorded by time-lapse TIRF microscopy focusing on the first 90nm from the basal membrane. The frames represent snaps at the beginning of the experiment or after 2 hours of culture. B. HeLa cells transiently expressing HaloAQP8 myc-out were stained with fluorescent anti-myc before (red) or after heat stress (blue) and analysed by FACS. Data are represented by

overlaying the 647nm signals in control or stress conditions. Cells expressing surface AQP8 are labelled as "Myc+ cells".
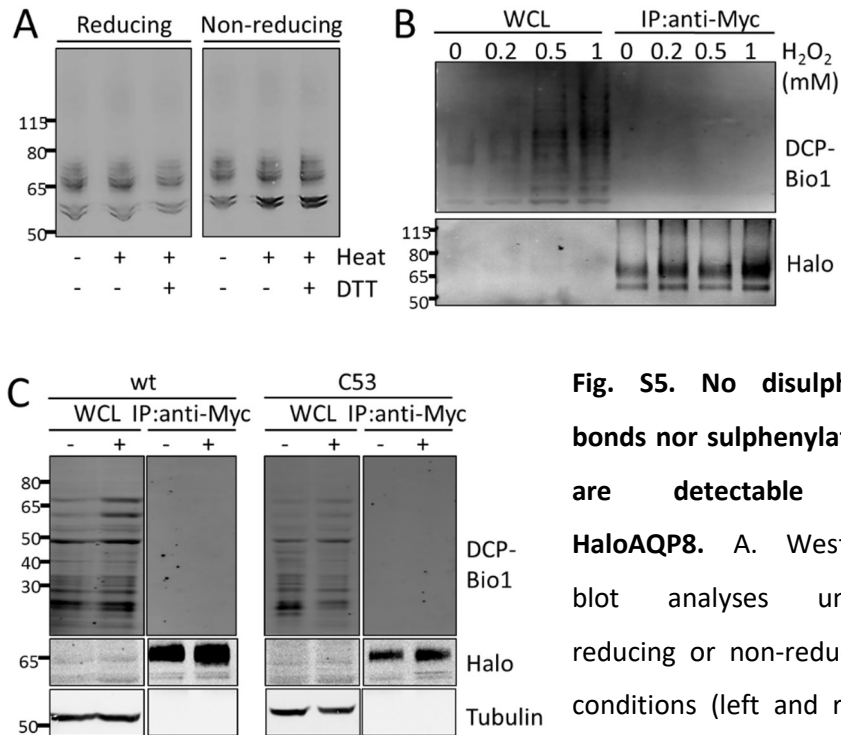
Fig. S5. No disulphide bonds nor sulphenylation are detectable in HaloAQP8. A. Western blot analyses under reducing or non-reducing conditions (left and right panels, respectively) do not reveal changes in the electrophoretic mobility of HaloAQP8 recombinant protein. The bands stained by anti-Halo correspond to HaloAQP8 non-glycosylated (a doublet of approximately 60-62 KDa) or glycosylated monomers (~71 KDa) and SDS-insoluble oligomers (~142 KDa). B. HeLa cells expressing myc-tagged HaloAQP8 were exposed to increasing amounts of H_2O_2 and treated during lysis in NP40 with a biotinylated probe designed to detect sulphenylated proteins (DCP-Bio 1). Aliquots of the lysates (WCL) and of the anti-myc immunoprecipitates were then resolved

electrophoretically and blotted to detect sulphenylated proteins (streptavidin-FITC, top panel) and HaloAQP8 (anti-Halo, lower panel).

C. HeLa cells expressing myc-tagged wt or C53S HaloAQP8 were heat stressed and lysed in the presence of DCP-Bio1 as in panel B. The same blot was then decorated with anti-tubulin (lower panel).
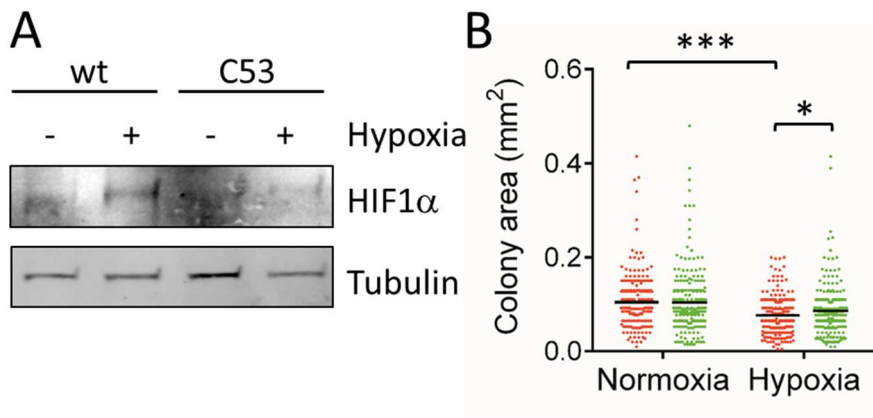
Fig. S6. Different sensitivity of wt and C53S AQP8 expressing cells to hypoxia A. Cells stably expressing AQP8 wt or C53S were cultured in hypoxic conditions (24 h at 1% oxygen), lysed and aliquots of the NP40 insoluble fraction decorated with anti HIF1α and anti-tubulin antibodies (top and bottom panels, respectively).

B. Measurement of colony area distribution in both AQP8 wt and C53S-expressing HeLa cells cultured in normoxic or hypoxic conditions for 24h and then for further 7 days at 37°C in normoxia. Each dot represents a single colony and their area is displayed in mm^2.

Movie SM1. The expression of a recombinant Halo-tagged AQP8 rescues H_2O_2 transport in silenced HyPerCyto-HeLa cells

Representative video (n≥3) showing the kinetics of exogenous H_2O_2 (50μM) entry into HeLa cells expressing *HyPerCyto* (ratio in pseudo-colour) and transfected with HaloAQP8 wt (white). The scale bar corresponds to 50μm.

Movie SM2. DTT pre-treatment rescues H_2O_2 transport in stressed HaloAQP8-positive cells

In this representative video (n≥3) cells were heat stressed and then treated for 5min with 5mM DTT before filming them as in Movie SM1.

Movie SM3. Gap filling HaloAQP8 wt in control conditions

Representative video (n≥3) showing the kinetics of gap closure by HeLa cells stably expressing HaloAQP8 wt filmed for 24h. The scale bars correspond to 200μm.

Movie SM4. Gap filling HaloAQP8 C53S in control conditions

Representative video (n≥3), as in SM3, of unstressed HeLa cells stably expressing HaloAQP8 C53S.

Movie SM5. Gap filling HaloAQP8 wt after 3h heat-shock at 42°C

This representative video (n≥3) clearly shows how heat stress slows down gap filling by HeLa cells stably expressing HaloAQP8 wt. See SM3 for details.

Movie SM6. Gap filling HaloAQP8 C53S after 3h heat-shock at 42°C

This representative video (n≥3), taken as in SM5, shows faster gap closure by heat-stressed HaloAQP8 C53S stable transfectants.

Chapter 3: Reversible inhibition of hydrogen peroxide transport by cysteine sulphydration of Aquaporin-8 upon cell stress

Stefano Bestetti[§], Iria Medraño-Fernandez[§], Mauro Galli, Andrea Orsi, Gerd P. Bienert, Anna Rubartelli and Roberto Sitia

[§]These authors contributed equally

Abstract

AQP8-mediated H_2O_2 transport allows efficient amplification of tyrosine kinase signalling, therefore influencing pathways frequently dysregulated under tumour progression. Besides, control of H_2O_2 cell permeability impacts life-death cell decisions in response to stress. Despite the important consequences of AQP8 gating, the precise biochemical modification that inhibits H_2O_2 transport still remains to be identified. We show here that the mechanism of regulation implies sulphydration of AQP8. Addition of an exogenous H_2S donor (NaHS) is sufficient to block H_2O_2 entry and dampen EGF receptor signalling, mimicking stress. Moreover, cells expressing non-inhibitable AQP8 mutants (e.g. C53S) are able to transport H_2O_2 also upon H_2S-mediated inhibition. Stress-induced blockade of transport requires cystathionine-β- synthase, a key enzyme in the transulphuration pathway. These findings identify a novel circuit modulating the strength and duration of key signalling pathways based on AQP8 regulation by sulphydration.

Introduction

Cysteine thiols can undergo many modifications (-SS-, -SOH, -SO2H, -SNO, -SSH) providing versatile regulatory switches for tuning protein activity and stability. Short-lived molecular species such as nitric oxide (NO) and hydrogen peroxide (H_2O_2) have emerged as essential endogenously synthesized modulators of these redox-induced pathways (1, 2). Recently, an additional gaseous compound, hydrogen sulphide (H_2S), has been added to the growing list of second messengers (3, 4). Long known to be produced by living cells, H_2S has been involved in various physiological processes, including cell viability, synaptic potentiation, blood vessel relaxation, platelet aggregation and inflammation (5). In mammals, H_2S biosynthesis depends mainly on the activity of two pyridoxal phosphate-dependent enzymes, cystathionine-β-synthase (CBS) and cystathionine-γ-lyase (CSE). Both are key steps in the transulphuration pathway converting methionine to cysteine (6). H_2S released through this pathway reacts with cysteine residues, when oxidised (7, 8), in target proteins leading to the formation of persulphides (R-S-SH), a process also referred to as sulphydration (3). Several reports suggest that both CBS and CSE contribute to maintain cellular redox homeostasis (9-11), their levels and/or activity being

affected by stress (12-15). Accordingly, H_2S can suppress oxidative stress and protect from cell death (16, 17), while deficiency of H_2S promotes cellular aging (18, 19). These observations led to suggest that -owing to its reversibility- persulphidation may protect protein function from irreversible oxidation (20). Thus, identifying specific H_2S targets and clarifying their roles are issues of great pathophysiological relevance.

Aquaporins (AQPs) are membrane channels that facilitate transport of water or other small solutes. AQP8 is an efficient H_2O_2 transporter (21) that can be gated by reversible redox-dependent modifications induced by different cellular stresses. Cysteine 53, and to lesser extent cysteine 173 were identified as the targets, but the biochemical nature of the modification(s) remain to be determined (22).

Considering that stress induces ROS (23-25) and H_2S production (26, 27), we surmised that sulphydration could be the modification that reversibly blocks AQP8. Accordingly, we found that addition of exogenous H_2S is sufficient to block AQP8-dependent H_2O_2 transport and downstream EGF-induced H_2O_2-mediated signalling. Furthermore, silencing of CBS prevents the inhibition. Finally, we identified a sequential modification of the C53 residue that appeared to be first sulphenylated and then sulphydrated after cell stress.

These findings identify a novel molecular mechanism for regulating signal intensity during stress, based on the H_2S –dependent AQP8 gating.

Results

Inhibitory effect of H_2S on H_2O_2 cell permeability

Sodium hydrogen sulphide (NaHS) is utilised commonly as a H_2S source, because it is stable and much easier to work with than using its gaseous forms (28). In solution, NaHS rapidly dissociates to Na+ and hydrogen sulphide anion (HS−) and, nearly instantaneously, HS– associates with H^+ to form H_2S (5, 29). This situation leads to a dynamic equilibrium at physiological pH in which about two-thirds of H_2S exists as HS^- and one-third as undissociated H_2S (5, 30). By convention, hereinafter, H_2S in the text refers to NaHS addition.

As a first step to investigate the effect of H_2S on H_2O_2 cell permeability, we measured exogenous H_2O_2 import in HeLa cells stably expressing in their cytosol the HyPer H_2O_2-specific probe (HyPerCyto, (31)) using confocal laser scanning. Addition of 50µM H_2O_2 clearly activated the sensor in control conditions, as determined by the profound 488/405 nm shifts observed in live cell imaging (Fig. 1A, red trace). In contrast, 30 minutes of treatment with 100µM H_2S before analysing transport caused a complete block of

H$_2$O$_2$ import (Fig. 1A, blue trace), mimicking the results obtained under stress conditions (22). H$_2$S-mediated blockade resulted to be time-dependent, as shorter incubation periods resulted in partial inhibition phenotypes (Supp. Fig. 1A). Dose-response experiments showed that H$_2$S caused a decrease in H$_2$O$_2$ transport capacity starting at 50µM at 30min with comparable effects at concentrations from 100 to 500µM (Supp. Fig. 1B)
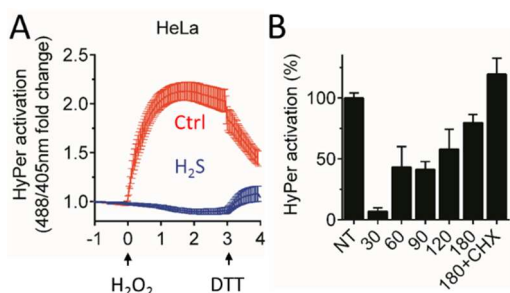

Figure 1. H$_2$S treatment is sufficient to block H$_2$O$_2$ transport and C53 is confirmed to be the primary target of the inhibition. A. Kinetics of HyPerCyto activation in H$_2$S-treated HeLa cells upon addition of exogenous H$_2$O$_2$ reveals an impairment of its transport though the plasma membrane. Data are shown as mean fold changes of the 488/405nm ratio measured by confocal laser scanning, plotted against time ± standard error of the mean (SEM). Ctrl, control conditions; H$_2$S, Hydrogen Sulphide. B. Quantification of H$_2$O$_2$-uptake performed 90 seconds after addition of exogenous H$_2$O$_2$ to HyPerCyto-HeLa cells after a treatment of H$_2$S. The quantification was done 30-60-90-120-180 minutes in presence or absence of cycloheximide after washing the compound to test the capability of cells to recover from the inhibition. Data were normalized to the uptake of untreated cells. Average of ≥3 experiments ±SEM. NT, untreated cells; CHX, cycloheximide.

H$_2$O$_2$-derived oxidation of the HyPer probe can be efficiently counteracted by adding the reducing agent dithiothreitol (DTT) during the live acquisition (Fig. 1A, red trace). The treatment indeed causes an initial abrupt HyPer reduction, followed by a slower rate

of fluorescent signal decrease elicited by the combined action of DTT-mediated probe reduction and sensor oxidation by the H_2O_2 that is still entering inside the cells. Quenching the remaining extracellular H_2O_2 at the end of the time-course by adding catalase causes a different reduction profile, leading to a drastic decrease in HyPer signal to basal levels (Suppl. Fig. 1C, red trace). Instead, addition of DTT to H_2S-inhibited cells caused a transient spike of probe oxidation (Fig. 1B, blue trace), implying that, paradoxically, a reducing agent, DTT, allowed the entry of an exogenous oxidant, H_2O_2, and further demonstrating HyPer functionality after the H_2S challenge. The presence of extracellular catalase prevented this spike (Suppl. Fig. 1C, blue trace). These findings suggested that H_2S impedes H_2O_2 transport across the plasma membrane by creating a DTT-sensitive modification(s), as described before for stress conditions (22). Moreover, as it was true for stress, H_2O_2 transport inhibition by H_2S showed to be time-reversible (Fig. 1B), and cicloheximide (CHX) supplementation during the maximum recovery time-point (3h) did not abrogate transport restoration, indicating that no newly synthesised protein is taking part in the process.

Having shown before that cysteine 53 (C53) of AQP8 is the main target of a redox-mediated modification that inhibits H_2O_2 transport upon cell stress (22), we investigated whether this residue is also involved in the H_2S-mediated H_2O_2 transport blockade. Therefore,

HeLa HyPerCyto cells were transfected either with wild-type (wt) or with a C53S mutant Halo-tagged recombinant protein (see material and methods for details) and the uptake of exogenous H_2O_2 evaluated before or after a 30min treatment with H_2S. Staining using fluorescent Halo ligands (32) allowed detection of cells positive for the expression of the transgenes, negative cells serving as efficient controls. As expected, neither untransfected cells nor wt transfectants displayed HyPer oxidation upon exposure to H_2O_2 when treated with H_2S (Fig. 1C, left panel, blue trace).
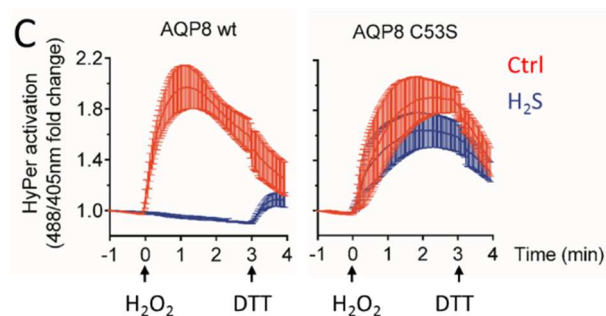
Figure 1C. Kinetics of HyPerCyto activation in H_2S-treated HeLa cells transfected with AQP8-wt or AQP8-C53S upon addition of exogenous H_2O_2 confirm that also recombinant AQP8 is inhibited after H_2S treatment, while the mutant C53S is almost unaffected by the same treatment. Data are shown as in figure 1A.

Remarkably, C53S mutants were resistant to the H_2S-driven transport inhibition (Fig. 1C, right panel, blue trace), implicating that the mechanism hits the same cysteine residue than stress. Moreover, DTT addition at the end of the time-course analysis of H_2S-treated C53S-expressing cells caused a reduction of the HyPer probe similar to the one observed in control conditions, while H_2S-treated wt-

expressing cells manifested the transient spike attributed to the transient reopening of the channel caused by the reducing agent.

As one of the main biochemical ways described for H_2S modulation of protein function is based on its reactivity with cysteine residues, these data suggest that AQP8 sulphydration could be the mechanism deployed by cells to regulate H_2O_2 permeability during stress.

Radioactive labelling of AQP8 sulphydration

Current biochemical protein persulphide detection methods imply the biotinylation of the sulphydrated moiety in so-called tag-switch assays (33-36). However, using these protocols, we did not achieve any AQP8 biotin labelling in conditions that assured that no further oxidation events occur in the samples. To overcome this technical issue and test the hypothesis of a stress-induced AQP8 sulphydration, we employed a radioactive sulphur transfer tracking strategy able to detect ^{35}S-persulphide formation. Thus, providing ^{35}S-Methionine/^{35}S-Cysteine to cells in the presence of a protein synthesis inhibitor, will result on labelling of the persulphidated pool via the H_2S generated during transulphuration of these amino acids (Fig. 2A).
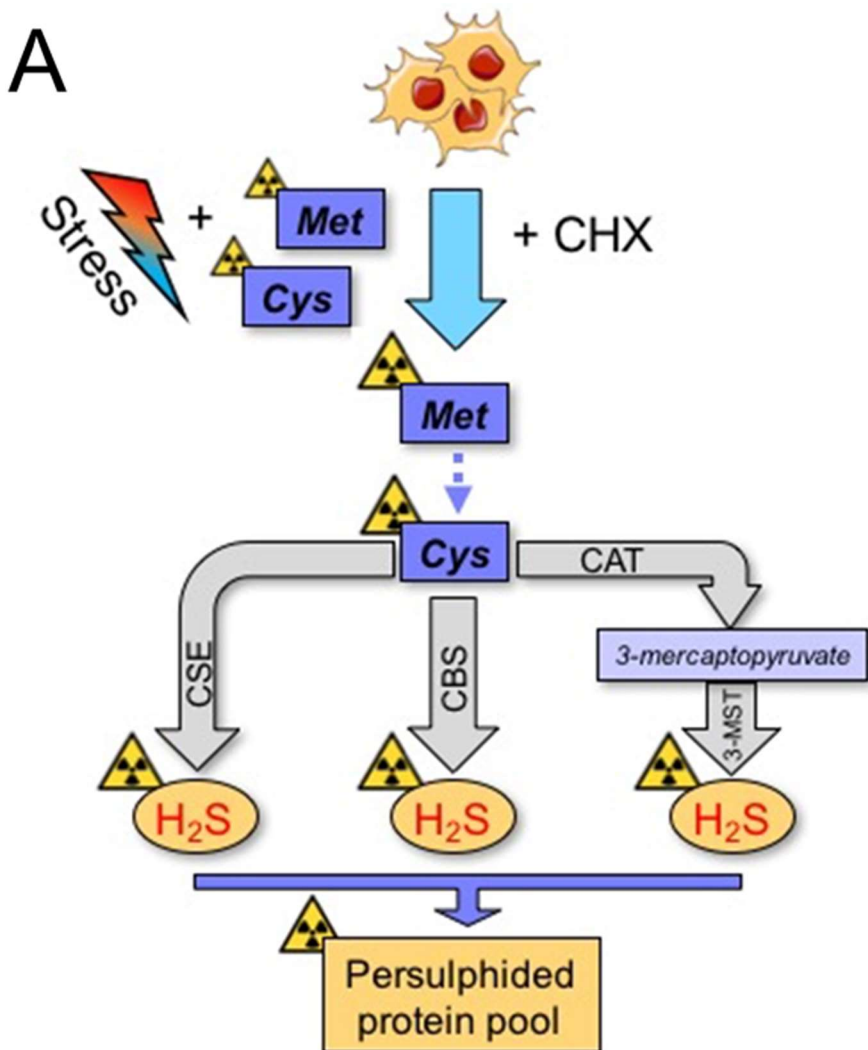
Figure 2. Dissecting the sulphydration pathway A. Rationale for producing radioactive H2S. To radioactive label the transulphuration pathway we incubate cells at 37°C (ctrl) or 42°C (stress) in complete medium without cysteines and methionines for 30mins then we add CHX for 1h to block proteins synthesis and finally we add radioactive labelled cysteines and methionines in presence of CHX. Thus, cells were forced to produce radioactive H2S that will be incorporated only in proteins that undergo persulfidation.

In addition, the covalent persulphides formed will be sensitive to DTT-dependent cleavage, allowing discrimination from putative background incorporation under reducing conditions.

Thus, incubation with ^{35}S-Methionine/^{35}S-Cysteine in the presence of cycloheximide resulted in great reduction of protein synthesis (Suppl. Fig. 2A), forcing cells to incorporate the radioactive sulphur into proteins mostly by using the H_2S produced via transulphuration of these amino acids (Fig. 2B). Persulphide formation was detected by non-reducing SDS-PAGE followed by autoradiography and should not be present when samples are treated with DTT prior to gel electrophoresis.

As stated before, persulphides are sensitive to reducing agents so the covalent ^{35}S persulphided label could be identified by analysing immunoprecipitated samples by non-reducing SDS-PAGE followed by autoradiography (Fig. 2B). Halo ligand served to control the total amount of recombinant immunoprecipitated protein (Suppl. Fig. 2B). As expected, a radiolabelled persulphide was formed on AQP8-wt protein under stress conditions (lane 2) and this signal was weaker in cells expressing AQP8-C53S (lane 4) showing that less radioactive sulphur is incorporated during the stress. Importantly, DTT addition prior to SDS-PAGE abrogate this difference, excluding that it was reflecting differential sulphur incorporation by protein synthesis between AQP8-wt and -C53S expressing cells.

The radioactive assay as described here demonstrated to be sufficiently sensitive to detect the persulphide formation on AQP8, though the failure of cycloheximide to reduce protein synthesis to 0 during the length of the chase (3h) presumably is reflected in the dilution of the radioactive signal coming from the transulphuration pathway with the background signal of the rest of cysteines and methionines labelled by synthesis.
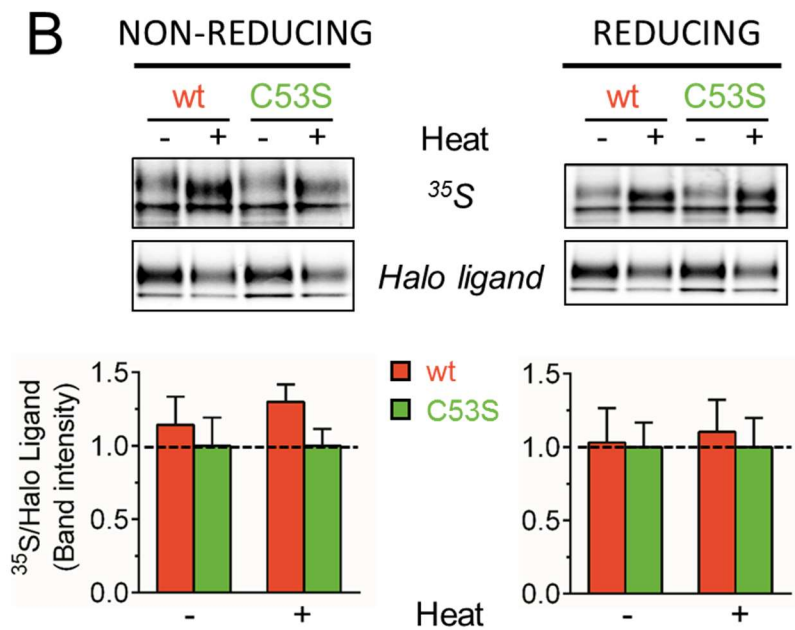
Figure 2B. Cells transfected with HaloAQP8-wt or -C53S mutant were treated as described in figure 2A and then lysed. Then, AQP8 was immunoprecipitated using anti-Flag beads, loaded on a gel in non-reducing (NR) or reducing (+DTT) and 35S signal was measured. The ratio between 35S and Halo-ligand was quantified and used as sulphydration index. The C53S 35S/Halo ligand ratio was used as background signal. Average of ≥3 experiments ±SEM.

C53 is located inside the pore far away from other thiols and thus hindering intra- and intermolecular reactions (22). These features make sulfenic acid the only plausible oxidative modification to be formed under stress. They are transient intermediates generated in thiol oxidation pathways. They are unstable and usually react with a second thiol to form disulphides. Sulfenilated cysteines can also be further oxidised to form sulfinic species, which can be enzymatically-reduced (37). If the oxidative conditions persist, sulfinic acid evolves in sulfonic acid, an irreversible status that completely inactivates the protein targeted by this modification. Moreover, sulfenic acid is a necessary intermediate for cysteines persulphydation (7, 8) which has been reported to be a possible mechanism that cell might exploit to prevent further oxidation of sulfenilated cysteines (38).

Here we hypothesize a two-step inhibition mechanism for AQP8 in which are involved an initial sulfenilation which is necessary for the following sulphydration (Fig. 2C, right panel).

We take advantage of DPI, a compound that impairs ROS production by inhibiting NOXes and other flavoproteins (39), that is sufficient to prevent stress-induced H_2O_2 transport inhibition (22). Therefore, we surmised that if a sulfenilation is the first step in the AQP8 inhibition mechanism, DPI can also prevent the H_2S-induced channel closure. Indeed, a pre-treatment with DPI (3h), completely prevent the

inhibition caused by H_2S (Fig. 2C) confirming our initial hypothesis in which a sulfenilation intermediate is necessary to inhibit AQP8.
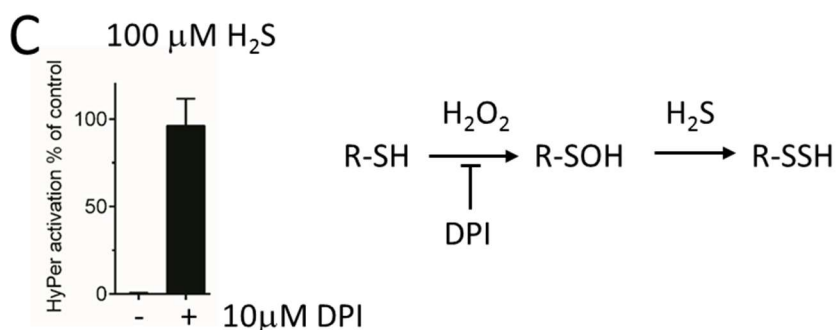
CBS Contribution

In mammals, cystathionine β-synthase (CBS) catalyses one of the first steps of the pathway, performing the condensation of serine and homocysteine to cystathionine (40). The second step is the hydrolysis of cystathionine to cysteine, ammonia, and α-ketobutyrate performed by cystathionine γ-synthase (CSE) (6). Both reactions generate H_2S and allow a coordinated control of cellular H_2S levels in a complex and overlapping manner. The contribution of these enzymes on H_2S production has been documented to be affected by their expression levels and the availability of substrates (41).

Therefore, to understand which role can CBS have in AQP8 inhibition mechanism we investigated if these two proteins can interact between each other. Thus, we performed a co-immunoprecipitation assay with lysates derived from cells overexpressing a flag-tagged version of AQP8 (Fig. 3A). As expected, we found that a band corresponding to CBS was enriched in the sample where AQP8-flag was present (Fig. 3A and S3A). Finally, we validated these results with a more functional approach. If CBS has a role in AQP8-sulphydration, its downregulation with specific siRNA may prevent stress-induced channel inhibition. Hence, we efficiently silenced the expression of CBS (Fig. S3B) in HeLa cells stably expressing HyPerCyto and heat-shocked them (42°C for 3h). In line with our hypothesis, the absence of CBS was sufficient to completely prevent the stress-induced H_2O_2 transport inhibition. In fact, no difference was found between stressed and control cells (Fig. 3B, red and blue traces), also suggesting that CSE play a minor role in our cellular model. Additionally, stressed cells remain sensitive to the H_2S-induced inhibition, meaning that the missing CBS activity can be rescued by adding exogenous H_2S (Fig. 3B, green trace).

CBS and, in particular, its metabolite H_2S have been demonstrated to play a major role in the regulation of H_2O_2 transport in HeLa cells

supporting the hypothesis that sulphydration of AQP8 is the modification that inhibits the channel.
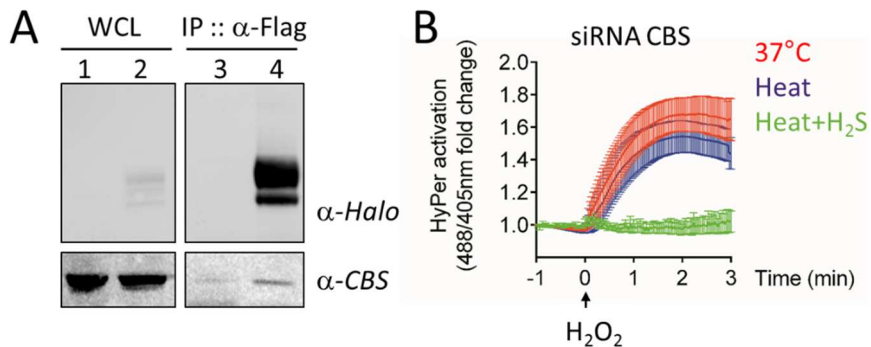
Figure 3. involvement of CBS in the inhibition mechanism. A. HeLa cells transiently transfected with HaloAQP8mycFlag or Halo, lysed and AQP8 was immunoprecipitated with anti-flag beads. B. Kinetics of H_2O_2 import into HeLa cells in which the expression of CBS was silenced heat shocked or not and treated or not with H_2S. Cells were silenced for CBS expression stressed at 42°C for 3 hours and then incubated with (blue trace) or without (green trace trace) 100 µM H_2S for 30min. Results represent the mean fold changes of the 488/405nm ratio measured by confocal laser scanning, plotted against time. Average of ≥3 experiments ±SEM.

EGFR-signalling modulation

Perturbing H_2O_2 permeability by silencing AQP8 has deep consequences on signalling downstream tyrosine kinase receptors (21, 42). Thus, we analysed protein tyrosine phosphorylation in cells that were either treated with H_2S or heat stressed and then stimulated with EGF (Fig. 4A). Clearly, both treatments severely affected phosphorylation compared with untreated cells (Ctrl). Heat

shock caused an increase in the basal level of cell phosphorylation in absence of stimulation probably reflecting the inhibition of cellular phosphatases caused by the accumulation of intracellular ROS produced in response to stress (24, 25). In contrast, the H_2S treatment did not increase the basal level of tyrosine-phosphorylated proteins. This phenomenon indicates that the overall cellular redox balance was not affected by the short exposure with hydrogen sulphide.
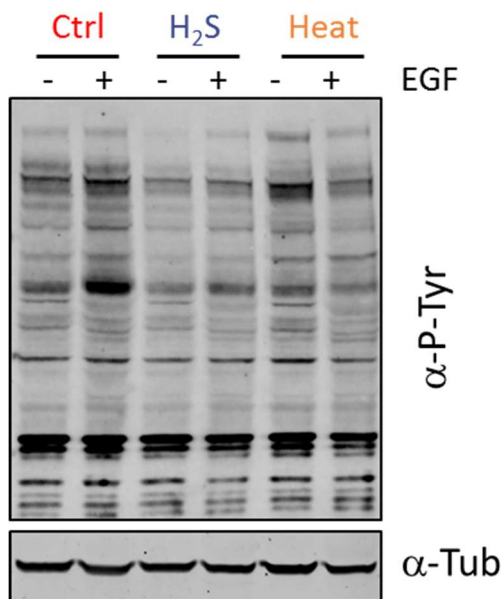
Figure 4. H_2S treatment: impact on TKR signalling. Western blot analysis with the indicated antibodies showing changes in phosphorylation of total cell tyrosines on whole HeLa cell extracts that were left untreated or treated with H_2S or stressed with heat shock before treatment with EGF. The intensity of specific bands was quantified by densitometry and normalized to tubulin. Bars show average band intensities relative to control cells ± SEM.

These results further confirm the importance of cell H_2O_2-transporting capacity for redox homeostasis and cell signalling and in particular the paramount role that the regulation of AQP8 plays in our cellular model.
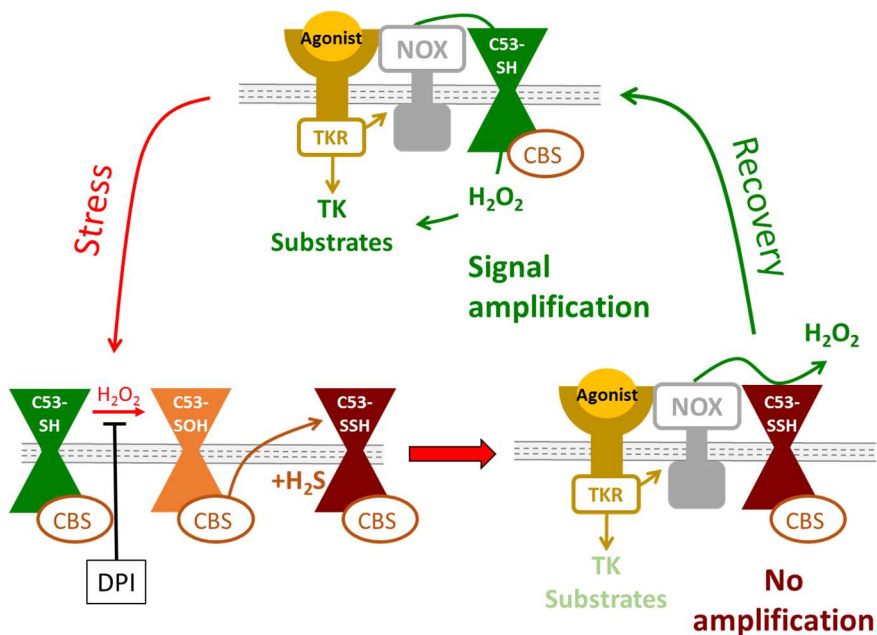
Figure 5. Schematic model of H_2O_2 generation and transport during signalling. Membrane NOX and DuOX enzymes are activated upon tyrosine kinase receptor (TKR) engagement to produce H_2O_2, which enters the cells via AQP8 and amplifies downstream signalling. Under stress conditions the DPI-sensitive increase in ROS production causes oxidation in C53 which now can be persulfidated by CBS-produced H_2S leading to AQP8 inhibition and, therefore, impairing EGF downstream phosphorylation cascade.

Discussion

The control of intracellular redox homeostasis uses a limited number of chemical reactions. One of these is sulfur-based chemistry. Probably the most important form of H_2S signalling is the modification of protein function by a process called S-sulfhydration. However, this field of research is at its beginning, and it is still facing challenges such as the proper choice of detection method, understanding of the mechanism(s) by which persulfidation takes place and the actual impact it has on the cellular functions.

H_2S production has been shown to be closely linked to cellular oxidative state as increased level of superoxide/peroxide production in cells activates H_2S generation. In fact, situations that lead to increased steady state levels of oxidized thiols increase persulphide formation. Experiments with cells in culture showed that treatment with H_2O_2 enhanced the formation of persulfides (43), which sustains the idea of oxidative stress increasing the persulphided protein pool. The steady-state concentration of H_2S is orders of magnitude lower than that of glutathione (44, 45), (44, 45), which makes it problematic for H_2S to compete for the reaction with protein sulfenic acids. Despite these difficulties, the high flux of H_2S generation (46), its free diffusion (47, 48) and therefore its ability to reach deeper

parts of the proteins suggest that the reaction of H_2S with sulfenic acids could still be a major source of protein persulphide formation. The localization of C53 buried in the AQP8 pore could constitutes the perfect target for hydrogen sulphide as it is in a position in which reductive elements such as GSH are not able to reach. Instead, H_2S will be the perfect modificator as its gaseous nature and its ability to freely cross membranes allow it to react with the buried cysteine.

Thiol oxidation, which initially starts with the formation of sulfenic acids (still reversible modification), could proceed further with the formation of irreversible sulfonic acids. H_2S could react with sulfenic acid preventing this oxidation. In addition, persulphidated protein will react faster with ROS/RNS and form an adduct that could be cleaved by the action of certain enzymes restoring free thiol. In this way, modification to obtain a persulphide cysteine could protect the sulfenylation to progress to an irreversible state that will cause cell death (38).

Accordingly, our results indicate a protective role of AQP8 gating, as its reversible C53-targeted, CBS-dependent sulphydration will represent the perfect switch for cells to choose between cell death or restore proliferation. Indeed, C53 sulphydration in mild-oxidative stress conditions will allow cells, after the insult, to re-establish cell growth by reducing C53, with a mechanism that is still under investigation. Instead, in harsher conditions the cysteine residue will

be further oxidised leading to an irreversible inhibition of the channel, accumulation of intracellular ROS and finally cell death.

Thus, AQP8 C53 sulphydration appears to have a dual role in cells, from one side it can finely tune AQP8 functionality impacting on cell signalling, on the other hand, in stress conditions, represents an important mechanism that cells can exploit to decide whether to live or die, depending on the duration and the strength of the insult. Therefore, the control of H_2O_2 fluxes can became a new tool to take advantage to manipulate cell fate. In fact, promoting them will fuel cell growth while imparing them will cause growth arrest and finally cell death. As indicated by these important consequences, AQP8-mediated H_2O_2 transport and its regulation deserve even more attention and efforts to understand, for instance, how AQP8 functionality is restored and which are the precise molecular players that regulate it.

Material and Methods

Cell culture

HeLa cells were cultured in DMEM+Glutamax™-I medium (Life Technologies, Carlsbad, CA, U.S.A.) supplemented with 10% fetal bovine serum (FBS, EuroClone, Pero, Italy) and 5mg/ml penicillin-streptomycin (Lonza, Basel, Switzerland).

Plasmids, siRNAs and transfection procedures

The plasmid for expression of the HyPer probe targeted to the cytosol (HyPerCyto) was a generous gift of Dr. V. Belousov (IBCh, Moscow, Russian Federation), while silencing‐resistant Halo‐AQP8 wt and C53S plasmids were generated as previously described (21). The flag-tagged HaloAQP8 was generated in two steps, first by cutting the AQP8 fragment from AQP8-GFP plasmid from Origene (RG219668) and inserting it in place of AQP11 in the AQP11mycFlag vector (Origene, RC 208083). The second step was to excide the fragment AQP8mycFlag from the previously generated vector and insert it in the construct HaloAQP8 (21) exchanging it with AQP8, thus generating HaloAQP8mycFlag plasmid.

The CBS-specific siRNA oligonucleotide (5′-CTCACATCCTAGACC-

AGTA-3′) and an unrelated control (Block‐it™) were purchased

from Ambion (Life Technologies, Carlsbad, CA, U.S.A.) and their

efficiency monitored by WB.

For silencing experiments, 8x104 HyperCyto-expressing HeLa stable

transfectants (see below) were grown overnight in 6-well plates and

transfected with 30pmol of siRNA, using RNAiMAX lipofectamin

(Invitrogen, Carlsbad, CA, U.S.A.), according to the manufacturer

instructions. Cells were analysed for efficient silencing and used after

48h of transfection.

For experiments in which AQP8 was transiently overexpressed using

HaloAQP8-wt or C53S recombinant proteins, cells were transfected

by JET-PEI (Polyplus-transfection, Illkirch, France), according to the

manufacturer instructions, and cultured for 48h before imaging or

biochemical analyses.

Reagents and treatments

NaHS was purchased from Sigma prepared freshly for each

experiment and used at the final concentrations of 100µM or 500µM

for 30min for untrasfected or AQP8-overexpressing cells,

respectively. Briefly, a stock solution of NaHS was prepared by

dissolving it in distilled water, then it was diluted 5000 times and incubated with 1mM DTNB (Sigma) for 1-2 minutes to exactly estimate H_2S concentration. A yellow product will be obtained and its absorbance will be read at a spectrophotometer set at 412nm and the actual concentration of H_2S will be calculated with this formula:

$$[H_2S] = cuvette\ volume * dilution * [OD_{412}]$$

Extracellular catalase, epidermal growth factor (EGF), diphenyleneiodonium (DPI), dithiothreitol (DTT), hydrogen peroxide (H_2O_2) and cycloheximide were all purchased from Sigma.

Heat-shock treatment was performed by putting the plates for 3 hours in a water bath set at 42°C.

H_2S treatment was performed by washing cells twice to remove all the serum from cells to avoid that serum proteins quench it. Then H_2S was added for 30 minutes at room temperature in ringer buffer for microscopy experiment and in DMEM with no serum for biochemical assays. Finally, H_2S was washed twice before analysing the cells.

Imaging HyPer‐oxidation

To perform confocal live imaging experiments, 8x104 HyperCyto-expressing HeLa cells were silenced and/or transfected on glass‐

coverslips as described above. To identify HaloAQP8‑expressing cells, 2nM HaloTag® TMR Direct Ligand was added 24h after transfection. After 24h of culture with the fluorescent ligand, cells on coverslips were equilibrated in Ringer Buffer (RB: 140mM NaCl, 2mM $CaCl_2$, 1mM $MgSO_4$, 1.5mM K_2HPO_4, 10mM Glucose, pH 7.3) for 10min at room temperature (RT) prior to addition of 50μM of H_2O_2, freshly prepared in RB. Cells were treated for 30min in RB with 100μM H_2S as described above with or without a pre-incubation of 3 hours with 10μM DPI, washed twice and analysed. Otherwise, cells, silenced or not for the expression of CBS, were heat-shocked for 3hours at 42°C and treated or not with 100μM H_2S, washed twice and analysed. A higher dose of H_2S was used when AQP8 transient overexpression was performed, to be sure to reach the maximum inhibitory effect. When indicated, extracellular catalase was added at a final concentration of 5000U/ml.

Confocal images were collected every 2sec for 5min or more by dual excitation with a 488nm argon and a 405nm violet diode lasers. We used an Ultraview confocal laser-scanning microscope equipped with a 40X oil‑immersion lens (Perkin Elmer, Waltham, MA). The 488/405nm ratios were calculated by ImageJ software for ≥25 cells, averaged, and showed as mean fold change ratio plotted against time ±SEM. Moreover, to facilitate quantification and statistical

analyses, we averaged the data obtained after 90 seconds from H_2O_2 addition in the time-course experiments performed, and represented them as the percentage of H_2O_2 transport in H_2S treated cells relative to the corresponding untreated cells. At least three independent experiments were performed for each condition, except for in which two different experiments gave almost identical results.

Antibodies and western blotting

Primary antibodies anti-CBS, anti-phosphotyrosine Antibody, clone 4G10® were purchased from Merck-Millipore (Darmstadt, Germania). Mouse anti-tubulin and anti-flag M2 affinity gel was from Sigma. Secondary antibodies α-rabbit AlexaFluor-488 or -AlexaFluor-647, were purchased from Invitrogen.

Images were acquired using a Typhoon FLA-9000 (GE HealthCare, Little Chalfont, U.K.), processed with ImageJ and densitometrically quantified when indicated by ImageQuant TL software (GE HealthCare, Little Chalfont, UK) ±SEM.

To follow EGF responses biochemically, sub-confluent HeLa cells were cultured in FCS-free DMEM for 3h before incubation with or without H_2S or at 42°C before EGF addition. Cells were then washed with ice-cold PBS containing 0.4mM Na_3VO_4 to block phosphatases

lysed in RIPA (0.1% SDS, 1% NP40, 150mM NaCl, 50mM Tris-HCl pH 7.4) supplemented with proteases inhibitors (Roche), 0.4mM Na_3VO_4, 10mM NEM and 10mM NaF and analyzed by electrophoresis and western blot.

Co-Immunoprecipitation

HeLa cells transfected with HaloAQP8mycFlag were lysed in RIPA buffer. Cell lysates in RIPA buffer were immunoprecipitated with anti-flag beads. Immune-complexes were electrophoresed in SDS-polyacrylamide gel, transferred to a nitrocellulose membrane and were immunoblotted with anti-CBS antibody.

Radioactive sulphydration assay

Cells transfected with HaloAQP8mycFlag wt or C53S, were seeded in 6cm dishes at $2.5*10^6$ cells/dish and incubated over-night in the presence of 30nM TMR-direct Halo ligand (Promega). Cells were-pre-incubated for 30 min in methionine/cysteine-free DMEM supplemented with 1% dialyzed fetal bovine serum at 37°C, followed by further 60min in the same conditions but in the presence of 0.5mM CHX. Cells were then labelled for 3hrs with 0.22mCi/mL [^{35}S]cys/met (EasyTag, Perkin Elmer) at either 37°C (ctrl) or 42°C (stress), in the continuous presence of 0.5mM CHX. Cells were then

washed in ice cold PBS and lysed in RIPA buffer containing 1mM NEM, protease and phosphatase inhibitors. AQP8 was immune-precipitated with anti-flag M2 affinity gel (Sigma #A2220) and then analysed on 3-8% Tris-Acetate NuPAGE gel (Novex). Signal from TMR-direct Halo ligand, which labels all AQP8 present at the start of the radioactive labelling, acted as convenient loading control. Under these labelling conditions we expect most of the radioactivity to be incorporated into the proteins via the sulphydration pathway, since protein synthesis is shut down. However, due to the prolonged labelling, we could not completely abolish amino acid incorporation. To account for this, samples were denatured in the presence of 200mM DTT before analysis by SDS-PAGE, as DTT will get rid of sulphydrated groups but not of incorporated amino acids. The difference between the signal in non-reduced and reduced conditions represent the extent of sulphydration that has occurred in the 3hrs labelling.

Statistical analyses

Statistics were calculated either by using the two-sample t-Test for independent samples or the one-way ANOVA method for multiple samples. When using the latter, the Tukey HSD post-hoc test was also applied to find out which groups were significantly different

from which others. In all cases, statistical significance was defined as P<0.05 (*), P<0.01 (**) or P<0.001(***).

References

1.   Sawa T, Arimoto H, Akaike T. Regulation of redox signaling involving chemical conjugation of protein thiols by nitric oxide and electrophiles. Bioconjugate chemistry. 2010;21(7):1121-9.

2.   Sies H. Role of metabolic H_2O_2 generation: redox signaling and oxidative stress. The Journal of biological chemistry. 2014;289(13):8735-41.

3.   Mustafa AK, Gadalla MM, Sen N, Kim S, Mu W, Gazi SK, et al. H_2S signals through protein S-sulfhydration. Sci Signal. 2009;2(96):ra72.

4.   Kimura H. Signaling molecules: hydrogen sulfide and polysulfide. Antioxidants & redox signaling. 2015;22(5):362-76.

5.   Wang R. Physiological implications of hydrogen sulfide: a whiff exploration that blossomed. Physiol Rev. 2012;92(2):791-896.

6.   Castro R, Rivera I, Blom HJ, Jakobs C, Tavares de Almeida I. Homocysteine metabolism, hyperhomocysteinaemia and vascular disease: an overview. Journal of inherited metabolic disease. 2006;29(1):3-20.

7.   Zhang X, Bian JS. Hydrogen sulfide: a neuromodulator and neuroprotectant in the central nervous system. ACS Chem Neurosci. 2014;5(10):876-83.

8.   Cuevasanta E, Lange M, Bonanata J, Coitino EL, Ferrer-Sueta G, Filipovic MR, et al. Reaction of Hydrogen Sulfide with Disulfide and Sulfenic Acid to Form the Strongly Nucleophilic Persulfide. The Journal of biological chemistry. 2015;290(45):26866-80.

9.   Hamelet J, Seltzer V, Petit E, Noll C, Andreau K, Delabar JM, et al. Cystathionine beta synthase deficiency induces catalase-mediated hydrogen peroxide detoxification in mice liver. Biochimica et biophysica acta. 2008;1782(7-8):482-8.

10.   Robert K, Nehme J, Bourdon E, Pivert G, Friguet B, Delcayre C, et al. Cystathionine beta synthase deficiency promotes oxidative stress, fibrosis, and steatosis in mice liver. Gastroenterology. 2005;128(5):1405-15.

11.   Bryan S, Yang G, Wang R, Khaper N. Cystathionine gamma-lyase-deficient smooth muscle cells exhibit redox imbalance and apoptosis under hypoxic stress conditions. Exp Clin Cardiol. 2011;16(4):e36-41.

12.   Niu WN, Yadav PK, Adamec J, Banerjee R. S-glutathionylation enhances human cystathionine beta-synthase activity under oxidative stress conditions. Antioxidants & redox signaling. 2015;22(5):350-61.

13.   Romero I, Tellez J, Romanha AJ, Steindel M, Grisard EC. Upregulation of Cysteine Synthase and Cystathionine beta-Synthase Contributes to Leishmania braziliensis Survival under Oxidative Stress. Antimicrob Agents Chemother. 2015;59(8):4770-81.

14.   Zhao Y, Wu S, Gao X, Zhang Z, Gong J, Zhan R, et al. Inhibition of cystathionine beta-synthase is associated with glucocorticoids over-secretion in psychological stress-induced hyperhomocystinemia rat liver. Cell Stress Chaperones. 2013;18(5):631-41.

15.   Zhao K, Li H, Li S, Yang G. Regulation of cystathionine gamma-lyase/H(2)S system and its pathological implication. Front Biosci (Landmark Ed). 2014;19:1355-69.

16.   Kimura Y, Goto Y, Kimura H. Hydrogen sulfide increases glutathione production and suppresses oxidative stress in mitochondria. Antioxidants & redox signaling. 2010;12(1):1-13.

17.   Yang M, Huang Y, Chen J, Chen YL, Ma JJ, Shi PH. Activation of AMPK participates hydrogen sulfide-induced cyto-protective effect against dexamethasone in osteoblastic MC3T3-E1 cells. Biochem Biophys Res Commun. 2014;454(1):42-7.

18.   Qabazard B, Li L, Gruber J, Peh MT, Ng LF, Kumar SD, et al. Hydrogen sulfide is an endogenous regulator of aging in Caenorhabditis elegans. Antioxidants & redox signaling. 2014;20(16):2621-30.

19.   Yang G, Zhao K, Ju Y, Mani S, Cao Q, Puukila S, et al. Hydrogen sulfide protects against cellular senescence via S-sulfhydration of Keap1 and activation of Nrf2. Antioxidants & redox signaling. 2013;18(15):1906-19.

20.   Filipovic MR. Persulfidation (S-sulfhydration) and H_2S. Handbook of experimental pharmacology. 2015;230:29-59.

21.   Bertolotti M, Bestetti S, Garcia-Manteiga JM, Medrano-Fernandez I, Dal Mas A, Malosio ML, et al. Tyrosine kinase signal modulation: a matter of H_2O_2 membrane permeability? Antioxidants & redox signaling. 2013;19(13):1447-51.

22.   Medrano-Fernandez I, Bestetti S, Bertolotti M, Bienert GP, Bottino C, Laforenza U, et al. Stress Regulates Aquaporin-8 Permeability to Impact Cell Growth and Survival. Antioxidants & redox signaling. 2016;24(18):1031-44.

23.   Jiang F, Zhang Y, Dusting GJ. NADPH oxidase-mediated redox signaling: roles in cellular stress response, stress tolerance, and tissue repair. Pharmacological reviews. 2011;63(1):218-42.

24.   Santos CX, Tanaka LY, Wosniak J, Laurindo FR. Mechanisms and implications of reactive oxygen species generation during the unfolded protein response: roles of endoplasmic reticulum oxidoreductases, mitochondrial electron transport, and NADPH oxidase. Antioxidants & redox signaling. 2009;11(10):2409-27.

25.   Shaughnessy DT, McAllister K, Worth L, Haugen AC, Meyer JN, Domann FE, et al. Mitochondria, energetics, epigenetics, and cellular responses to stress. Environ Health Perspect. 2014;122(12):1271-8.

26.   Christou A, Filippou P, Manganaris GA, Fotopoulos V. Sodium hydrosulfide induces systemic thermotolerance to strawberry plants through transcriptional regulation of heat shock proteins and aquaporin. BMC Plant Biol. 2014;14:42.

27.   Kwak WJ, Kwon GS, Jin I, Kuriyama H, Sohn HY. Involvement of oxidative stress in the regulation of H_2S production during ultradian metabolic oscillation of Saccharomyces cerevisiae. FEMS Microbiol Lett. 2003;219(1):99-104.

28.   Cavallini D, Federici G, Barboni E. Interaction of proteins with sulfide. European journal of biochemistry / FEBS. 1970;14(1):169-74.

29.   DeLeon ER, Stoy GF, Olson KR. Passive loss of hydrogen sulfide in biological experiments. Analytical biochemistry. 2012;421(1):203-7.

30.   Reiffenstein RJ, Hulbert WC, Roth SH. Toxicology of hydrogen sulfide. Annu Rev Pharmacol Toxicol. 1992;32:109-34.

31.   Belousov VV, Fradkov AF, Lukyanov KA, Staroverov DB, Shakhbazov KS, Terskikh AV, et al. Genetically encoded fluorescent indicator for intracellular hydrogen peroxide. Nat Methods. 2006;3(4):281-6.

32.   Mossuto MF, Sannino S, Mazza D, Fagioli C, Vitale M, Yboue ED, et al. A dynamic study of protein secretion and aggregation in the secretory pathway. PloS one. 2014;9(10):e108496.

33.   Doka E, Pader I, Biro A, Johansson K, Cheng Q, Ballago K, et al. A novel persulfide detection method reveals protein persulfide- and

polysulfide-reducing functions of thioredoxin and glutathione systems. Science advances. 2016;2(1):e1500968.

34.   Park CM, Macinkovic I, Filipovic MR, Xian M. Use of the "tag-switch" method for the detection of protein S-sulfhydration. Methods Enzymol. 2015;555:39-56.

35.   Wedmann R, Onderka C, Wei S, Szijarto IA, Miljkovic JL, Mitrovic A, et al. Improved tag-switch method reveals that thioredoxin acts as depersulfidase and controls the intracellular levels of protein persulfidation. Chem Sci. 2016;7(5):3414-26.

36.   Zhang D, Macinkovic I, Devarie-Baez NO, Pan J, Park CM, Carroll KS, et al. Detection of protein S-sulfhydration by a tag-switch technique. Angew Chem Int Ed Engl. 2014;53(2):575-81.

37.   Lo Conte M, Carroll KS. The redox biochemistry of protein sulfenylation and sulfinylation. The Journal of biological chemistry. 2013;288(37):26480-8.

38.   Ono K, Akaike T, Sawa T, Kumagai Y, Wink DA, Tantillo DJ, et al. Redox chemistry and chemical biology of H_2S, hydropersulfides, and derived species: implications of their possible biological activity and utility. Free radical biology & medicine. 2014;77:82-94.

39.   Li Y, Trush MA. Diphenyleneiodonium, an NAD(P)H oxidase inhibitor, also potently inhibits mitochondrial reactive oxygen species production. Biochem Biophys Res Commun. 1998;253(2):295-9.

40.   Banerjee R, Evande R, Kabil O, Ojha S, Taoka S. Reaction mechanism and regulation of cystathionine beta-synthase. Biochimica et biophysica acta. 2003;1647(1-2):30-5.

41.   Yuan G, Vasavda C, Peng YJ, Makarenko VV, Raghuraman G, Nanduri J, et al. Protein kinase G-regulated production of H_2S governs oxygen sensing. Sci Signal. 2015;8(373):ra37.

42.   Vieceli Dalla Sega F, Zambonin L, Fiorentini D, Rizzo B, Caliceti C, Landi L, et al. Specific aquaporins facilitate Nox-produced hydrogen peroxide transport through plasma membrane in leukaemia cells. Biochimica et biophysica acta. 2014;1843(4):806-14.

43.   Cuevasanta E, Moller MN, Alvarez B. Biological chemistry of hydrogen sulfide and persulfides. Arch Biochem Biophys. 2017;617:9-25.

44.   Kabil O, Banerjee R. Enzymology of H_2S biogenesis, decay and signaling. Antioxidants & redox signaling. 2014;20(5):770-82.

45.   Olson KR, DeLeon ER, Liu F. Controversies and conundrums in hydrogen sulfide biology. Nitric oxide : biology and chemistry / official journal of the Nitric Oxide Society. 2014;41:11-26.

46.   Vitvitsky V, Kabil O, Banerjee R. High turnover rates for hydrogen sulfide allow for rapid regulation of its tissue concentrations. Antioxidants & redox signaling. 2012;17(1):22-31.

47.   Cuevasanta E, Denicola A, Alvarez B, Moller MN. Solubility and permeation of hydrogen sulfide in lipid membranes. PloS one. 2012;7(4):e34562.

48.   Mathai JC, Missner A, Kugler P, Saparov SM, Zeidel ML, Lee JK, et al. No facilitator required for membrane transport of hydrogen sulfide. Proceedings of the National Academy of Sciences of the United States of America. 2009;106(39):16633-8.
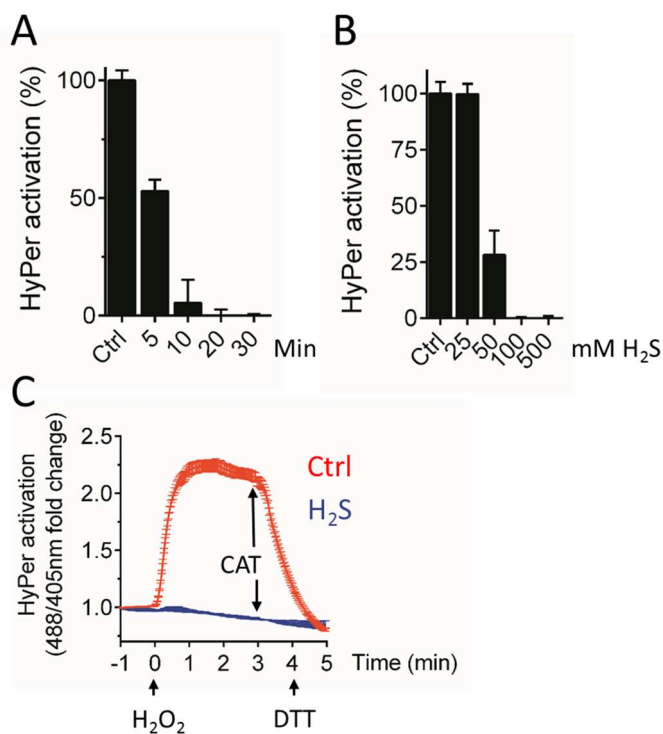
Supplementary figures

Figure 1. A. Time course of H_2S inhibition in HeLa cells stably expressing *HyPerCyto*. Quantification of H_2O_2-uptake performed 90 seconds after addition of exogenous H_2O_2 to *HyPerCyto*-HeLa cells after a treatment of H_2S at different time points. Data were normalized to the uptake of control cells. Average of ≥3 experiments ±SEM. B. Titration of H_2S concentration in HeLa cells stably expressing *HyPerCyto*. The quantification is performed as in supplementary figure 1B. C. Kinetics of HyPerCyto activation in H_2S-treated HeLa cells upon addition of exogenous H_2O_2. Catalase was added 1 minute before DTT addition to prove that the exogenously added H_2O_2 was responsible of the HyPer activation detectable after DTT addition (Fig.1A, blue trace). Data are shown as mean fold changes of the 488/405nm ratio measured by confocal laser scanning, plotted against time ± standard error of the mean (SEM). Ctrl, control conditions; H_2S, Hydrogen Sulphide; CAT, extracellular catalase.

A HaloAQP8mycFlag

-	-	+	-	+	Heat
-	+	+	+	+	^{35}S
-	-	-	0.5	0.5	CHX mM

^{35}S
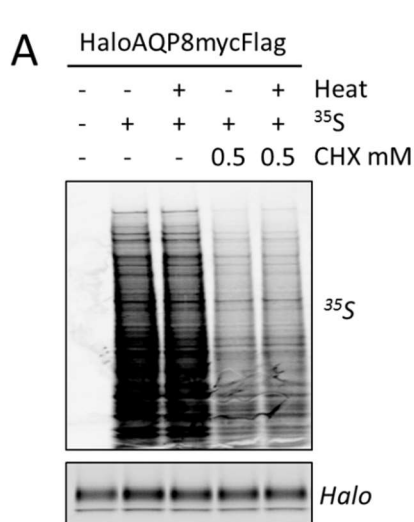
Halo

Figure 2 A. Radioactive sulphur incorporation. Cells transfected with flag-tagged version of AQP8 were treated as described in Fig. 2A-B with or without CHX to assess the strength of its inhibition. B. Halo-ligand signal in reducing or non-reducing conditions used to compare the total levels of HaloAQP8-wt or -C53.

Figure 3 A. Quantification of the signals of the band corresponding to CBS (Fig. 3A) in cell expressing or not a flagged version of AQP8. B. Representative blot and its quantification showing the efficacy of CBS silencing in HeLa cells transfected with specific siRNA against that transcript.

Chapter 4: Conclusions

Summary

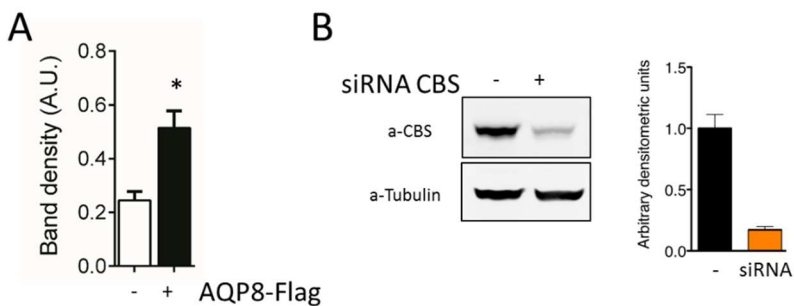In these past three years, we were able to demonstrate that regulation of AQP8-mediated H_2O_2 transport plays a crucial role in cell life-death decisions when subjected to different stresses. In fact, a mutation in a particular AQP8 cysteine residue confers HeLa cells growth advantages under those conditions in comparison to cells expressing the wt protein. Moreover, I determined, for the first time, that AQP8 can be gated by a two-step mechanism, and the relevance of the protein CBS in the process. Upon stress, AQP8 cysteine 53, in order to be inhibited, must be first oxidised by a DPI-sensitive enzyme(s) then CBS-produced H_2S will sulphydrate this residue causing channel closure. Since ROS, and in particular H_2O_2, have a very important role in cancer onset and progression, the inhibition of AQP8 could be an advantageous tool to slow-down cancer cells growth. Besides, finding other proteins that collaborate with CBS in AQP8 regulation, will increase the number of targets that could be exploited in cancer therapy.

Discussion and Future perspective

My PhD. project was initially conceived to investigate the role of H_2O_2-transporting capacity of AQP8 in MM, since increasing evidence pointed to a relevant and innovative role of ROS in this particular type of cancer (1-4). At the time, we started to get into the project, we realized that the scope of this thesis might have wider implications as the regulation of ROS fluxes showed to be relevant also for other cancer types.

As described above, a delicate redox balance is a feature of many cancers (5, 6) and thus the regulation of redox homeostasis could be used to treat the disease from a new approach. Indeed, many treatments against cancer are known to generate intracellular ROS (chemotherapeutics, such as arsenic trioxide, cisplatin, and radiotherapies) (7, 8) but their efficacy has been proved to be far from satisfactory for still unknown reasons. Therefore, it is important to understand which are these mechanisms and how to circumvent them to improve the efficacy of these ROS-generating therapeutic drugs.

Our hypothesis is that direct or indirect AQP8 modulation may be a tool that may increase chemotherapy effectiveness and avoid cancer progression. Thus, from one side, the sulphydration-mediated

closure of AQP8 will further increase the intracellular level of ROS, as it hampers their transport to the extracellular space therefore limiting damage. Moreover, gating also inhibits the entry of NOX-derived H_2O_2 thus impairing its growth-promoting effects. This new redox-homeostasis should increase therapeutics effects by impeding cancer cells to buffer the excess of ROS and inhibiting the uptake of growth-promoting ones.

The results obtained during this PhD will predict that the use of specific AQPs inhibitors might be a good method to block AQPs function. Although it is a very attractive possibility, so far the application of the already described compounds is still limited (9). Indeed, finding a good inhibitor with specificity limited to a particular isoform is quite challenging, probably because all the members of this family of proteins have a very similar structure (10). It is expectable that molecules with high AQPs selectivity and specificity of action will be hard to find.

A hypothesis that will allow to translate the findings presented in this PhD project into cancer therapy will rely instead on the indirect regulation of AQP8 function by forcing its inhibition in cancer cells. In order to survive, tumours must rapidly adapt to the endemic stress in which they live. In this sense, one of the adaptation mechanisms tumours frequently deploy is to upregulate their antioxidant capacity (11, 12). This characteristic leaves them predisposed to suffer more

when a second "redox-insult" is applied, compared to their normal counterparts. Having demonstrated that AQP8 sulphydration to occur need a first oxidation step, it is tempting to speculate that tumour cells prevent AQP8 inhibition because of their upregulated antioxidant defences. In that view, AQP8 cysteine 53 residue, that lays inside the pore and it is the main target of the inhibition machinery, would be kept in a non-sulphydratable state, hampering the channel closure.

The overall result of keeping AQP8 in a chronical open conformation is that cancer cells will obtain a growth advantage under stress conditions compared to surrounding cells. Thus, indicating that a functional redoxtat is fundamental for the maintenance of physiological signalling.

Therefore, we can speculate that shifting redox homeostasis towards a more oxidising balance would recover AQP8 inhibition mechanism, driving tumour cells to apoptosis as described in the second chapter of this thesis. In comparison with the design of specific inhibitors, this strategy has many advantages, since it can be directed towards to two different objectives. As the goal is to force AQP8 inhibition by increasing intrinsic cancer oxidative stress we can imagine a possible therapy based on decreasing antioxidant defences (12) in combination with the standard chemotherapy directed to increase intracellular ROS levels. Thus, we would be able to restore AQP8

closure, block the channel and finally drive cancer cells to ROS-induced apoptosis. Nonetheless, a possible pitfall in this strategy would be that antioxidant defences must not be completely ablated, otherwise redox-influenced signalling will be abrogated and all cells will suffer because of the treatment. Therefore, antioxidants level must be maintained to a certain threshold causing damage mostly to cancer cells taking advantage of the wider therapeutically window opened up by their intrinsic level of stress.

Having so far described the basis of AQP8 inhibition mechanism, the new scope of the study will be to unveil the molecular pathway leading to its closure, and the mechanisms the cell uses to reopen the channel. We have demonstrated that CBS-produced H_2S sulphydrates AQP8 but we did not found yet the source(s) responsible of the initial oxidation step in cysteine 53. Finding out the molecular identity of this (these) enzyme(s), and other AQP8-interactors, would add another layer of regulation to the inhibition process and render channel activity even more modulable, thus increasing its importance as a mean to impact cancer therapy. So far the AQP8 interactome has been poorly investigated, as reported on the web-tool *String (*https://string-db.org/*)*. In fact, no experimental data has been retrieved to support any of the described interactions. Deeper and systematic investigation must be carried out, using for

example a mass-spectrometry approach, to determine the truth of AQP8 interactions.

Another interesting question to be investigated in the future could be whether the stress-induced inhibition mechanism that we defined for AQP8 (or a similar one) is also present in AQP3 and AQP9, the other two already described H_2O_2-transporting AQPs. These two AQPs have been shown to be implicated in different type of tumours, particularly in cells migration and cancer development (13-15). The reason under our hypothesis that a similar regulation controls also these two AQPs is that, the main target of the inhibition mechanism here described (cysteine 53), is conserved also in these H_2O_2-transporting AQPs while absent in the rest of the members of the family (16, 17). If our hypothesis is confirmed and considering the importance of AQP3 and 9 in cancer, they will represent druggable targets also in those systems where AQP8 is absent or the effects of its inhibition are counteracted by compensatory mechanisms.

Thus, our final goal is to investigate if AQPs regulation occurs also in primary cells derived from MM patients: this would demonstrate that our findings could indeed represent a new promising path for the improvement of cancer therapy.

Publications

1. Tyrosine kinase signal modulation: a matter of H_2O_2 membrane permeability?

Bertolotti M*, Bestetti S*, García-Manteiga JM*, Medraño-Fernandez I*, Dal Mas A, Malosio ML, Sitia R.

Antioxid Redox Signal. 2013 Nov 1;19(13):1447-51. doi: 10.1089/ars.2013.5330.

*these authors equally contributed to this work and are listed in alphabetical order

2. Response to Marinelli and Marchissio.

Bertolotti M, Bestetti S, Medrano-Fernandez I, Sitia R.

Antioxid Redox Signal. 2013 Sep 10;19(8):897. doi: 10.1089/ars.2013.5505rs. No abstract available.

3. Stress Regulates Aquaporin-8 Permeability to Impact Cell Growth and Survival.

Medraño-Fernandez I*, Bestetti S*, Bertolotti M, Bienert GP, Bottino C, Laforenza U, Rubartelli A, Sitia R.

Antioxid Redox Signal. 2016 Jun 20;24(18):1031-44. doi: 10.1089/ars.2016.6636.

*the authors equally contributed to this work

Ringraziamenti

Grazie Iria, my darling scientific mother.

Grazie Enrica Maria e Fernando Primo, my biological parents.

Grazie Bob e grazie Anna, my scientific lighthouse.

Grazie professor Biondi e signora Elisabetta, my Dimet guardian angels.

Grazie la Benedetta, my beautiful love.

Grazie lab members and relatives, my scientific brothers.

Grazie adjacent-lab members and relatives, my scientific neighbours.

Grazie Campionissimi, my life-time friends.

Grazie Nipo and Nipo-makers, the "*smallest*" joy of my life.

Grazie G.S.O, my stupid, irreplaceable team (un po' meno? Cit.).

Grazie a tutti voi, i motivi li conoscete.

References

1.   Tavel L, Fontana F, Garcia Manteiga JM, Mari S, Mariani E, Caneva E, et al. Assessing Heterogeneity of Osteolytic Lesions in Multiple Myeloma by (1)H HR-MAS NMR Metabolomics. International journal of molecular sciences. 2016;17(11).

2.   Nerini-Molteni S, Ferrarini M, Cozza S, Caligaris-Cappio F, Sitia R. Redox homeostasis modulates the sensitivity of myeloma cells to bortezomib. British journal of haematology. 2008;141(4):494-503.

3.   Campanella A, Santambrogio P, Fontana F, Frenquelli M, Cenci S, Marcatti M, et al. Iron increases the susceptibility of multiple myeloma cells to bortezomib. Haematologica. 2013;98(6):971-9.

4.   Bordini J, Galvan S, Ponzoni M, Bertilaccio MT, Chesi M, Bergsagel PL, et al. Induction of iron excess restricts malignant plasma cells expansion and potentiates bortezomib effect in models of multiple myeloma. Leukemia. 2016.

5.   Cenci S, Sitia R. Managing and exploiting stress in the antibody factory. FEBS letters. 2007;581(19):3652-7.

6.   Liou GY, Storz P. Reactive oxygen species in cancer. Free radical research. 2010;44(5):479-96.

7.   Tiligada E. Chemotherapy: induction of stress responses. Endocr Relat Cancer. 2006;13 Suppl 1:S115-24.

8.   Zhou S, Ye W, Shao Q, Zhang M, Liang J. Nrf2 is a potential therapeutic target in radioresistance in human cancer. Crit Rev Oncol Hematol. 2013;88(3):706-15.

9.   Martins AP, Marrone A, Ciancetta A, Galan Cobo A, Echevarria M, Moura TF, et al. Targeting aquaporin function: potent inhibition of aquaglyceroporin-3 by a gold-based compound. PloS one. 2012;7(5):e37435.

10.   Almasalmeh A, Krenc D, Wu B, Beitz E. Structural determinants of the hydrogen peroxide permeability of aquaporins. The FEBS journal. 2014;281(3):647-56.

11.   Castellani P, Balza E, Rubartelli A. Inflammation, DAMPs, tumor development, and progression: a vicious circle orchestrated by redox signaling. Antioxidants & redox signaling. 2014;20(7):1086-97.

12.   Benlloch M, Obrador E, Valles SL, Rodriguez ML, Sirerol JA, Alcacer J, et al. Pterostilbene Decreases the Antioxidant Defenses of Aggressive Cancer Cells In Vivo: A Physiological Glucocorticoids- and Nrf2-Dependent Mechanism. Antioxidants & redox signaling. 2016;24(17):974-90.

13.   Satooka H, Hara-Chikuma M. Aquaporin-3 Controls Breast Cancer Cell Migration by Regulating Hydrogen Peroxide Transport and Its Downstream Cell Signaling. Molecular and cellular biology. 2016;36(7):1206-18.

14.   Thiagarajah JR, Chang J, Goettel JA, Verkman AS, Lencer WI. Aquaporin-3 mediates hydrogen peroxide-dependent responses to environmental stress in colonic epithelia. Proceedings of the National Academy of Sciences of the United States of America. 2017;114(3):568-73.

15.   Watanabe S, Moniaga CS, Nielsen S, Hara-Chikuma M. Aquaporin-9 facilitates membrane transport of hydrogen peroxide in mammalian cells. Biochem Biophys Res Commun. 2016;471(1):191-7.

16.   Marino A, Morabito R, La Spada G, Adragna NC, Lauf PK. Evidence for aquaporin-mediated water transport in nematocytes of the jellyfish Pelagia noctiluca. Cellular physiology and biochemistry : international journal of experimental cellular physiology, biochemistry, and pharmacology. 2011;28(6):1211-8.

17.   Putker M, Vos HR, van Dorenmalen K, de Ruiter H, Duran AG, Snel B, et al. Evolutionary acquisition of cysteines determines FOXO paralog-specific redox signaling. Antioxidants & redox signaling. 2015;22(1):15-28.